NewCompStar School 2016
"Neutron stars: gravitational physics theory and observations"

NS-NS and BH-NS coalescing binaries

Toni Font (Universitat de València, Spain)

Suggested reading

M. Alcubierre, "Introduction to 3+1 Numerical Relativity", Oxford (2007)

T.W. Baumgarte & S.L. Shapiro, "Numerical Relativity: Solving Einstein's equations on the computer", Cambridge University Press (2010)

E. Gourgoulhon, "3+1 Formalism in General Relativity", Springer (2012)

M. Shibata, "Numerical Relativity (100 Years of General Relativity)" World Scientific (2015)

J.A. Faber & F.A. Rasio, "Binary neutron star mergers", Living Reviews in Relativity (2012) (livingreviews.org)

L. Baiotti & L. Rezzolla, "Binary neutron-star mergers: a review of Einstein's richest laboratory" (2016) arXiv:1607.03540

M. Shibata & K. Taniguchi, "Coalescence of Black Hole-Neutron Star Binaries", Living Reviews in Relativity (2012) (livingreviews.org)

G. Cook, "Initial data for Numerical Relativity" (2000) (livingreviews.org)

J.A. Font, "Numerical hydrodynamics and magnetohydrodynamics in general relativity", Living Reviews in Relativity (2008) (livingreviews.org)

L. Rezzolla & O. Zanotti, "Relativistic hydrodynamics", Oxford (2013)

Reason #1 to study BNS and BH-NS mergers

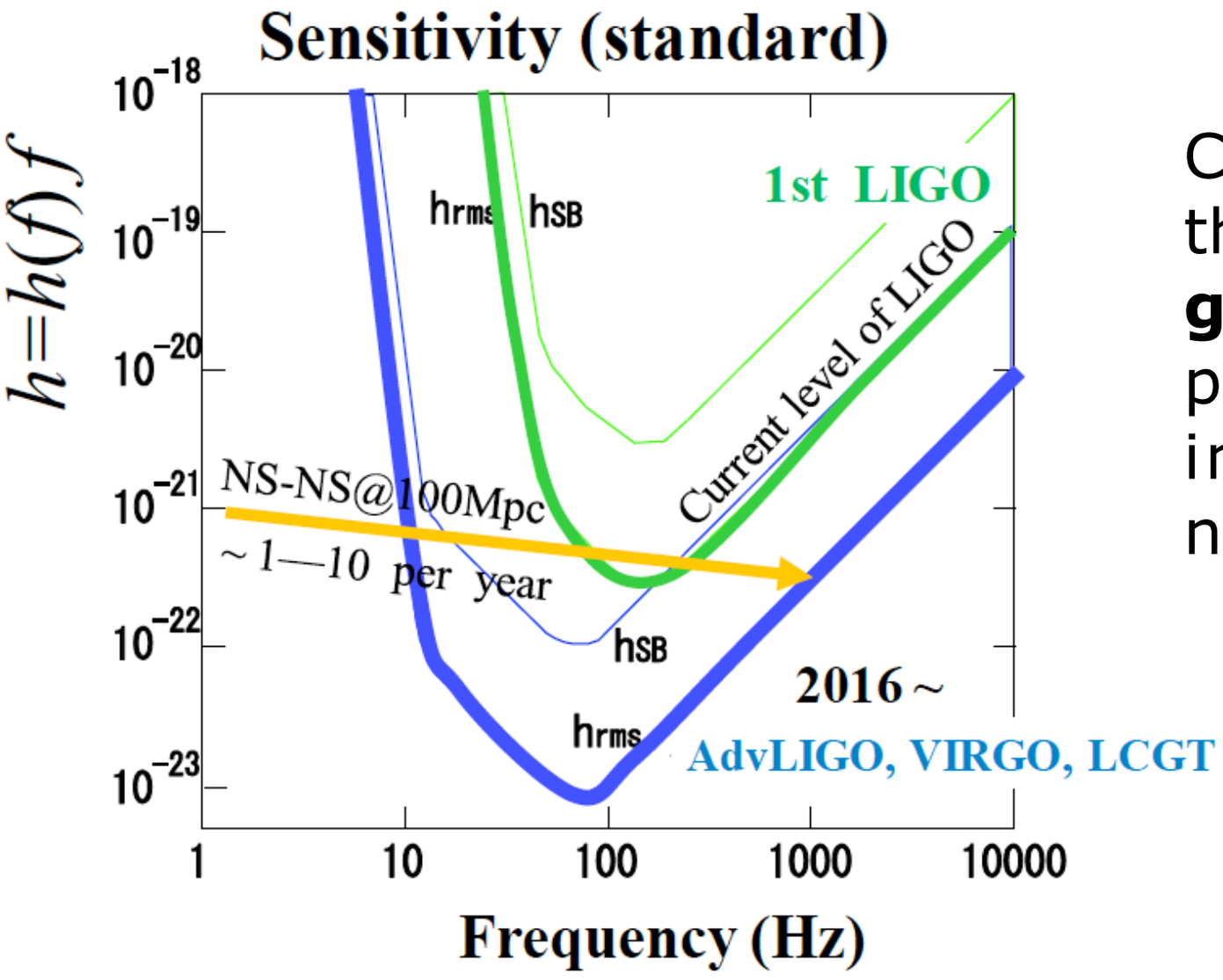

Compact binaries are among the most powerful sources of **gravitational waves.** Could provide key information to improve understanding of neutron star physics and EOS.

BNS mergers = GW source

Before merger ($10 < f <$ ~kHz)

after merger ($f >$ ~kHz)

Post-Newtonian

EOB

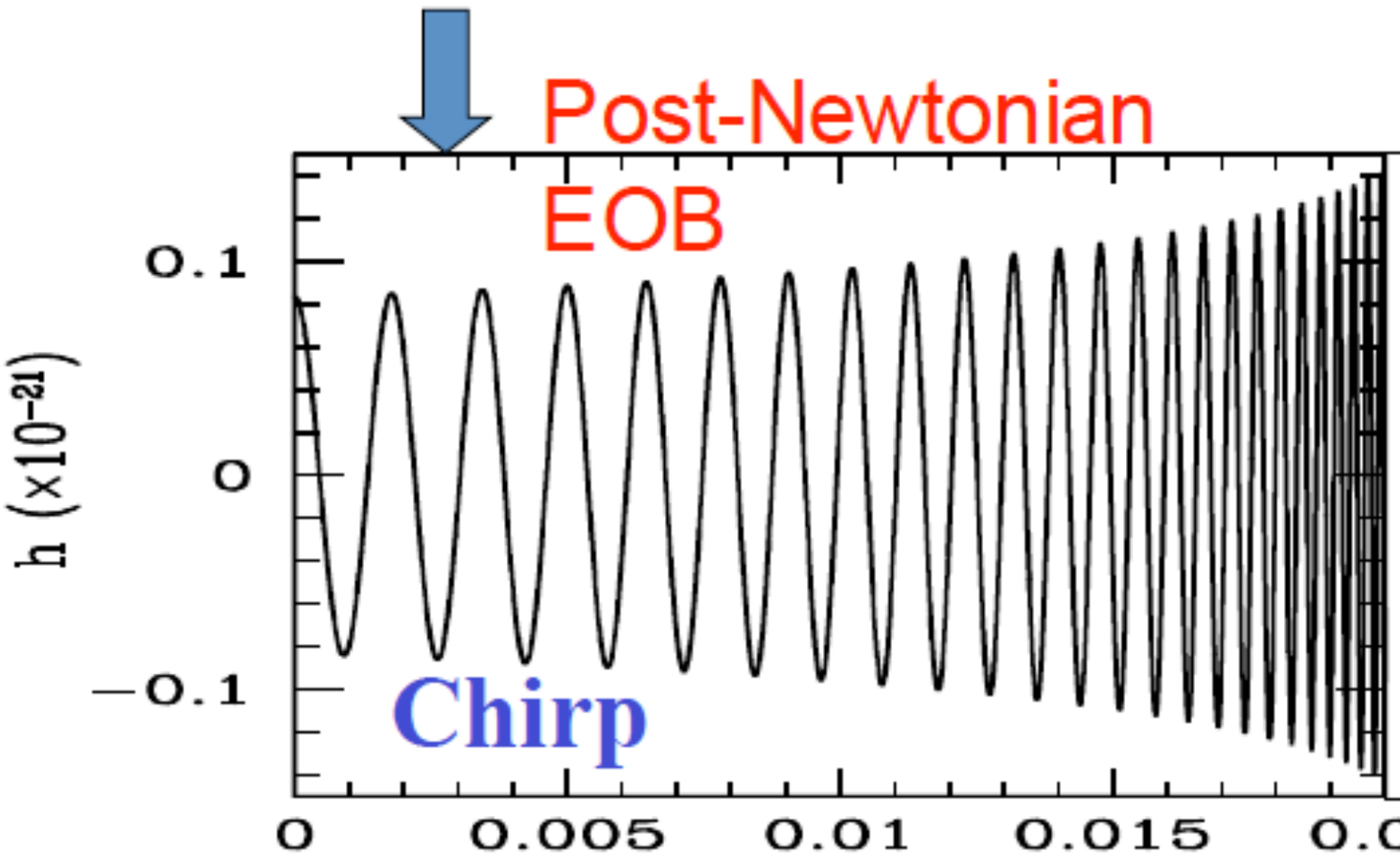

?

GR gravity

Hydro-interaction

Neutrino emission

Magnetic field

Numerical relativity

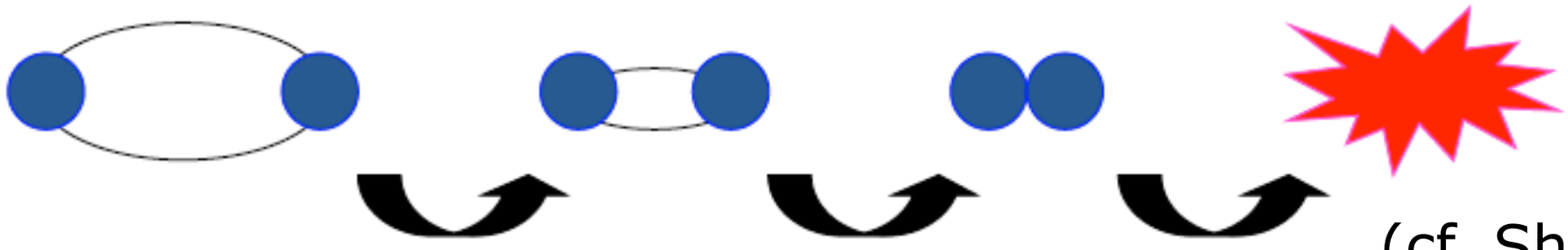

(cf. Shibata)

GW astronomy with BH-NS mergers

GWs emitted during the **tidal disruption** of a NS in a BH-NS merger will provide invaluable information about the radius and the EOS of the NS, because the orbital frequency at tidal disruption depends strongly on the compactness of the NS (Kyutoku et al 2010, 2011).

The masses of the NS and the BH will be determined by the data analysis for GWs emitted in the inspiral phase (Cutler & Flanagan 1994; parameter estimation techniques).

If the NS radius could be determined or constrained from the observation of GWs emitted during tidal disruption, the resultant relation between the mass and the radius of the observed NS (Ferrari et al 2010) may be used for constraining the EOS of the high-density nuclear matter .

Theoretical templates for a variety of possible EOS have yet to be prepared.

Reason #2 to study BNS and BH-NS mergers

Excellent laboratory to study high-density nuclear physics (key to decipher the NS physics)

Neutron star composition still unknown

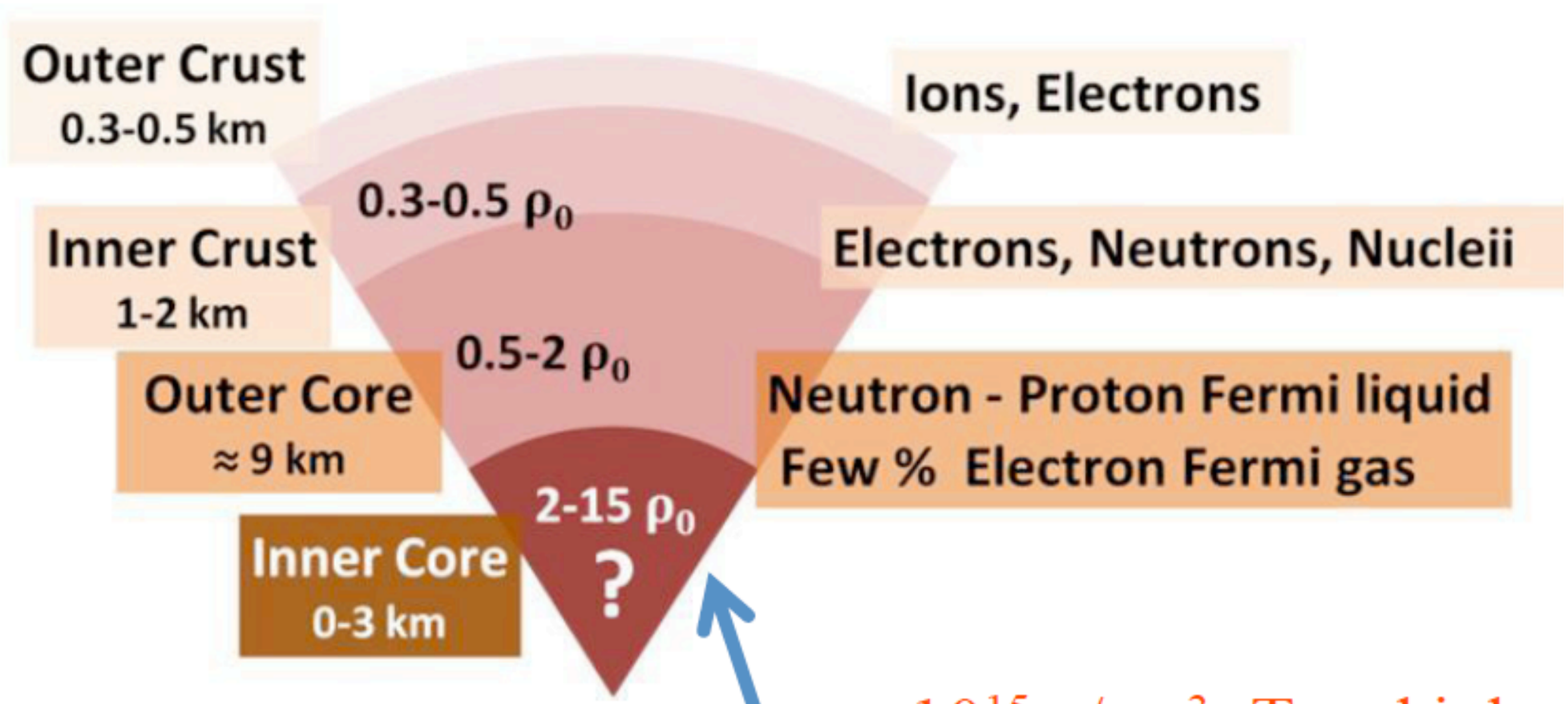

ρ_0=2.8*10^{14} g/cm^3

$\rho \sim 10^{15}$ g/cm^3: Too high

Components: Neutron + ?????

Radius: 10—15 km ?

Many different possibilities depending on the EOS

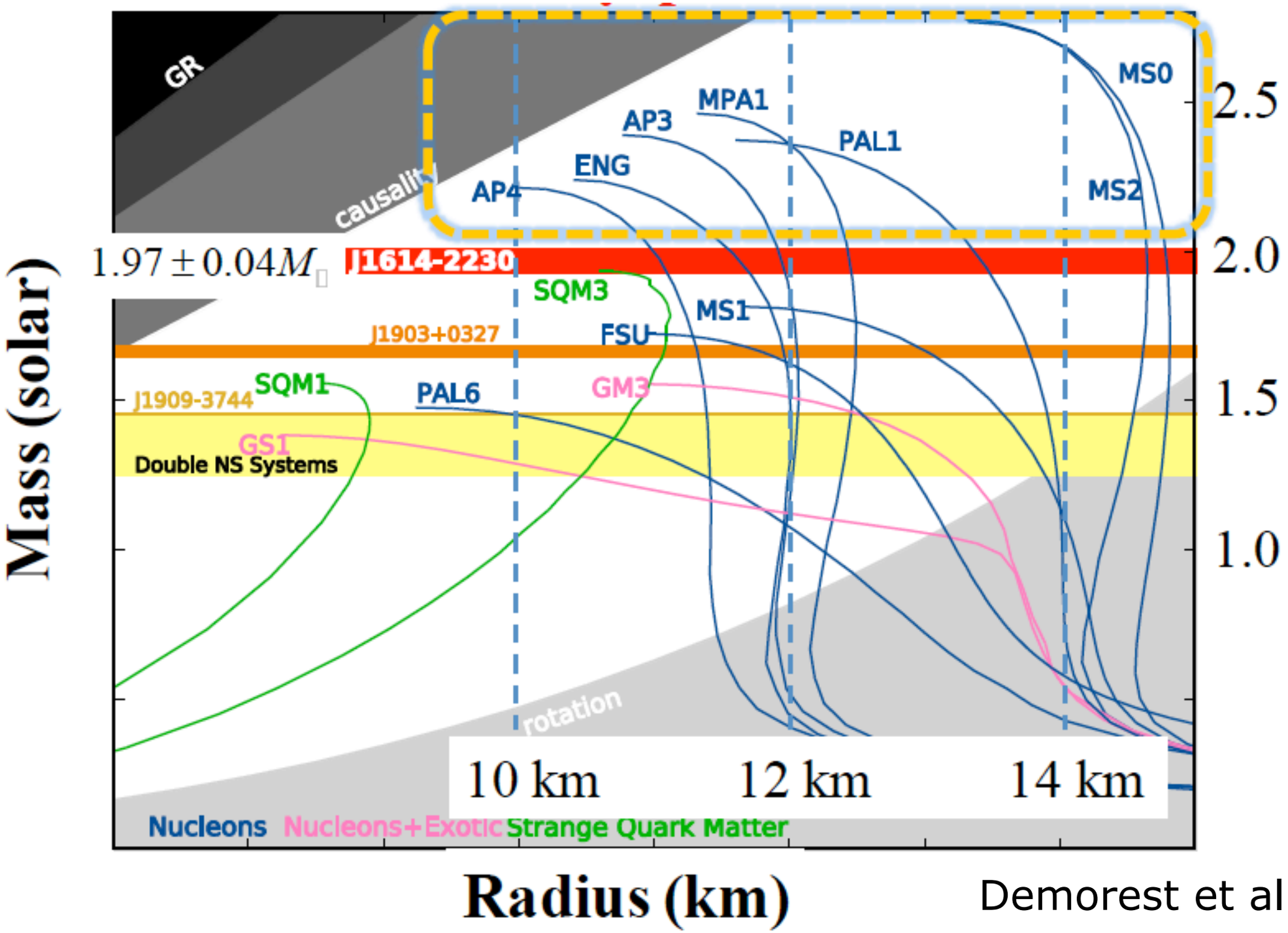

Demorest et al (2010)

GWs in the late inspiral and merger phases could constrain NS EOS.
Many GW templates from Numerical Relativity are necessary

Reason #3 to study BNS and BH-NS mergers

Their mergers lead to BH+torus systems: central engines of one of the most powerful phenomena in the universe: **short Gamma Ray Bursts** (GRBs)

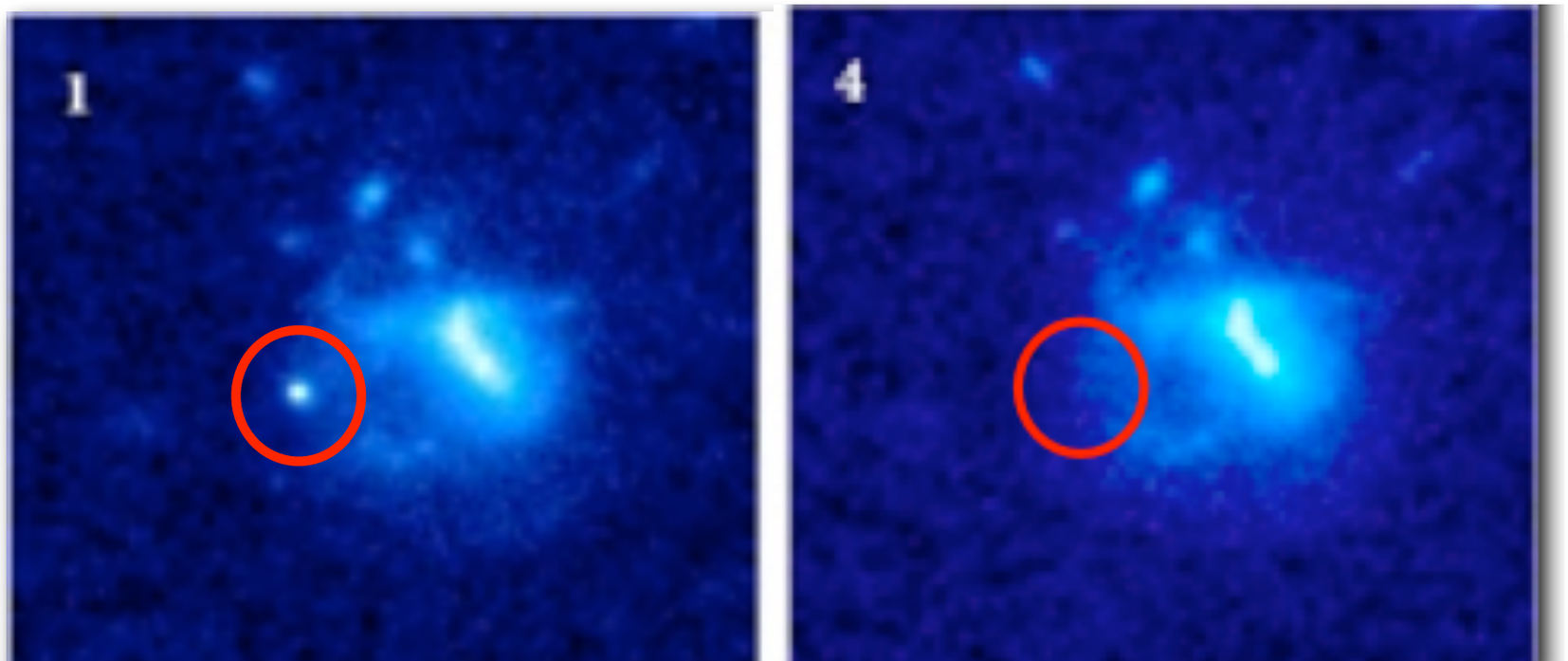

HST images of July 9, 2005 GRB taken 5.6, and 34.7 days after the burst (Derek Fox, PSU)

Possible evidence that a BNS/BH-NS merger can be behind SGRBs has emerged recently from the infrared excess in the afterglow curve of Swift's SGRB 130603B (Berger et al 2013, Tanvir et al 2013).

Interpreted as a **"kilonova/macronova"** emission (Li and Paczynski 1998, Metzger et al 2010) i.e., as due to the **radioactive decay** of by-products of the r-processed matter from the material ejected in the merger **(nucleosynthesis)**.

BH-NS mergers as central engines of short GRBs

If tidal disruption occurs outside the ISCO, a tidally-disrupted NS may form a disk or torus around the remnant BH of

$$M_{\rm d} > 0.01 M_\odot, \;\; \rho_{\rm d} \geq 10^{11}\,{\rm g/cm}^3, \;\; T_{\rm d} \geq 10\,{\rm MeV}$$

A **spinning BH** surrounded by a **massive, hot, and dense torus** has been proposed as one of the likely sources for the central engine of a GRB (Berger 2014 and references therein). BH-NS binaries have been proposed as progenitors of short GRBs, as lifetime of disk is short (<1s).

The typical energies of sGRB can be explained if 1 – 10% of the thermal energy generated in a compact disk around a BH is converted in gamma rays:

$$L = \eta_{\rm eff} \frac{G M_{\rm BH} \dot{M}}{r_{\rm d}} \approx 2 \times 10^{49}\,{\rm erg/s} \left(\frac{\eta_{\rm eff}}{10^{-2}}\right) \left(\frac{10 G M_{\rm BH}}{r_{\rm d} c^2}\right) \left(\frac{\dot{M}}{10^{-2} M_\odot/{\rm s}}\right)$$

The issue to be resolved through NR simulations is whether or not the mass and thermal energy of the torus formed after the merger are large enough for driving an SGRB of such **huge total luminosity**.

A more challenging issue is whether or not the longterm X-ray flares of duration 10^3 – 10^4 s, often observed in association with sGRB, may be explained in the BH-NS merger scenario.

Reason #4 to study BNS and BH-NS mergers

Sites for r-process nucleosynthesis

Material ejected from a BNS merger or a tidally-disrupted NS may be important for understanding **observed abundances of heavy elements** that are formed by rapid neutron capture in the r-process (Lattimer & Schramm 1974).

r-process happens if neutron flux density is so high that the atomic nucleus has no time to decay via beta emission in between neutron captures. Afterwards, highly unstable nuclei decay via many beta decays to stable or unstable nuclei of high atomic number.

β^- decay $\qquad {}^{A}_{Z}X \rightarrow {}^{A}_{Z+1}X' + e^- + \bar{\nu}_e$

Is it possible for a fraction of **material to escape** from the system?

Tidal disruption of a NS occurs at an orbital separation of $\sim 10 G M_{\rm BH}/c^2$

For a test particle of mass *m* in a circular orbit around a BH the total energy is ~ $G M_{\rm BH} m/2r = 0.05\, mc^2$

For a free nucleon $0.05\, mc^2 \sim 50\,\mathrm{MeV}$

Is it possible to give 50 MeV energy to each nucleon? Relevant process?

Galactic compact BNS observed

	PSR	P(day)	e	$M(M_{\rm sun})$	M_1	M_2	$T_{\rm GW}$
1.	B1913+16	0.323	0.617	2.828	1.387	1.441	2.45
2.	B1534+12	0.421	0.274	2.678	1.333	1.345	22.5
3.	B2127+11C	0.335	0.681	2.71	1.35	1.36	2.2
4.	J0737-3039	0.102	0.088	2.58	1.35	1.24	0.85
5.	J1756-2251	0.32	0.18	2.58	1.31	1.26	1.69
6.	J1906-0746	0.166	0.085	2.62	1.25	1.37	3.0

[according to lowest-order dissipative contribution from GR (2.5PN level); both NSs point masses.]

10^8 yrs

$$\tau_{\rm GW} = \frac{5}{64}\frac{a^4}{\mu M^2} = 2.2\times 10^8 q^{-1}(1+q)^{-1}\left(\frac{a}{R_\odot}\right)^4\left(\frac{M_1}{1.4M_\odot}\right)^{-3}\ {\rm yr}$$

Merger time

6 (GC) NS-NS, which will merge within a Hubble time (13.7 Gyr), have been found.

see Lorimer (2008)

Evolution of BNS

Inspiral

Formation
(after two supernovae)
Evolve as a result
of GW emission

Last 1 hour at $r \sim 1000$ km
$f_{GW} \sim 7$ Hz

Merger starts when
$r \sim 30$ km ($f_{GW} \sim 1$ kHz)

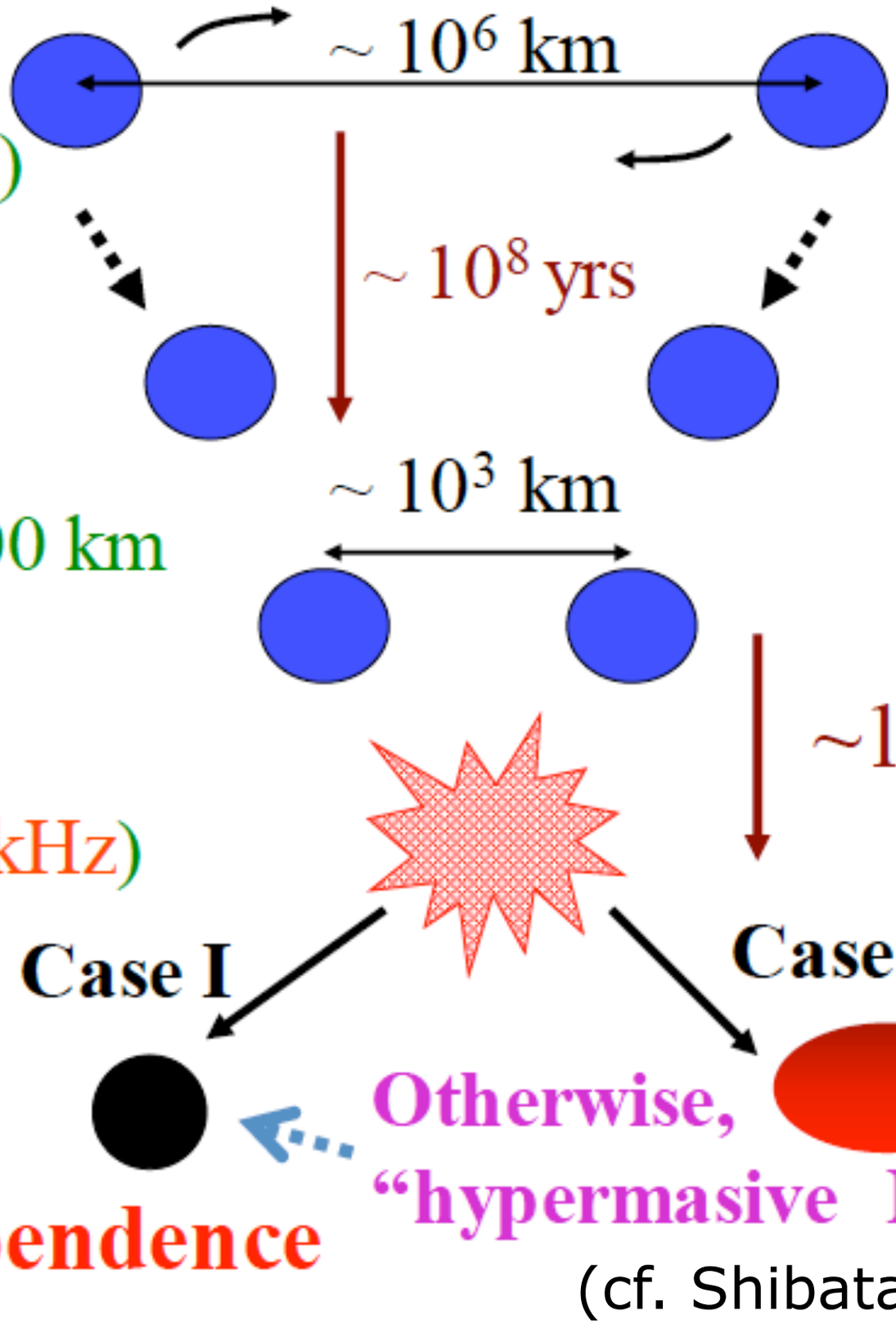

If mass is high enough, a black hole is formed

Otherwise, "hypermasive NS"

Large EOS-dependence

(cf. Shibata)

Evolution of BNS

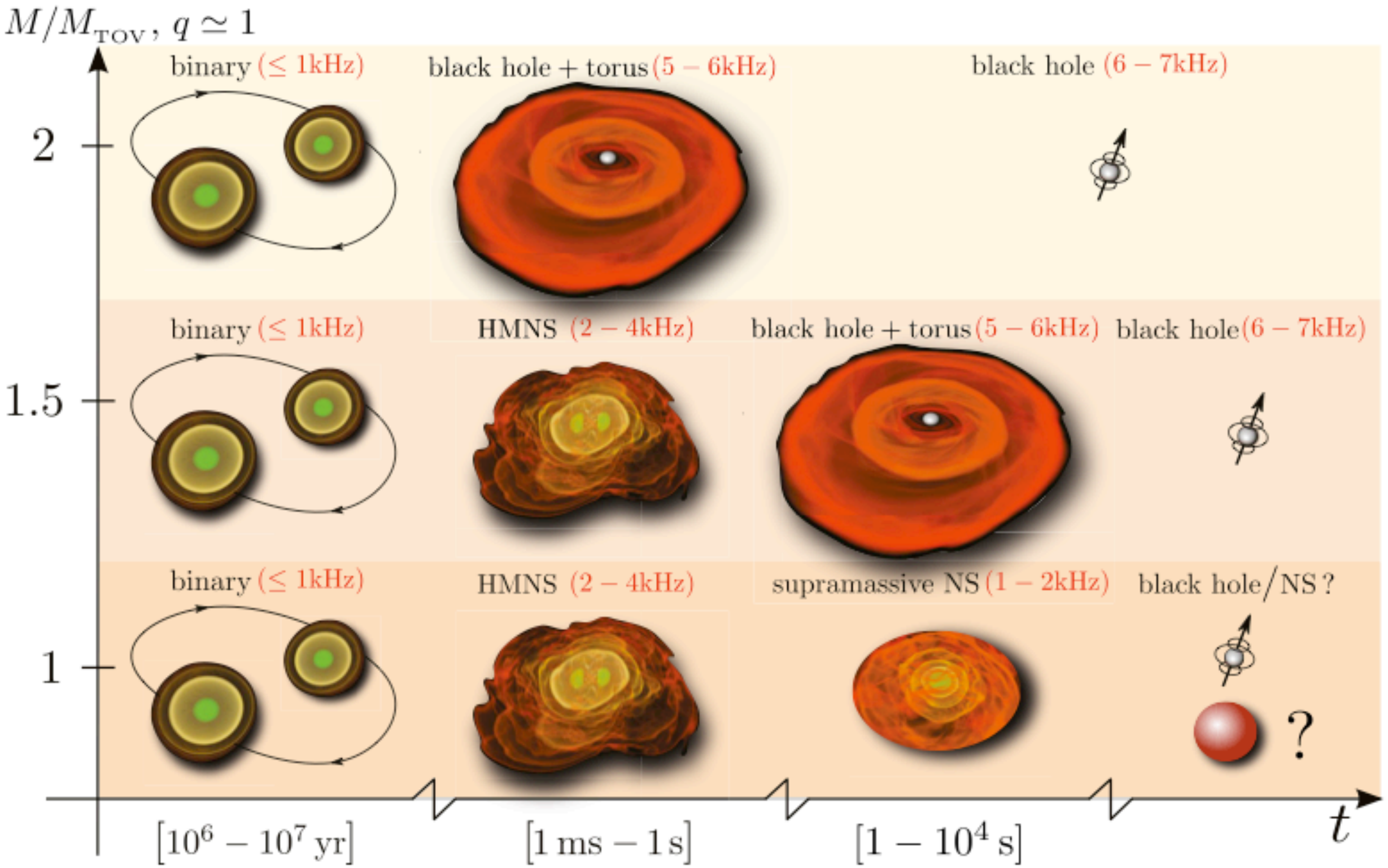

Baiotti & Rezzolla (2016)

Evolution of BH-NS binaries

BH-NS binaries are believed to be formed as a result of two supernovae in a massive binary system.

As BNS, orbital separation decreases gradually due to the longterm **gravitational radiation reaction** (objects are in an adiabatic inspiral motion). Eventually, the two objects merge to be a BH system.

Lifetime of a binary in quasi-circular orbit (Peters & Mathews 1963)

$$\tau_{\rm GW} = \frac{5c^5}{256G^3}\frac{r^4}{(M_{\rm BH}+M_{\rm NS})M_{\rm BH}M_{\rm NS}}$$
$$\approx 1.34\times10^{10}\,{\rm yrs}\left(\frac{r}{6\times10^6\,{\rm km}}\right)^4\left(\frac{M_{\rm BH}}{6M_\odot}\right)^{-1}\left(\frac{M_{\rm NS}}{1.4M_\odot}\right)^{-1}\left(\frac{M_{\rm BH}+M_{\rm NS}}{7.4M_\odot}\right)^{-1}$$

If initial semi-major axis is $<10^7$ km, **BH and NS merge within the Hubble timescale** after a substantial emission of GWs.

Inspiral phase: binary separation gradually decreases due to gravitational radiation reaction, objects well approximated by **point masses in an adiabatic orbit** since radii much smaller than orbital separation, finite-size effects (tidal deformation) negligible.

Gravitational-radiation-reaction timescale much longer than orbital period:

$$\frac{\tau_{\rm GW}}{P_{\rm orb}} \approx 1.8 \left(\frac{r}{6G(M_{\rm BH}+M_{\rm NS})/c^2}\right)^{5/2} \left(\frac{M_{\rm BH}}{6M_\odot}\right)^{-1} \left(\frac{M_{\rm NS}}{1.4M_\odot}\right)^{-1} \left(\frac{M_{\rm BH}+M_{\rm NS}}{7.4M_\odot}\right)^{2}$$

because $r \gg G(M_{\rm BH}+M_{\rm NS})/c^2$

The evolution through the inspiral phase is well understood within the **post-Newtonian (PN) approximation** (Blanchet 2006).

Late inspiral and merger phases: orbital evolution depends significantly on finite-size effects and the resulting modification on the interaction between the two objects.

In addition, adiabatic approximation for orbital evolution breaks down when

$$\tau_{\rm GW} \sim P_{\rm orb} \quad \text{i.e.} \quad r \sim 6G(M_{\rm BH}+M_{\rm NS})/c^2 \qquad \text{last orbit}$$

In the merger phase and remnant-formation phase, the **dynamics** of the system **depends strongly on NS structure** (radius and density profile, EOS) and **on BH spin**, as well as **on general relativistic gravity**. This implies that a numerical study in general relativity is required to understand the final evolution phase of BH-NS binaries.

BH-NS binaries not yet observed in contrast to BNS.

Statistical studies based on stellar evolution synthesis suggest that coalescence will occur ~1 – 10% as frequently as that of BNS binaries in our galaxy and hence in normal **spiral galaxies** every 10^6 - 10^7 years (Kalogera et al 2007).

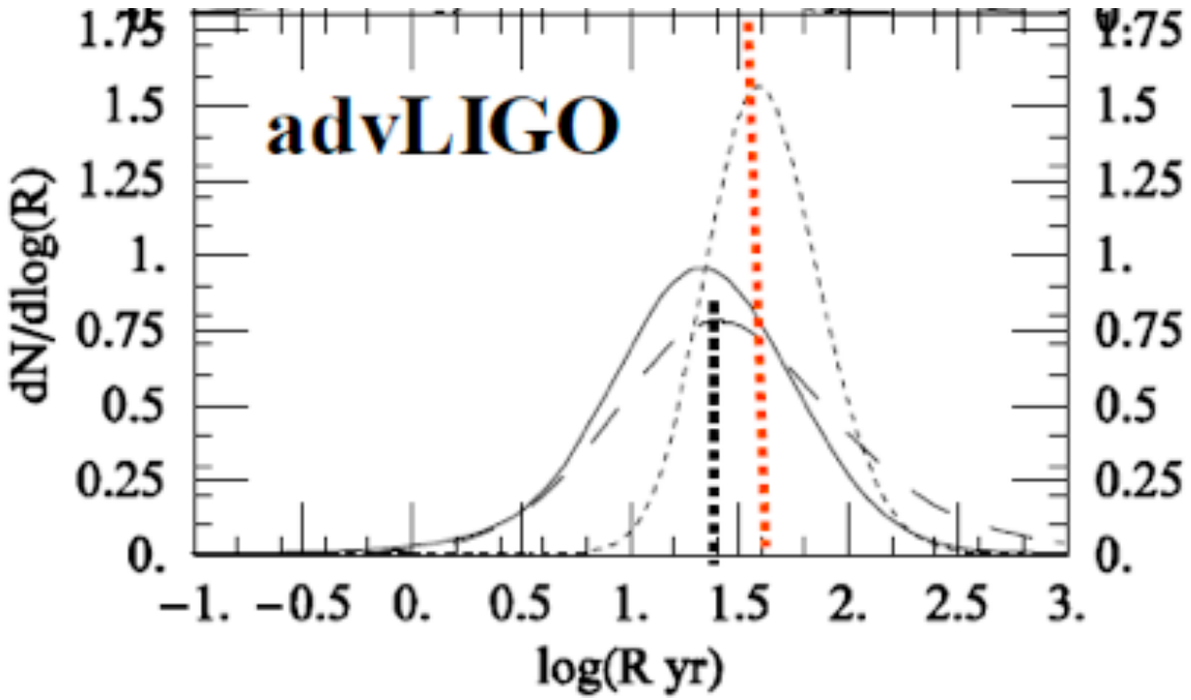

dot: BNS, solid: BH/NS, dashed: BBH

Events/year	BNS	BH/NS	BBH
aLIGO	0.4-400	0.2-300	2-4000
ET	10^3-10^7	10^3-10^7	10^4-10^8

Kalogera et al 2007

In addition, BH/NS coalescence in **elliptic galaxies** could significantly contribute to total coalescence rate of the universe (O'Shaughnessy et al 2010)

This implies that BH-NS coalescence is likely to occur frequently in the Hubble volume, and therefore, the evolution process and final fate of BH-NS binaries deserve a detailed theoretical study.

BH-NS binaries in close orbits are among most promising sources for large laser-interferometric GW detectors.

The frequency and amplitude of GW near the last orbit are estimated to give:

$$f \approx 594\,\mathrm{Hz} \left(\frac{6G(M_{\mathrm{BH}}+M_{\mathrm{NS}})}{c^2 r}\right)^{3/2} \left(\frac{M_{\mathrm{BH}}+M_{\mathrm{NS}}}{7.4M_\odot}\right)^{-1}$$

$$\begin{aligned} h &\approx \frac{4G\mu(M_{\mathrm{BH}}+M_{\mathrm{NS}})}{c^4 D r} \\ &\approx 3.6\times10^{-22} \left(\frac{6G(M_{\mathrm{BH}}+M_{\mathrm{NS}})}{c^2 r}\right) \left(\frac{M_{\mathrm{BH}}}{6M_\odot}\right) \left(\frac{M_{\mathrm{NS}}}{1.4M_\odot}\right) \left(\frac{D}{100\,\mathrm{Mpc}}\right)^{-1} \end{aligned}$$

Frequency within sensitivity range of advanced GW detectors, 10 Hz – 3 kHz.

10^{-22} amplitude is high enough for the signal to be detected.

Final fate of BH-NS binaries classified into two categories:

- NS tidally disrupted by the BH before being swallowed
- NS simply swallowed by its companion BH

Final fate of NS depends primarily on the mass of companion BH and compactness of the NS. If BH mass is small enough or NS radius is large enough, NS will be tidally disrupted before being swallowed by the BH.

Mass shedding of a non-spinning NS occurs when the tidal force of its companion BH at the surface of the NS (lhs) is stronger than the self-gravity of the NS (rhs):

$$\frac{2Gc_{\rm R}M_{\rm BH}R_{\rm NS}}{r^3} \geq \frac{GM_{\rm NS}}{(c_{\rm R}R_{\rm NS})^2}$$

$c_{\rm R}$ EOS-dependent parameter (degree of tidal deformation)

If the binary is in a circular orbit with the Keplerian angular velocity, previous equation may be written in terms of the angular velocity:

$$\Omega^2 \geq C_\Omega^2 \frac{GM_{\rm NS}}{R_{\rm NS}^3}(1+Q^{-1}) \qquad Q \equiv \frac{M_{\rm BH}}{M_{\rm NS}} \qquad C_\Omega \leq 0.3$$

(Taniguchi et al 2007, 2008)

Above $f = \dfrac{\Omega}{\pi} \geq 1.0\,{\rm kHz}$ tidal disruption likely to occur irrespective of BH mass.

A challenging numerical problem

The accurate simulation of BNS and BH-NS mergers is among the most challenging tasks in NR.

Scenarios involve **strong gravitational fields**, matter motion with **relativistic speeds**, **shock waves**, and **strong magnetic fields.**

Numerical difficulties aggravated by intrinsic **multidimensional** character and by the inherent complexities in Einstein's theory of gravity, such as **coordinate degrees of freedom** and the possible formation of **curvature singularities** (BH formation).

Not surprisingly, early simulations were performed in Newtonian framework (see Faber & Rasio 2012, Baiotti & Rezzolla 2016 for reviews).

Despite difficulties, major progress achieved during ~ **last 15 years** in NR simulations of **BNS** mergers.

Breakthrough simulations of BBH in 2005 sparked off NR simulations of the merger of **BH-NS** binaries (~ **a decade long**).

Important advances have been achieved in our understanding of all topics of research listed above.

More than a decade of NR progress

Drastic **improvements** in simulation front

- **mathematics** (formulation of equations)
- **physics** (nuclear physics EOS, thermal effects, cooling, and MHD)
- **numerical methods** (use of high-resolution methods and adaptive mesh refinement)
- ever increasing **computational resources**

have all allowed to extend scope of early numerical relativity simulations (seminal work by **Shibata and Uryu 2000**).

Increasing attention in recent years by growing number of groups: Kyoto/Tokyo, AEI/Frankfurt, Jena, UIUC, Caltech/Cornell, Princeton, UWM, LSU/BYU/Perimeter, AUTH, MPA, Trento, Parma, Valencia ...

Larger initial separations have recently started being considered and some of the existing simulations have expanded the range spanned by the models well beyond black-hole formation.

Still, most simulations: cold EOS; few include thermal EOS, neutrino effects, and MHD.

State-of-the-art NR codes

- SACRA code: Kyoto/Tokyo group
- Whisky/WhiskyMHD/WhiskyTHC code: AEI / Frankfurt / Trento / (Caltech) ... whiskycode.org, cactuscode.org
- HAD code: Anderson et al (2008) arXiv:0708.2720 (GHF)
- Illinois code: Etienne et al (2010) arXiv:1007.2848
- Einstein Toolkit: LSU / ... Löffler et al (2012) arXiv:1111.3344 einsteintoolkit.org (public domain code)
- Jena code (BAM): Thierfelder et al (2011) arXiv:1104.4751
- Code by East et al: East et al (2016) arXiv:1511.01093 (GHF)
- SpEC: GHF for spacetime (spectral methods) Duez et al (2008) arXiv:0809.0002, www.black-holes.org/SpEC.html
- SPH codes of Rosswog (Newtonian) and Bauswein (CFC)
- LORENE: Initial Data, public domain www.lorene.obspm.fr

Numerical framework for the simulations

Gravitational field eqs

Use conformal and traceless "3+1" formulation of EEs (BSSN) or GHF

Gauge: "1+log" slicing for lapse; hyperbolic "Gamma-driver" for shift

Use consistent configurations of irrotational binary NSs in quasi-circular orbit (eccentric orbits and NS spin more recent)

Use 4th-8th order finite-differencing

Wave-extraction with Weyl scalars and gauge-invariant perturbations

Hydrodynamics/MHD eqs

Riemann-solver-based HRSC TVD methods (HLLE, Roe, Marquina) with high-order cell reconstruction (minmod, PPM)

Method of lines for time integration (high-order conservative RK schemes)

Use excision if needed

Divergence-free magnetic field condition (CT, divergence cleaning)

AMR with moving grids

Basic set of equations to solve
Hydrodynamics

3+1 formulation. Details in Banyuls et al 1997, Font 2008.

$$\frac{\partial}{\partial x^\mu}(\sqrt{-g}\rho u^\mu) = 0\,, \qquad \frac{\partial}{\partial x^\mu}(\sqrt{-g}T^{\mu\nu}) = \sqrt{-g}\Gamma^\nu_{\mu\lambda}T^{\mu\lambda}$$

Hyperbolic system:

$$\frac{1}{\sqrt{-g}}\left(\frac{\partial\sqrt{\gamma}\mathbf{U}}{\partial x^0} + \frac{\partial\sqrt{-g}\mathbf{F}^i}{\partial x^i}\right) = \mathbf{S}$$

$$\begin{aligned}
\mathbf{U} &= (D, S_j, \tau) \\
\mathbf{F}^i &= \left(D\left(v^i - \frac{\beta^i}{\alpha}\right), S_j\left(v^i - \frac{\beta^i}{\alpha}\right) + p\delta^i_j, \tau\left(v^i - \frac{\beta^i}{\alpha}\right) + pv^i\right) \\
\mathbf{S} &= \left(0, T^{\mu\nu}\left(\frac{\partial g_{\nu j}}{\partial x^\mu} - \Gamma^\delta_{\nu\mu}g_{\delta j}\right), \alpha\left(T^{\mu 0}\frac{\partial \ln\alpha}{\partial x^\mu} - T^{\mu\nu}\Gamma^0_{\nu\mu}\right)\right)
\end{aligned}$$

First-order flux-conservative hyperbolic system

Basic set of equations to solve
Magneto-hydrodynamics

Conservation of mass: $\nabla_\mu(\rho u^\mu) = 0$

Conservation of energy and momentum: $\nabla_\mu T^{\mu\nu} = 0$

Maxwell's equations: $\nabla_\mu {}^*F^{\mu\nu} = 0 \quad {}^*F^{\mu\nu} = \frac{1}{W}(u^\mu B^\nu - u^\nu B^\mu)$

- Divergence-free constraint: $\vec{\nabla} \cdot \vec{B} = 0$
- Induction equation: $\frac{1}{\sqrt{\gamma}} \frac{\partial}{\partial t} \left(\sqrt{\gamma}\vec{B}\right) = \vec{\nabla} \times \left[\left(\alpha\vec{v} - \vec{\beta}\right) \times \vec{B}\right]$

Adding all up (Antón et al 2006):
first-order, flux-conservative, hyperbolic system + constraint

$$\frac{1}{\sqrt{-g}} \left(\frac{\partial \sqrt{\gamma}\mathbf{U}}{\partial t} + \frac{\partial \sqrt{-g}\mathbf{F}^i}{\partial x^i} \right) = \mathbf{S} \qquad \frac{\partial(\sqrt{\gamma}B^i)}{\partial x^i} = 0$$

$$D = \rho W \qquad S_j = \rho h^* W^2 v_j - \alpha b_j b^0 \qquad \tau = \rho h^* W^2 - p^* - \alpha^2 (b^0)^2 - D$$

Quite distinct methods used to deal with hyperbolic equations ...

The hyperbolic and conservative nature of the GR(M)HD equations allows to design a solution procedure based on characteristic speeds and fields of the system, translating to relativistic hydro existing tools of CFD.

Godunov-type or **high-resolution shock-capturing (HRSC)** schemes.

Divergence-free constraint not guaranteed to be satisfied numerically when updating the B-field with a HRSC scheme.

Ad-hoc scheme has to be used, e.g. the constrained transport (CT) scheme (Evans & Hawley 1988, Tóth 2000). Main physical implication of divergence constraint: magnetic flux through a closed surface is zero, essential to the CT scheme.

Basic set of equations to solve
Gravitational field equations

From standard (ADM) 3+1 to conformal, traceless BSSN

Details in Alcubierre 2007, Baumgarte & Shapiro 2010

Evolution equations

$$
\begin{aligned}
(\partial_t - \mathcal{L}_\beta)\tilde{\gamma}_{ij} &= -2\alpha\tilde{A}_{ij} \\
(\partial_t - \mathcal{L}_\beta)\phi &= -\frac{1}{6}\alpha K \\
(\partial_t - \mathcal{L}_\beta)K &= -\gamma^{ij}D_iD_j\alpha + \alpha\left[\tilde{A}_{ij}\tilde{A}^{ij} + \frac{1}{3}K^2 + \frac{1}{2}(\rho + S)\right] \\
(\partial_t - \mathcal{L}_\beta)\tilde{A}_{ij} &= e^{-4\phi}\left[-D_iD_j\alpha + \alpha(R_{ij} - S_{ij})\right]^{\mathrm{TF}} + \alpha\left(K\tilde{A}_{ij} - 2\tilde{A}_{il}\tilde{A}^l_j\right) \\
(\partial_t - \mathcal{L}_\beta)\tilde{\Gamma}^i &= -2\tilde{A}^{ij}\partial_j\alpha + 2\alpha\left(\tilde{\Gamma}^i_{jk}\tilde{A}^{kj} - \frac{2}{3}\tilde{\gamma}^{ij}\partial_j K - \tilde{\gamma}^{ij}S_j + 6\tilde{A}^{ij}\partial_j\phi\right) \\
&\quad + \partial_j\left(\beta^l\tilde{\partial}_l\gamma^{ij} - 2\tilde{\gamma}^{m(j}\partial_m\beta^{i)} + \frac{2}{3}\tilde{\gamma}^{ij}\partial_l\beta^l\right)
\end{aligned}
$$

Constraint equations

$$
\begin{aligned}
R + K^2 - K^{ij}K_{ij} &= 16\pi\rho \\
\nabla_i\left(K^{ij} - \gamma^{ij}K\right) &= 8\pi S^j
\end{aligned}
$$

Cauchy problem (IVP):

- Constraint-satisfying ID $\tilde{\gamma}_{ij}$, ϕ, K, $\tilde{A}_{ij}$, $\tilde{\Gamma}^i$
- Freely specifiable coordinates α β^i
- Evolve ID

Gravitational wave extraction in (3+1) NR

First approach: perturbations on a Schwarzschild background expanding spatial metric into a tensor basis of Regge-Wheeler harmonics. Allows for extracting gauge-invariant wavefunctions given spherical surfaces of constant coordinate radius.

Second approach: projection of the Weyl tensor onto components of a null tetrad. At a sufficiently large distance from the source and in a Newman-Penrose tetrad frame, the gravitational waves in the two polarizations can be written in terms of the Weyl scalar.

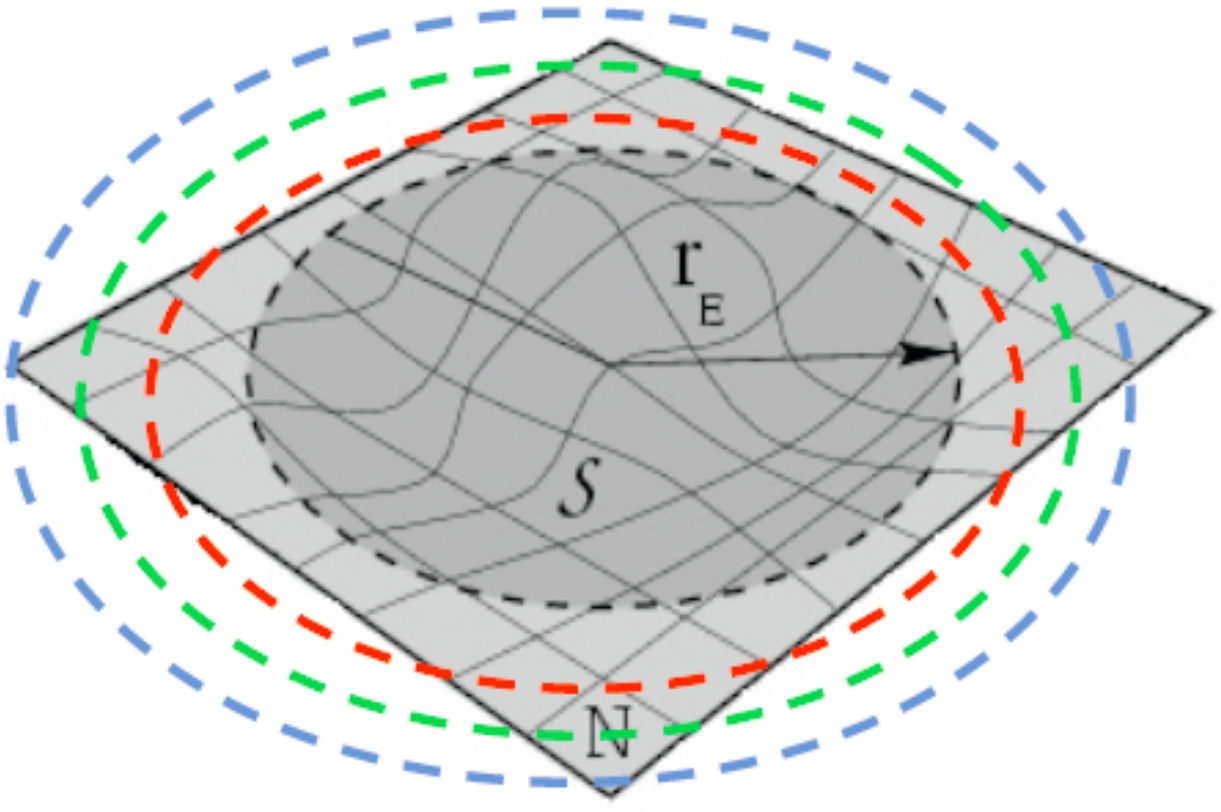

In both approaches observers are located at various positions from the source (nested spheres), where Weyl scalars are computed or where the metric is decomposed in tensor spherical harmonics to compute gauge invariant perturbations of a Schwarzschild black hole.

Results from BNS merger simulations

Shibata's massive body of work on BNS

Most dedicated study of BNS mergers in full general relativity performed by Shibata and coworkers (Kyoto/Tokyo)

Shibata **1999**, 2005
Shibata & Uryu **2000**, 2002
Shibata, Taniguchi & Uryu 2005
Shibata & Taniguchi 2006

...
Hotokezaka, Kyutoku, Okawa, Shibata, Kiuchi 2011
Sekiguchi, Kiuchi, Kyutoku, Shibata 2011
Kiuchi, Sekiguchi, Kyutoku, Shibata, 2012

...
Kiuchi, Kyutoku, Sekiguchi, Shibata, Wada 2014
Kyutoku, Ioka, Shibata 2014
Kiuchi, Cerdá-Durán, Kyutoku, Sekiguchi, Shibata 2015
Sekiguchi, Kiuchi, Kyutoku, Shibata, Taniguchi 2016
Hotokezaka, Kyutoku, Sekiguchi, Shibata 2016

...

Preparatory work

Simple EOS

Mycrophysical EOS

GRBs

Gravitational waves

MHD

neutrino transport

r-process

kilonova/macronova

Simulations incorporate following ingredients:

- self-consistent initial data for irrotational and corotational binaries
- long-term evolutions: from ISCO up to formation and ringdown of final collapsed object (either a BH or a HMNS)
- equal and unequal mass ratio
- apparent horizon finder
- microphysical (thermal) EOS and neutrino cooling (leakage, M1)
- gravitational waveform extraction from the collisions
- state-of-the-art numerical methodology: HRSC, AMR, ...
- GRMHD with very high resolution (KH and MRI instabilities)
- ejecta, r-process nucleosynthesis, radiative decay, electromagnetic counterparts (kilonova/macronova)

Most other groups have developed/are developing NR codes that incorporate same ingredients and can achieve similar scientific goals.

There is an increasing large body of results in the literature, impossible to capture in this lecture: see reviews of Faber & Rasio (2012), Baiotti & Rezzolla (2016) for complete list of references.

Main (initial, ideal fluid EOS) results

Final outcome of merger depends significantly on **initial compactness** of NSs before plunge, i.e. on the stiffness of the (ideal fluid) EOS

- If total mass of the system is 1.3–1.7 times larger than maximum rest mass of a spherical star in isolation, end product is a **BH**.
- Otherwise, a marginally-stable **HMNS** forms, supported against self-gravity by rapid differential rotation.

The HMNS will eventually collapse to a BH once sufficient angular momentum is dissipated via neutrino emission and/or gravitational radiation.

Ultimate outcome of BNS mergers is a BH + torus system (the more the NS mass ratio departs from unity the larger the disk mass).

Different outcome of the merger imprinted in the GW, as first noted by Shibata & Uryu 2002.

Future detection of GWs from BNS mergers could help constrain the maximum allowed mass of NSs along with the composition of NS matter.

Recently scrutinized in simulations performed by the various groups, in which new ingredients have been incorporated in the modelling (nucleonic and hyperonic finite-temperature EOS and neutrino cooling).

NS/NS: relativistic simulations with realistic EOS

(Shibata, Taniguchi & Uryu, PRD 71, 084021 (2005))

Case $1.30M_{sun}$ - $1.30M_{sun}$

Formation of a hypermassive neutron star

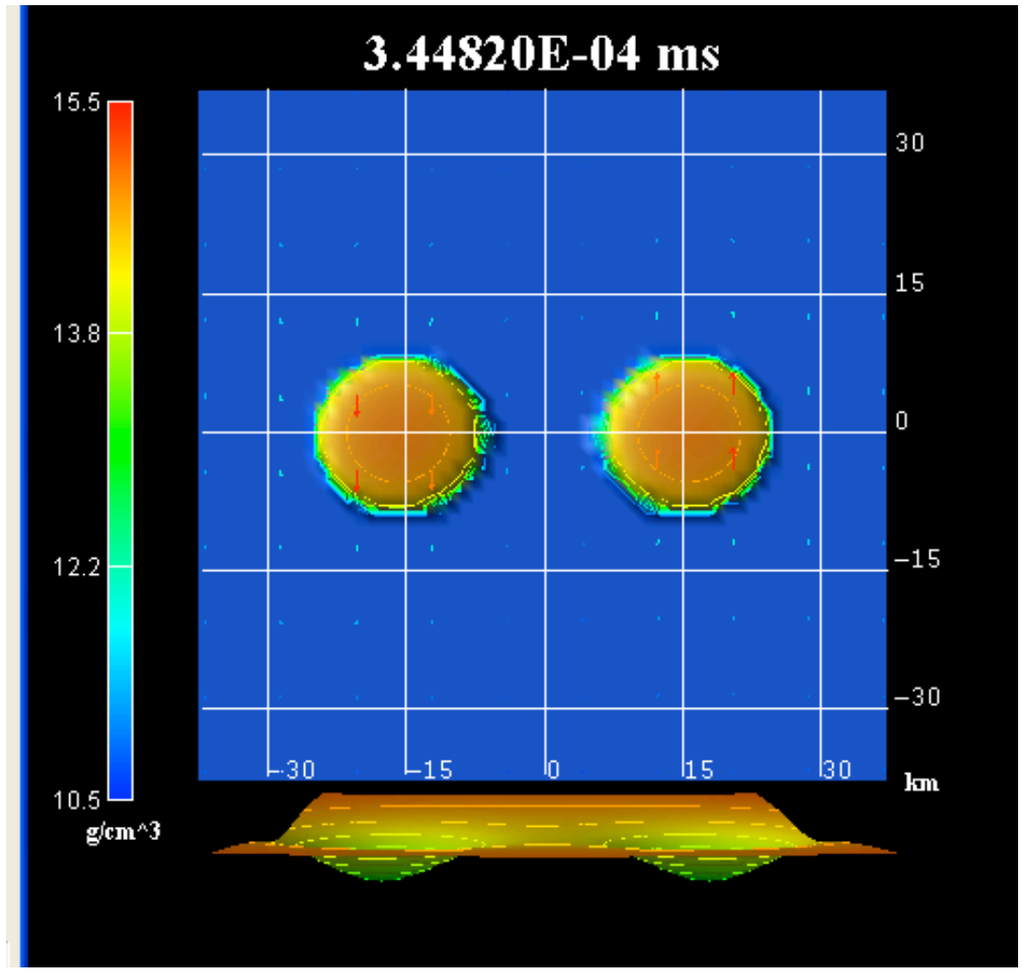

Case $1.35M_{sun}$ - $1.35M_{sun}$

Delayed formation of a rotating black hole

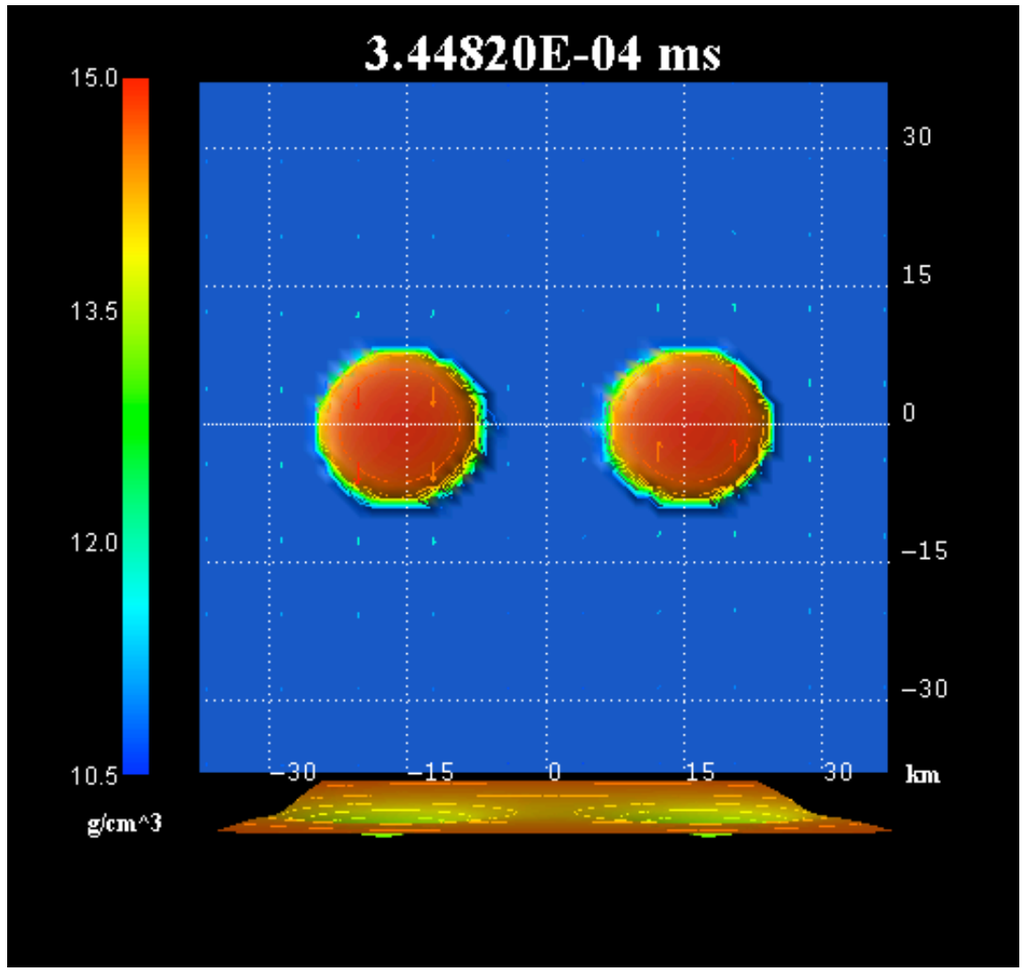

The gravitational waveform allows to unveil the final outcome: neutron star or black hole.

BNS merger → HMNS → BH+torus

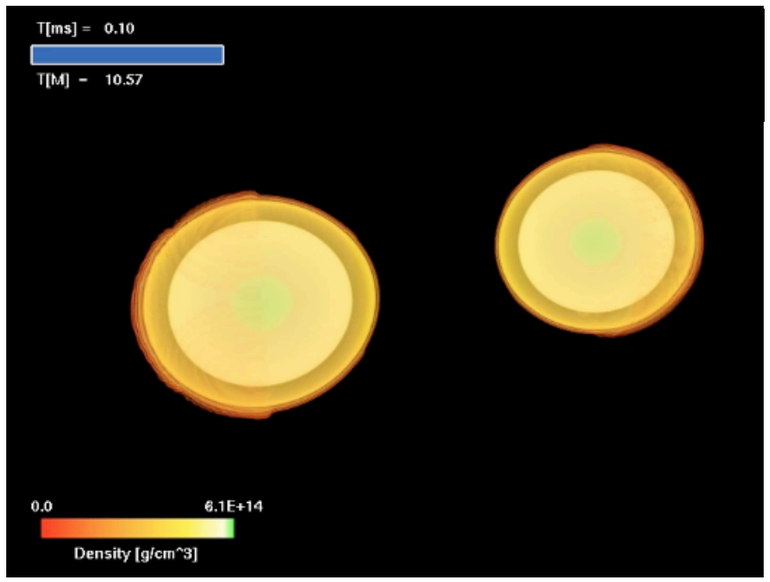

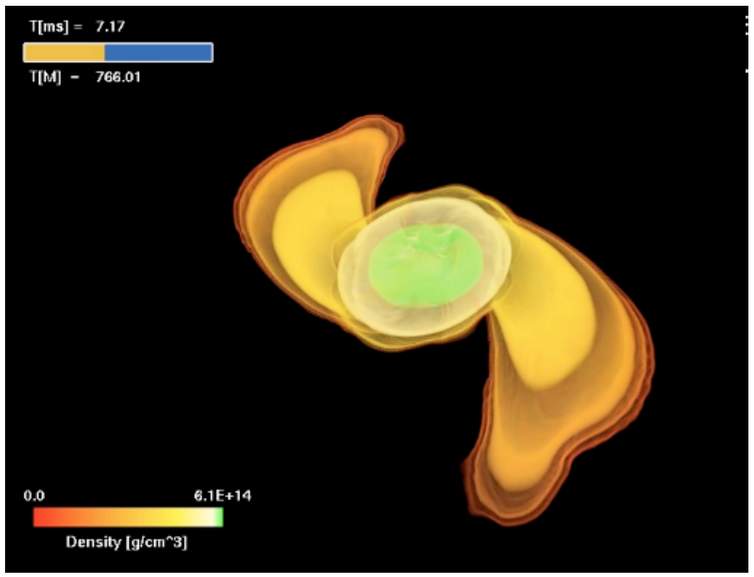

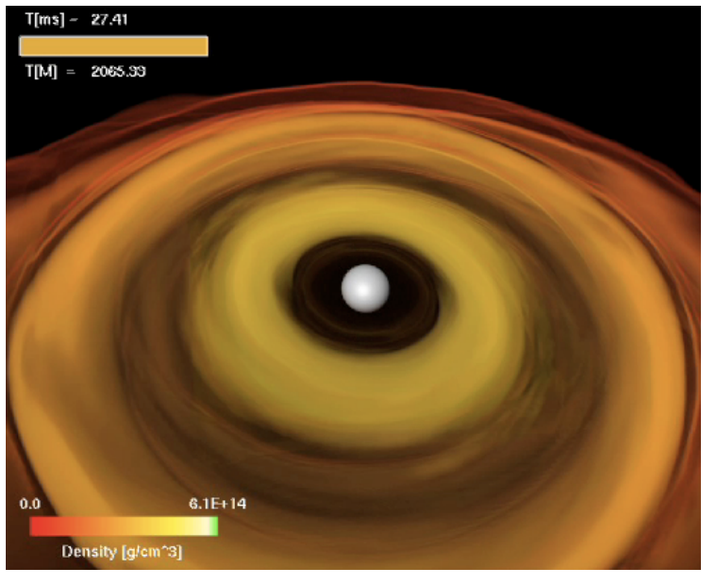

Credit: AEI

Variations on this **general trend** are produced by:

- differences in the mass for the same EOS:

a binary with smaller mass will produce a HMNS which is further away from the stability threshold and will collapse at a later time

- differences in the EOS for the same mass:

a binary with an EOS allowing for a larger thermal internal energy (ie hotter after merger) will have an increased pressure support and will collapse at a later time

Equal-mass BNS merger

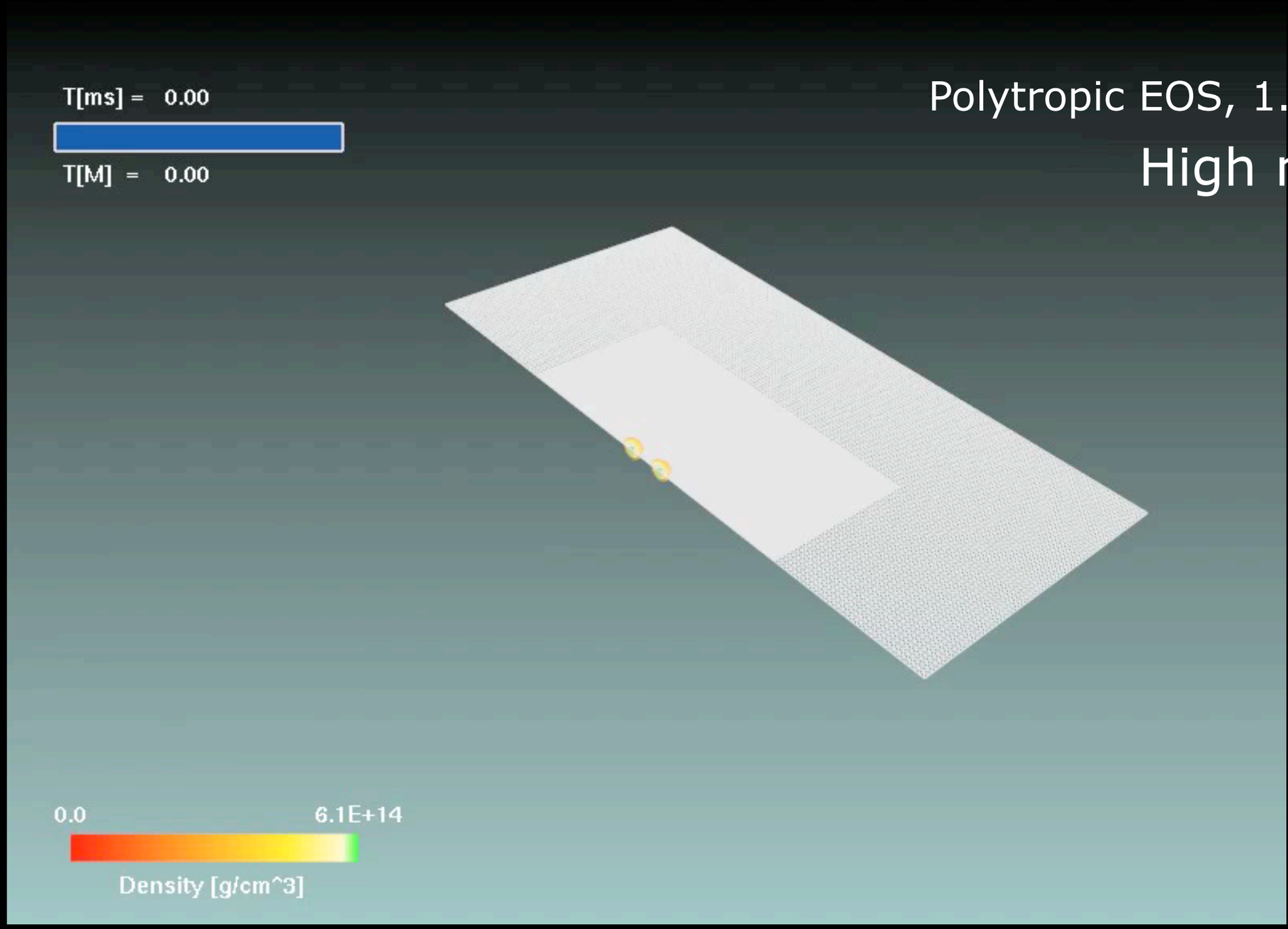

A hot, low-density torus is produced orbiting around the BH.
This is what is expected in short GRBs.

(Baiotti et al 2008)

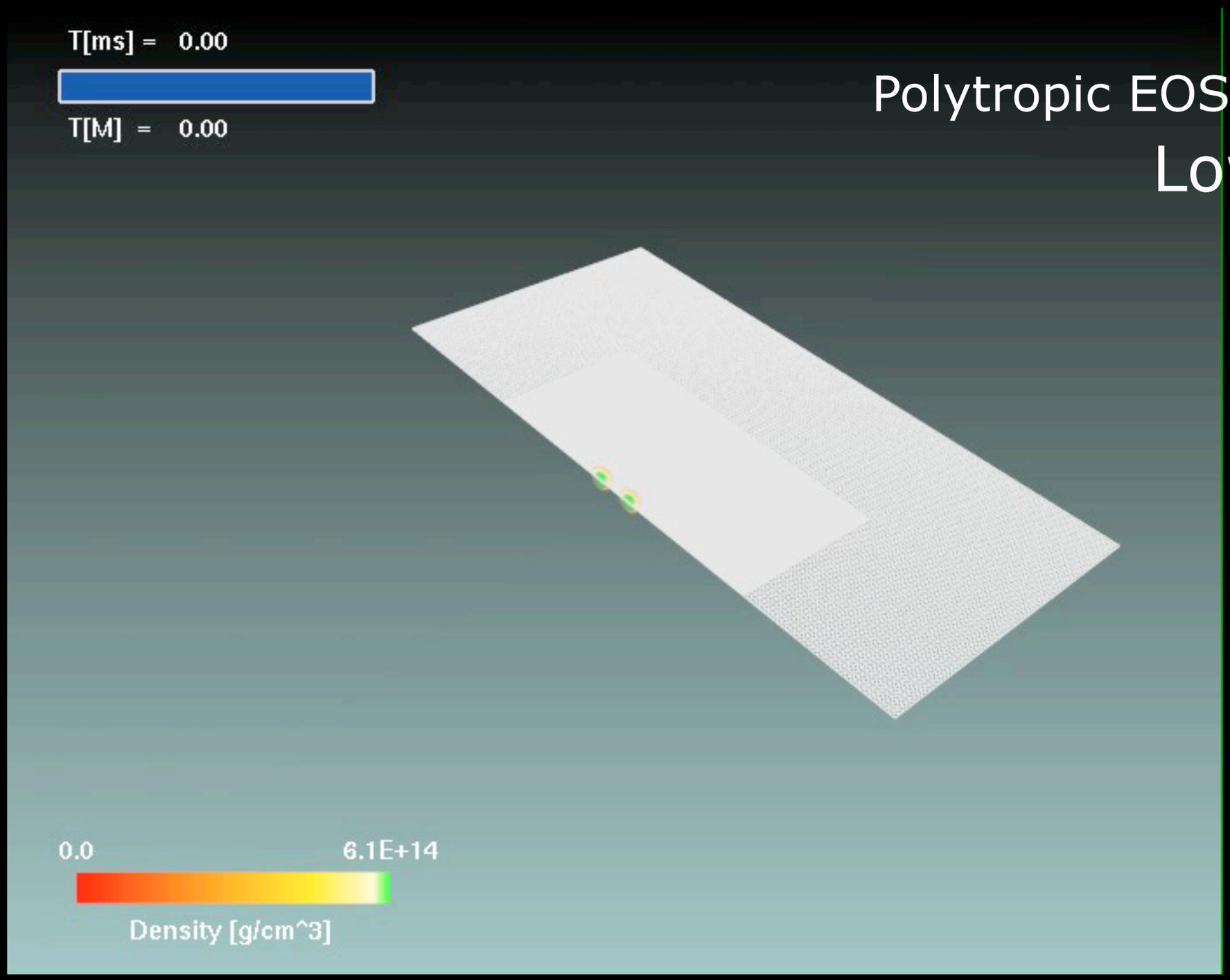

Polytropic EOS, 1.4 M_{sun}
Low mass

The HMNS is far from the instability threshold and survives for a longer time while losing energy and angular momentum.

After ~ 25 ms the HMNS has lost sufficient angular momentum and will collapse to a BH.

(Baiotti et al 2008)

Gravitational radiation from *the* merger

Dynamics

Signal amplitude

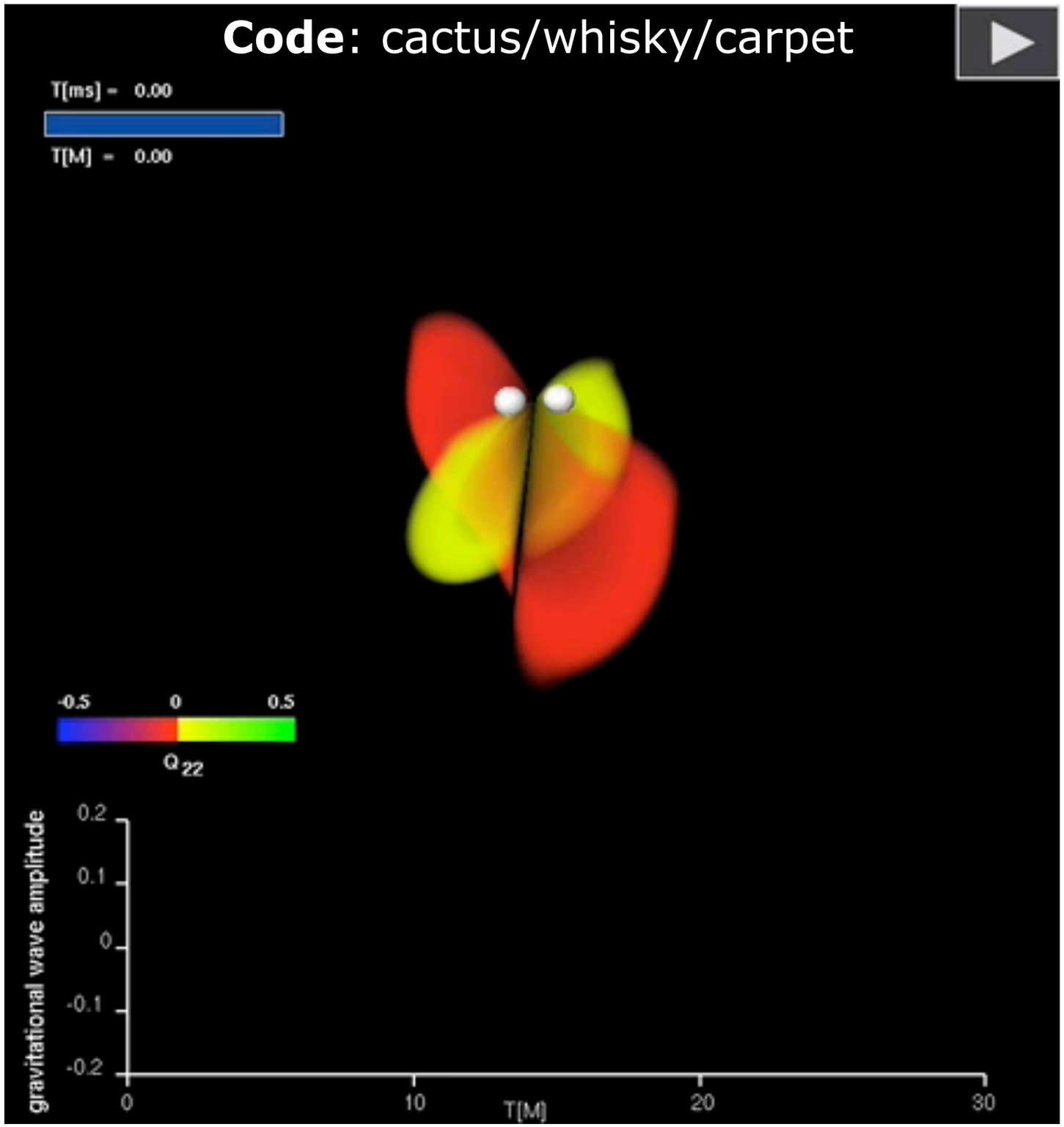

(AEI)

Waveforms: strong dependence on total mass

(Baiotti et al 2008)

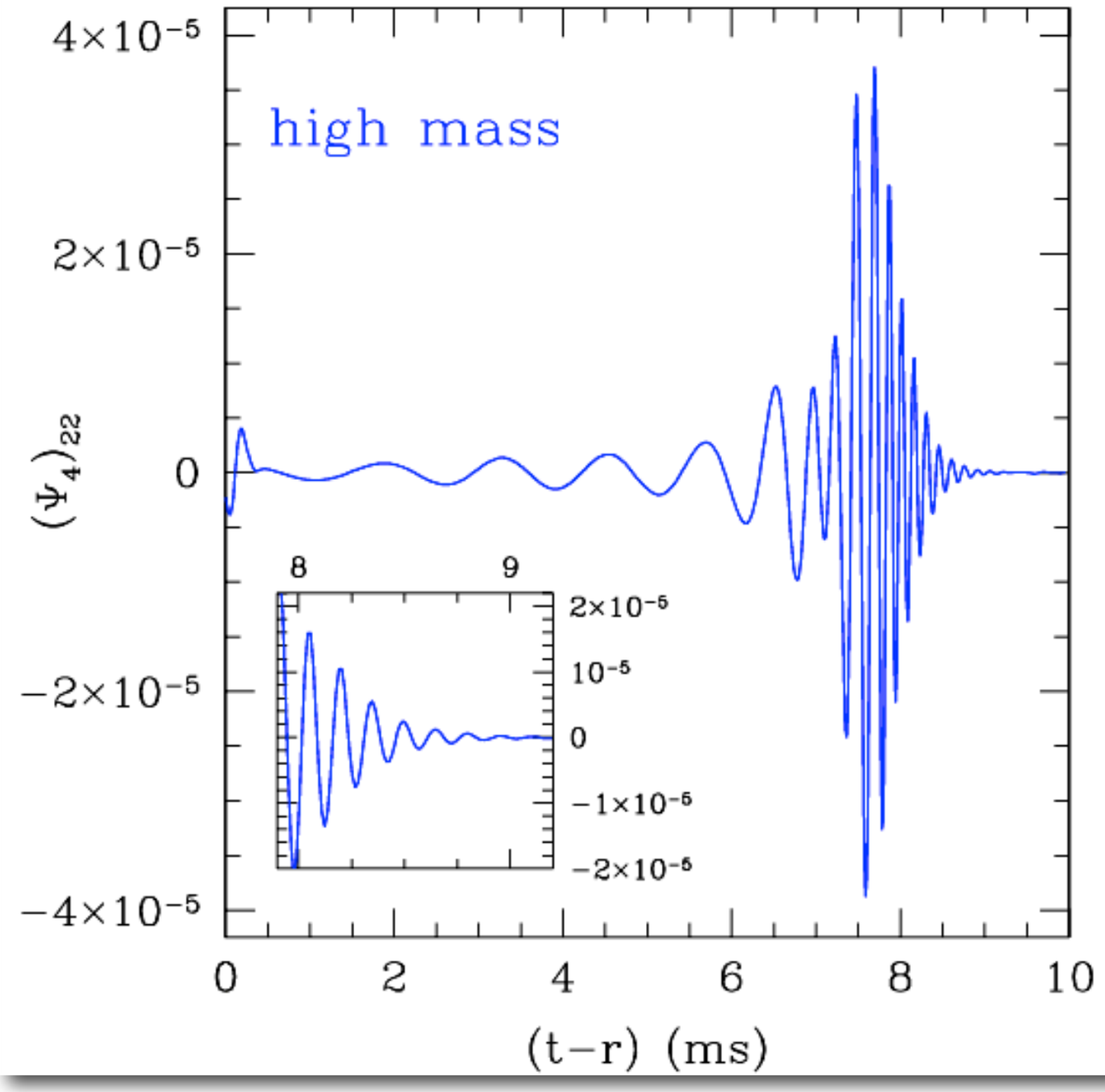

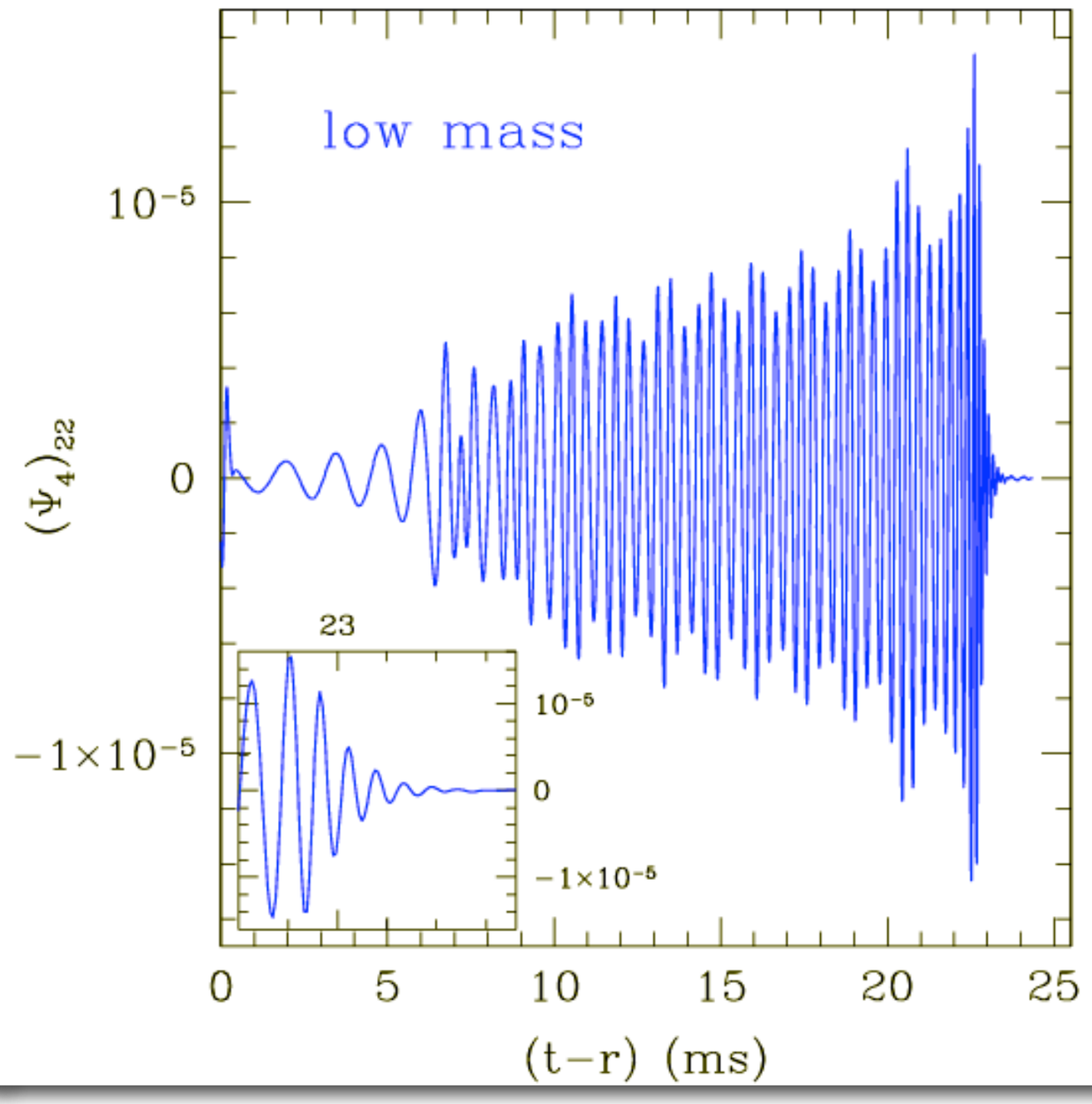

Small variations in the total mass of the initial models yield important differences in the gravitational waveforms

Increasing realism of simulations thermal conditions of BNSs

Late inspiral phase: neutron stars are **cold.**
Neutron stars with age > 10^7 years have undergone long-term cooling by neutrinos and photons.

$$\mathrm{T} < 10^5\,\mathrm{K} \sim 10\,\mathrm{eV} \ll E_\mathrm{F} \sim 100\,\mathrm{MeV}$$

Hence, neutron stars can be modelled by cold EOS.
Problem: such EOS is still unknown; need for a systematic survey.

Merger phase: neutron stars are **hot.** Shock heating increases temperature to about $\mathrm{kT} \sim 0.1 - 0.2\,E_\mathrm{F} \sim 10\,\mathrm{MeV}$

New effects likely to play important dynamical role: finite temperature effects, lepton fraction, neutrino thermal pressure, neutrino cooling.
Neutron stars modelled by thermal EOS.
Problem: systematic survey as well; few EOS available, more needed.

Dependence on the nuclear EOS

$$P(\rho,\varepsilon) = P_{\rm cold}(\rho) + P_{\rm th}(\rho,\varepsilon)$$

Piecewise-polytropic EOS for the cold part (Read et al 2009)

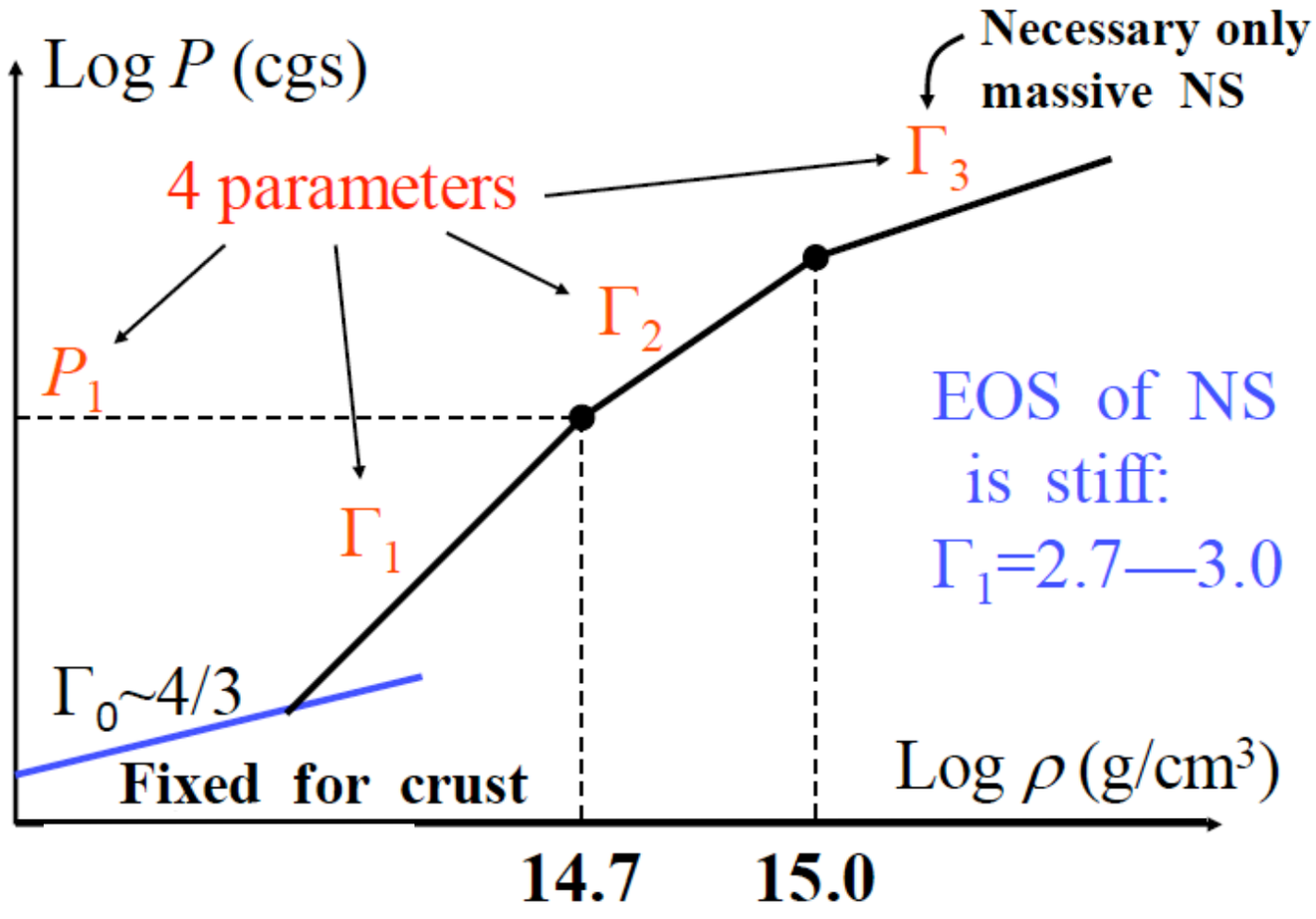

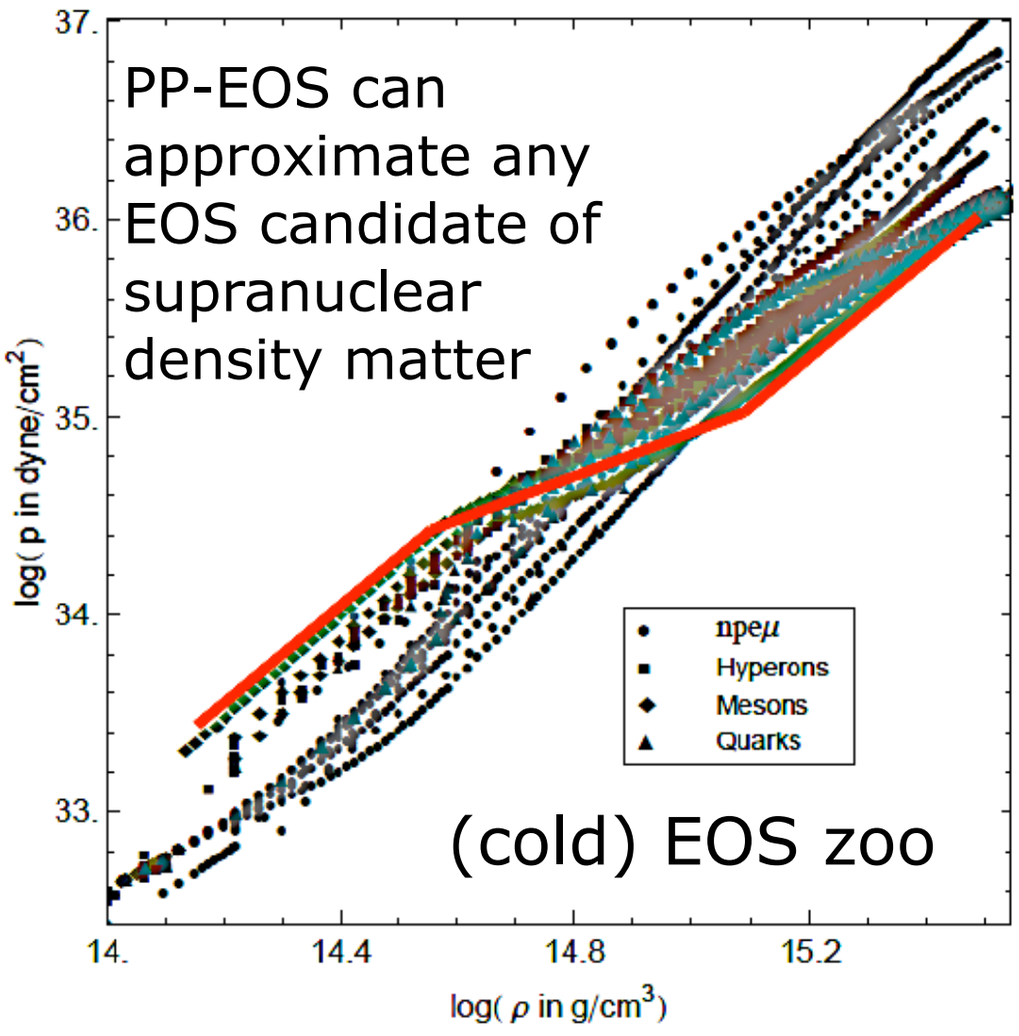

Thermal part of the pressure (shock heating) for hot, merged NS (T~10MeV) given by

$$P_{\rm th} = (\Gamma_{\rm th} - 1)(\varepsilon - \varepsilon_{\rm cold})\rho, \quad \Gamma_{\rm th} = 1.357 - 1.8$$

Type of final remnant depending on the nuclear EOS

Hotokezaka et al (2011)

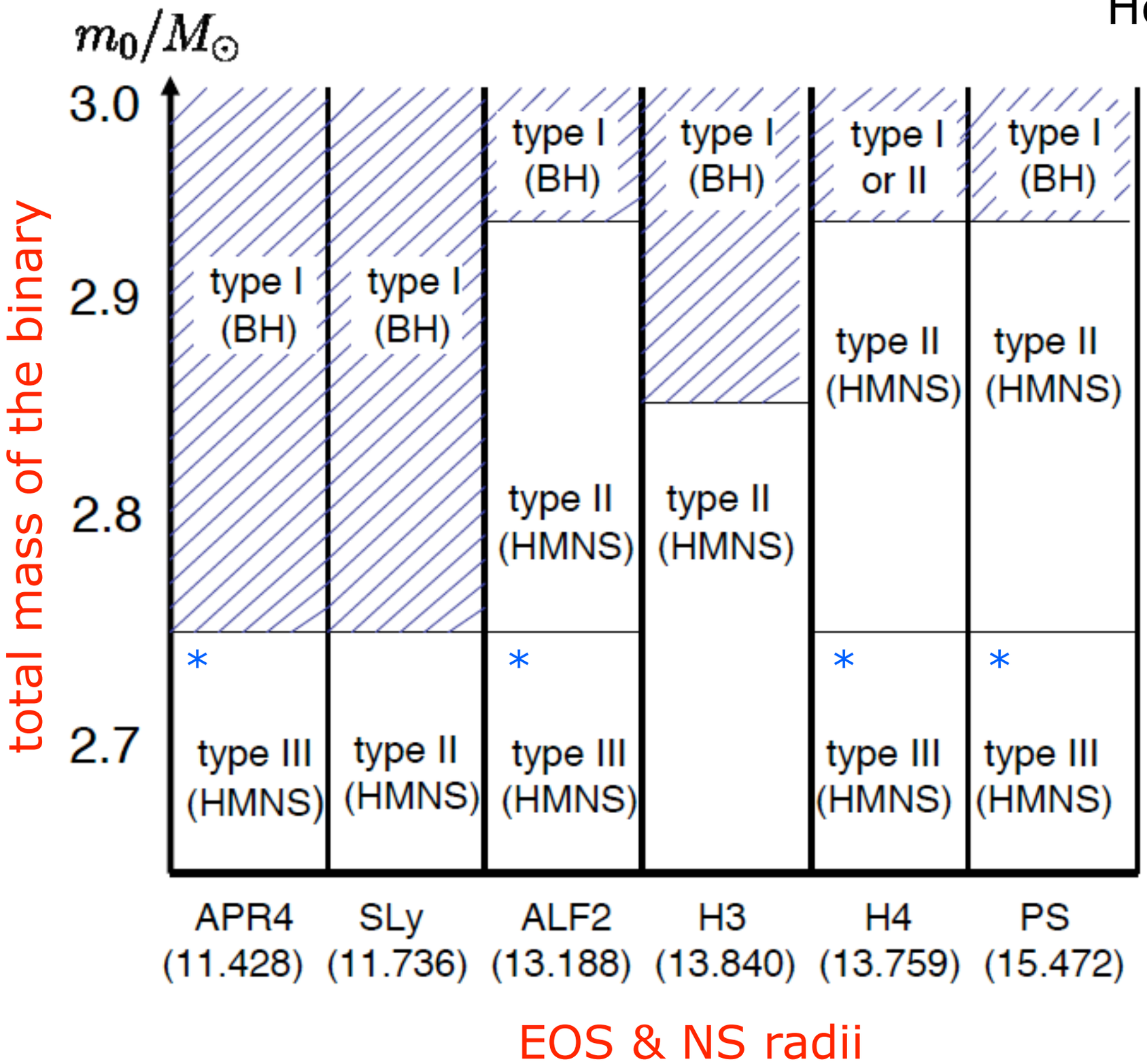

Type I: prompt collapse to BH

Type II: short-lived HMNS (<5 ms)

Type III: long-lived HMNS (>5 ms)

* EOS with $M_{max}>2M_{sun}$

Demorest et al (2010): discovery of NS with $M=1.97\pm0.04\ M_{sun}$

GW emission depending on the nuclear EOS

Qualitative form of high-frequency components of GW signal primarily determined by type of remnant formed.

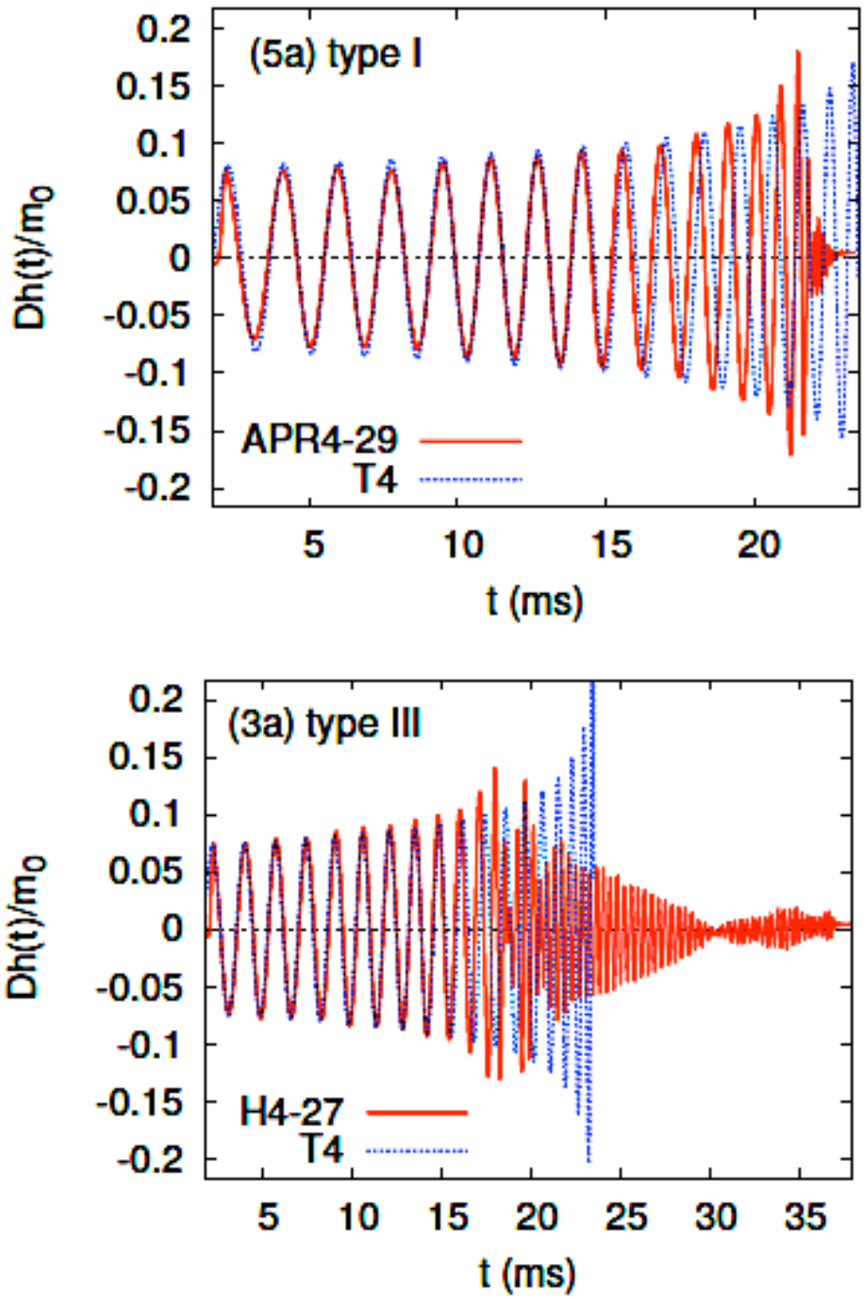

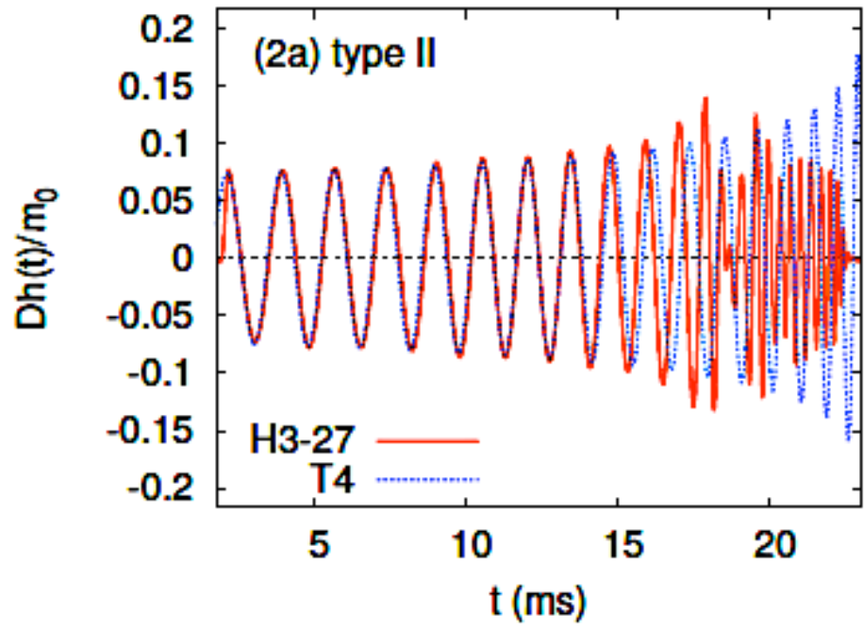

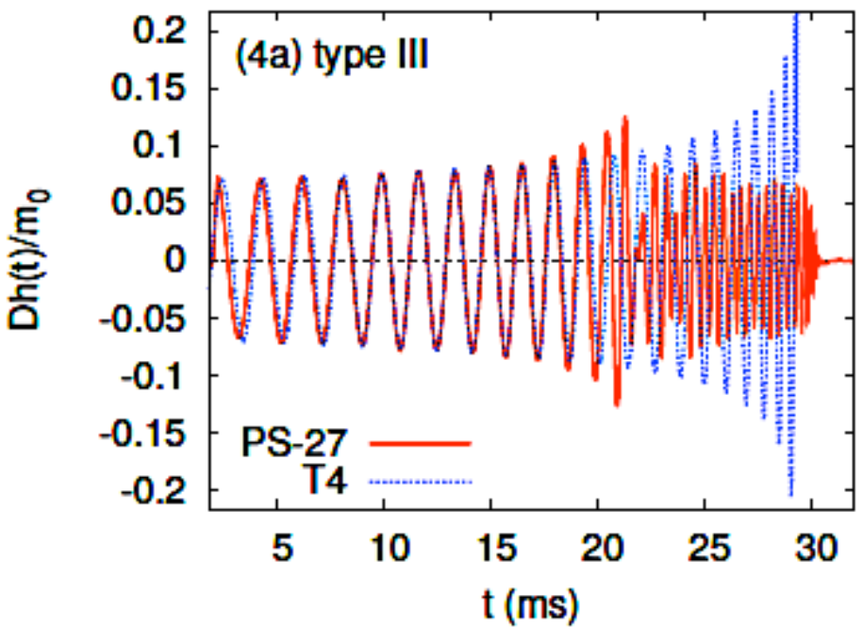

Red: Numerical Relativity

Blue: enhanced Post-Newtonian

Hotokezaka et al (2011)

Fourier spectrum (h_{eff} @ 100 Mpc)

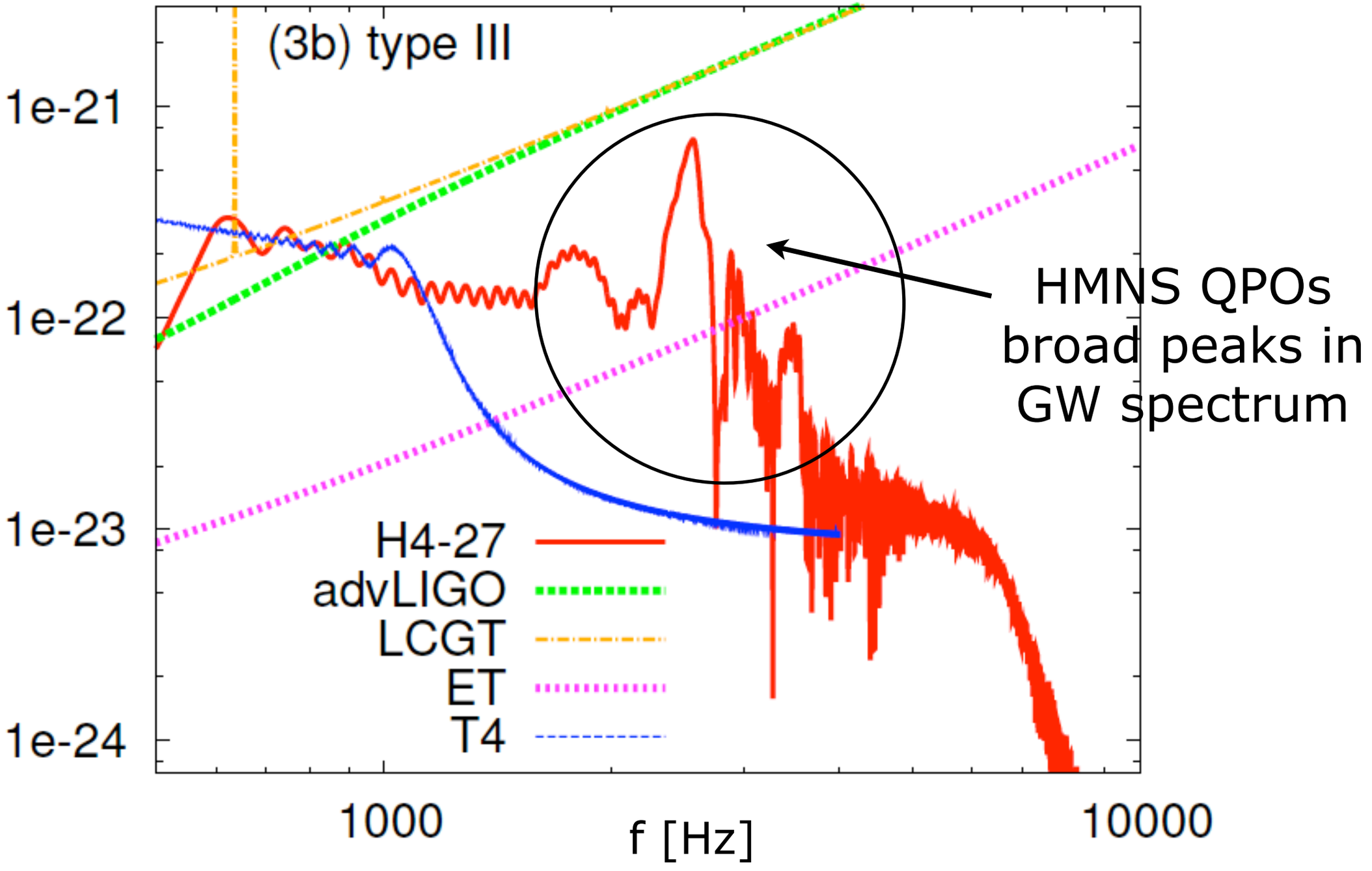

2-4 kHz peaks in spectrum detectable by 3rd generation detectors (ET) or advLIGO if source closer (20 Mpc)

Hotokezaka et al (2011)

Inspiral part of the signal

Read et al. (2013): systematic investigation of inspiral using extended set of EOS and multiple-group multiple-code collaborative effort to generate waveforms. Goal: improving data-analysis estimates of the measurability of matter effects in BNSs.

With a single source at a distance of ~100 Mpc, the NS radius or the dimensionless **quadrupole tidal deformability could be constrained to about 10%.**

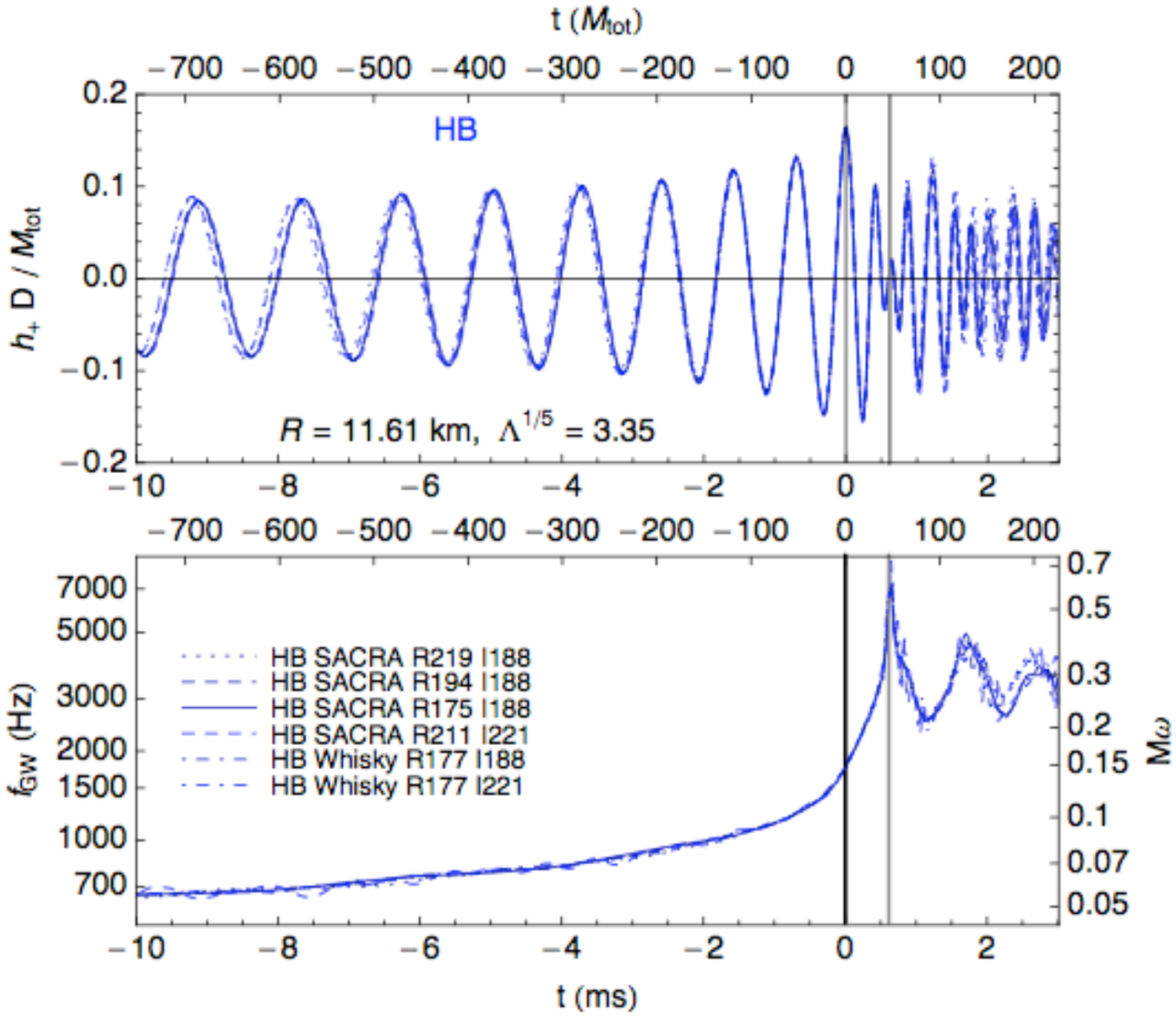

$$\Lambda = \frac{2}{3} k_2 \left(\frac{R}{M}\right)^5$$

k_2 quadrupole Love number

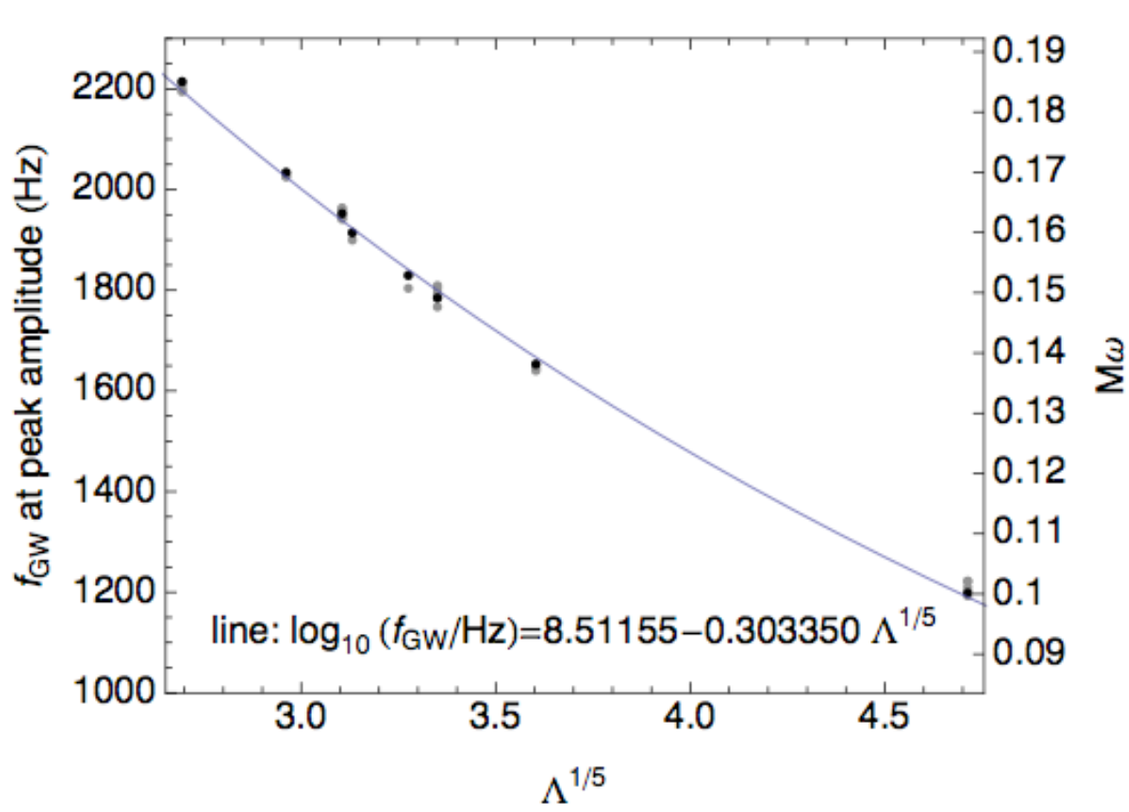

universal relation between frequency of merger and tidal deformability

Work of Read et al (2013) only valid for equal-mass binaries.

Bernuzzi et al (2014) proposed the use of the tidal polarizability parameter as a better choice of parameter to be related to the EOS, as it is also valid for unequal-mass binaries.

Hotokezaka et al (2016) extended results of Read et al (2013) adding more EOS to sample, better ID (less eccentric), longer inspirals, and lower frequencies (down to ~30 Hz) where aLIGO is more sensitive: **tidal deformability can be determined to about 10% accuracy for source up to 200 Mpc.**

Most of recent research on the inspiral phase is currently carried out with **post-Newtonian** expansions of the Einstein equations (Blanchet 2006; Poisson & Will 2014), coupled to results of NR simulations (use of **Taylor approximants**).

Another promising method based on an analytical approximation is the **Effective-One-Body (EOB)** formalism (Buonanno & Damour 1999).

The high nonlinearity of the Einstein equations makes it impossible to have satisfactory analytic approximations during the most nonlinear phases of the merger, but the **inspiral part can be very well approximated with EOB even up to very close before the merger** (Bernuzzi et al 2015, Hotokezaka et al 2016; Hinderer et al 2016).

Nonaxisymmetric oscillation modes in HMNS

Excitation of nonaxisymmetric modes in the post-merger phase of BNS mergers. Dominant m= 2 mode forms a **triplet** with two nonlinear components that are the result of coupling to the quasiradial mode. A corresponding triplet of frequencies is identified in the GW spectrum.

Identification of a **specific strong frequency peak** in the GW spectrum: difference between the m= 2 mode and the quasi-radial mode.

Once such observations become available, both the m=2 and quasiradial mode frequencies could be extracted, allowing for the application of GW asteroseismology to the post-merger remnant and leading to tight **constraints on the EOS**.

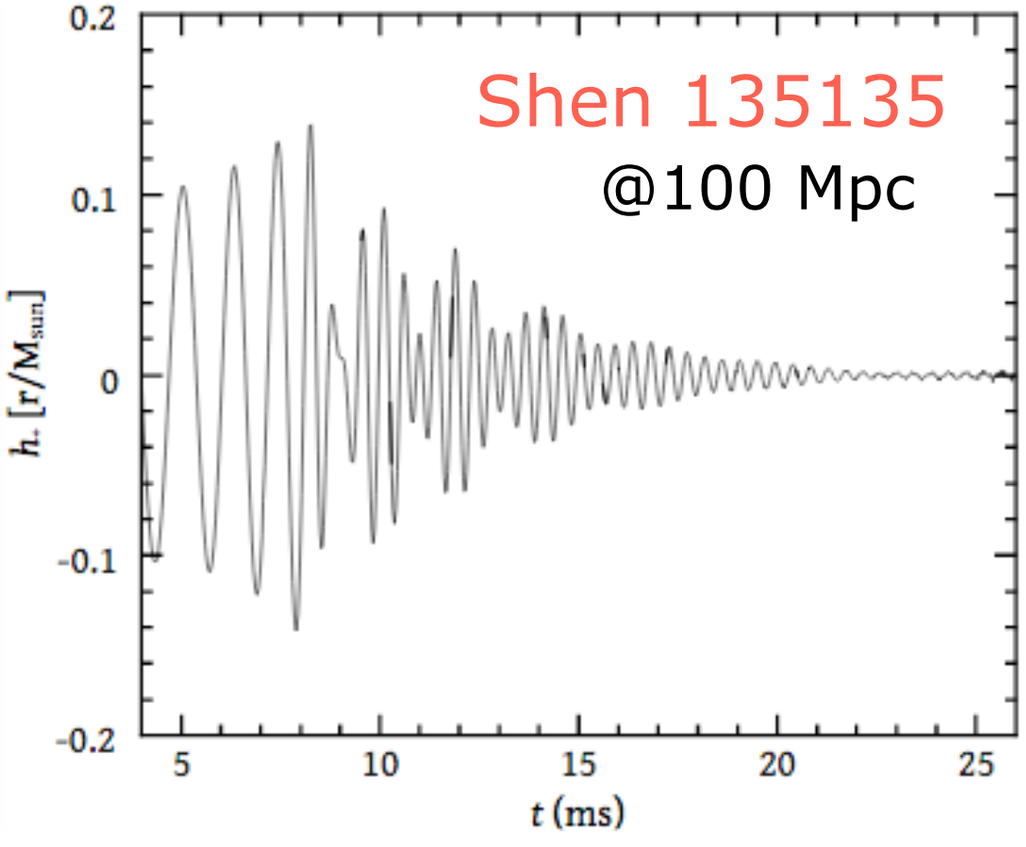

Stergioulas et al (2011)

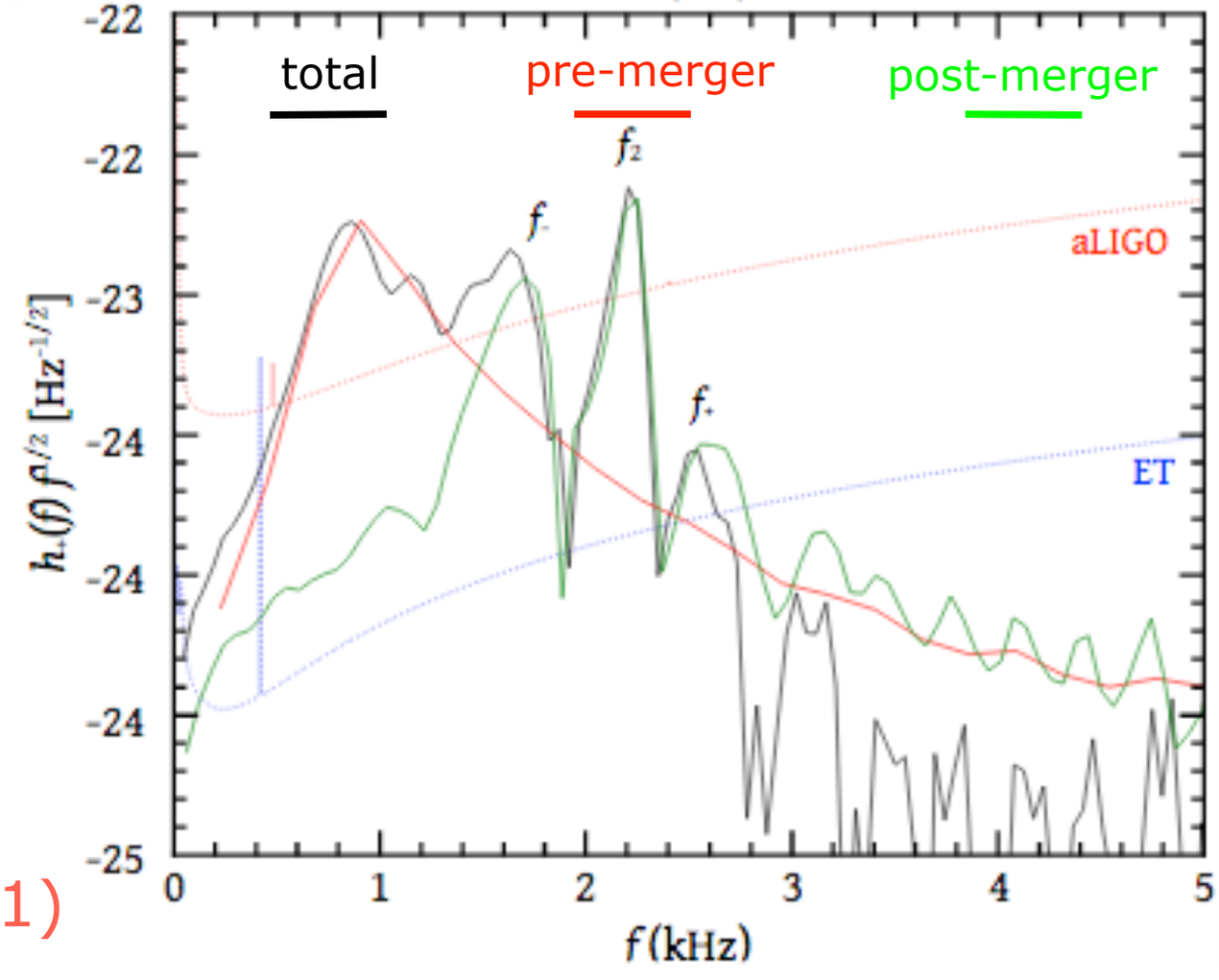

Constraining the EOS from HMNS oscillations

Bauswein et al (2014)

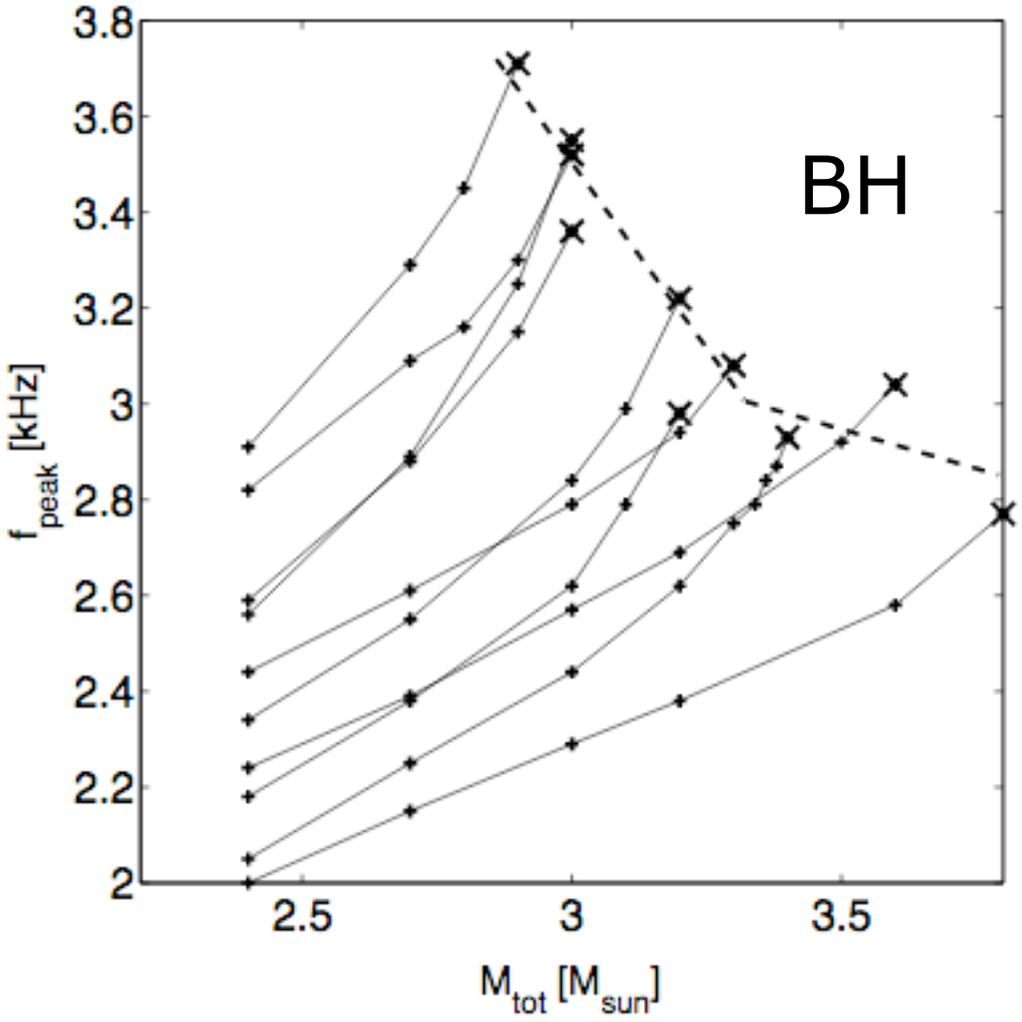

$f_{\rm peak}$ (quadrupolar m=2 HMNS fluid mode) vs M_{tot} for all EOS

x $f_{\rm peak}^{\rm thres}$ highest frequency beyond which no stable HMNS exists

Idea: two measurements of f_{peak} at slightly different masses yield slope that can be used for an extrapolation along corresponding EOS solid line.

$$\frac{df_{\rm peak}(M_{\rm tot})}{dM_{\rm tot}}$$

Extrapolation gives estimates of the threshold mass for BH formation.

Bauswein et al (2013) showed that such threshold can be used to estimate **maximum mass** of cold, non-rotating NS.

The estimation of the threshold peak frequency constrains the **radius** of the maximum-mass configuration of non-rotating NS.

Combining this with the actual determination of the radius of NS from the **measured** GW peak frequencies allows for a clear distinction of a particular EOS among a set of candidates.

Interpretation of low frequency secondary peak(s)

- Bausswein & Stergioulas (2015)

Dominant f_{peak} frequency and two secondary peaks at lower frequencies (f_{2-0} and f_{spiral}) with comparable SNR.

f_{2-0} is a nonlinear combination frequency between quadrupolar f_{peak} oscillation and quasi-radial oscillation. Most likely due to the interaction of the double-core structure produced in early post-merger phase.

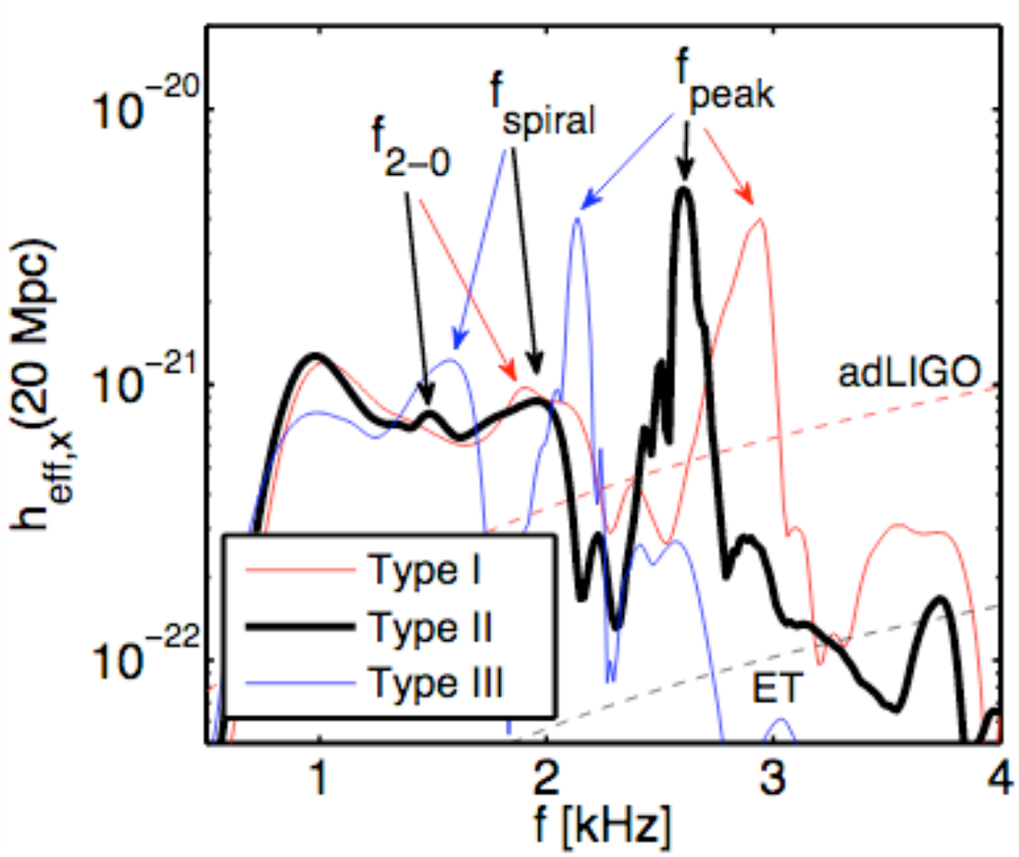

f_{spiral} produced by strong deformation initiated at time of merging, whose pattern rotates slower than the double-core structure of the inner remnant and lasts for a few rotational periods.

- Takami et al (2014, 2015)

Lower frequency single peak related to the merger process (first ~3ms after merger). Found universal correlation between frequency of this peak and average compactness of HMNS, for all EOS and masses.

Such correlation not found by Bauswein & Stergioulas (2015). Differences may be due to the stiffness of the EOS considered by each group and the corresponding maximum masses of non-rotating NSs.

Thermal EOS + hyperons - imprints on GWs

Weak interaction processes and neutrino cooling with GR leakage scheme. Shen EOS and thermal EOS including hyperons.

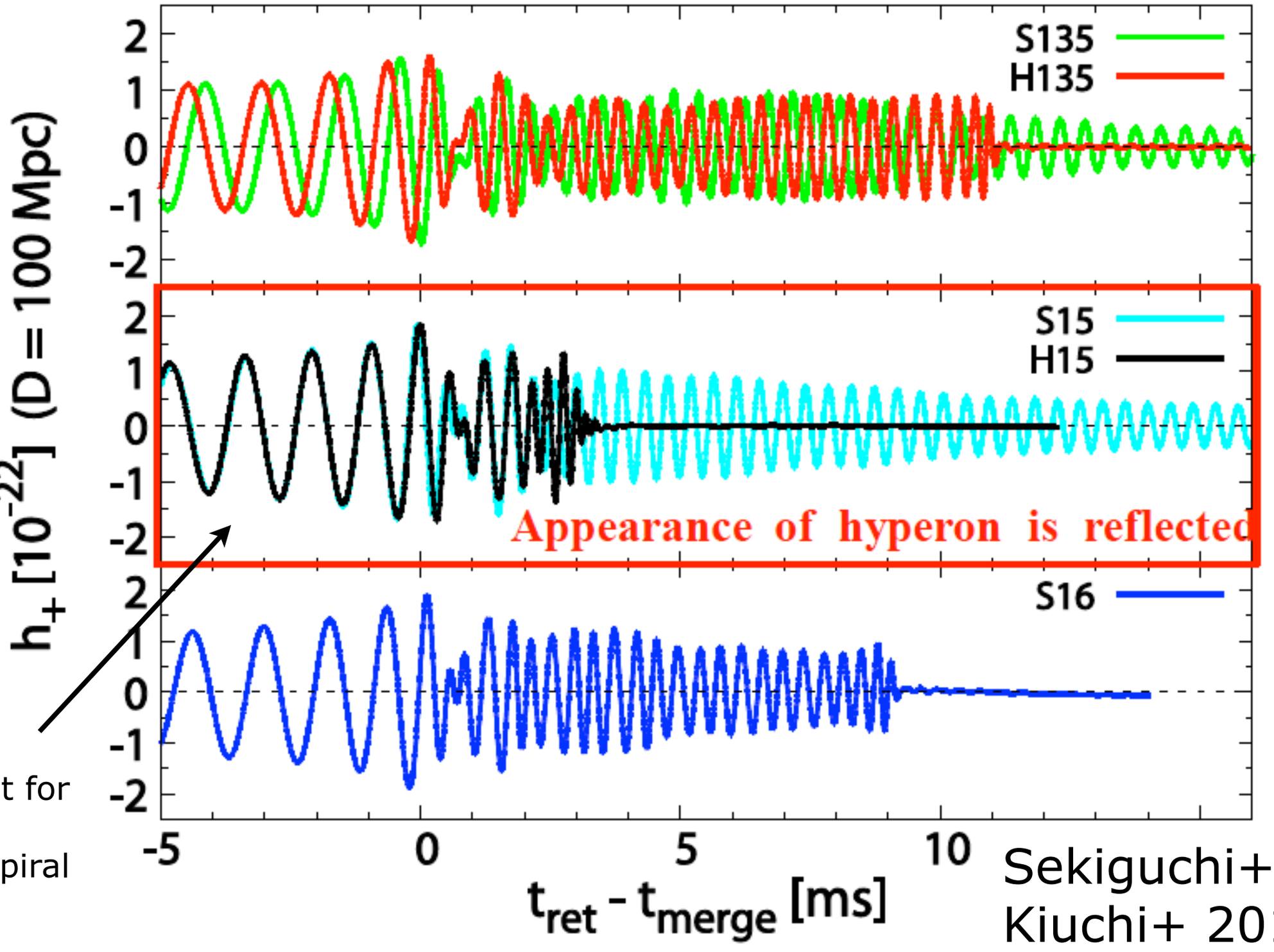

agreement for both EOS during inspiral

Sekiguchi+ 2011
Kiuchi+ 2012

Unequal-mass BNS merger

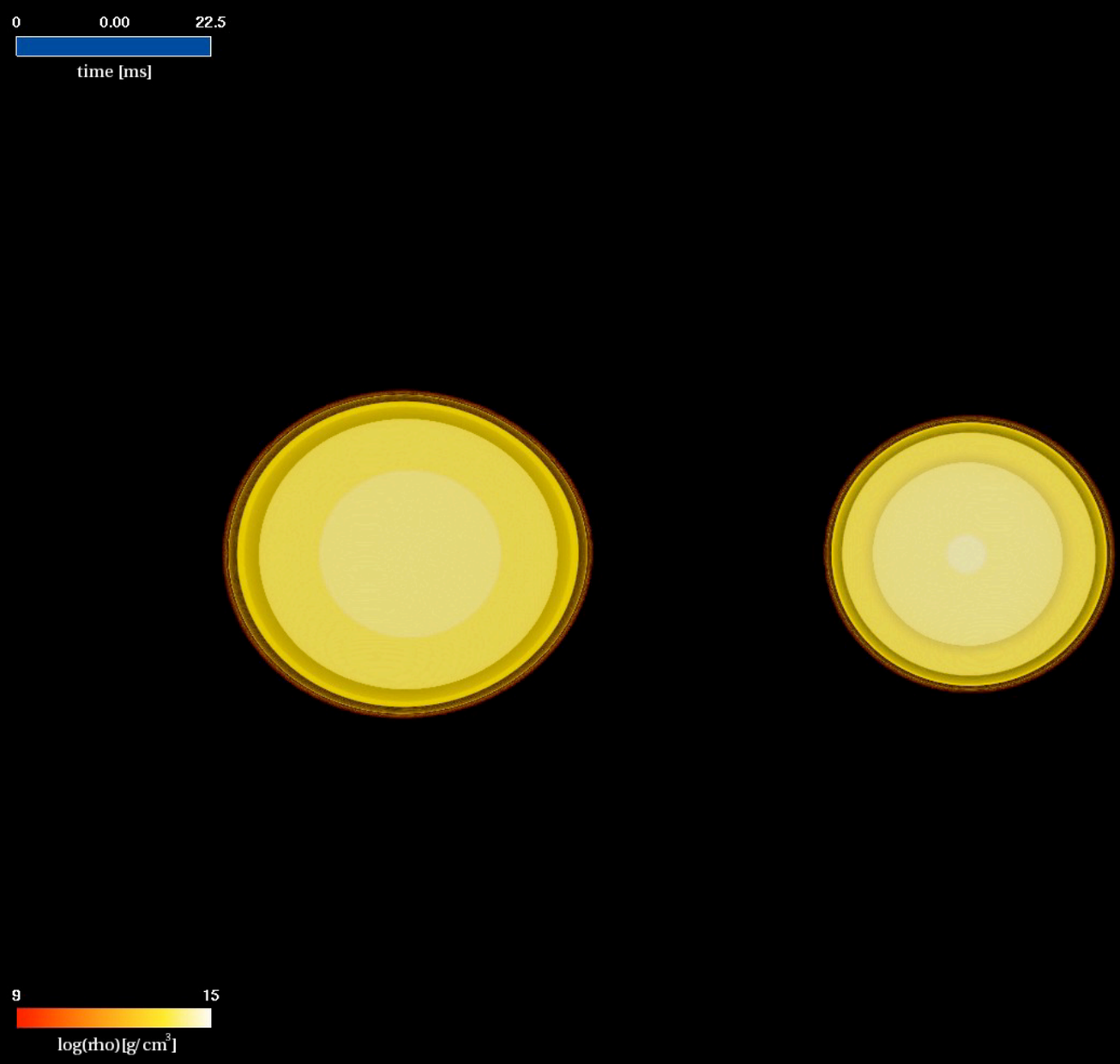

A significantly more massive torus is formed in this case.

(Rezzolla, Baiotti, Giacomazzo, Link & Font 2010)

Morphological differences (at end of simulation)

q=1.0 q=0.7

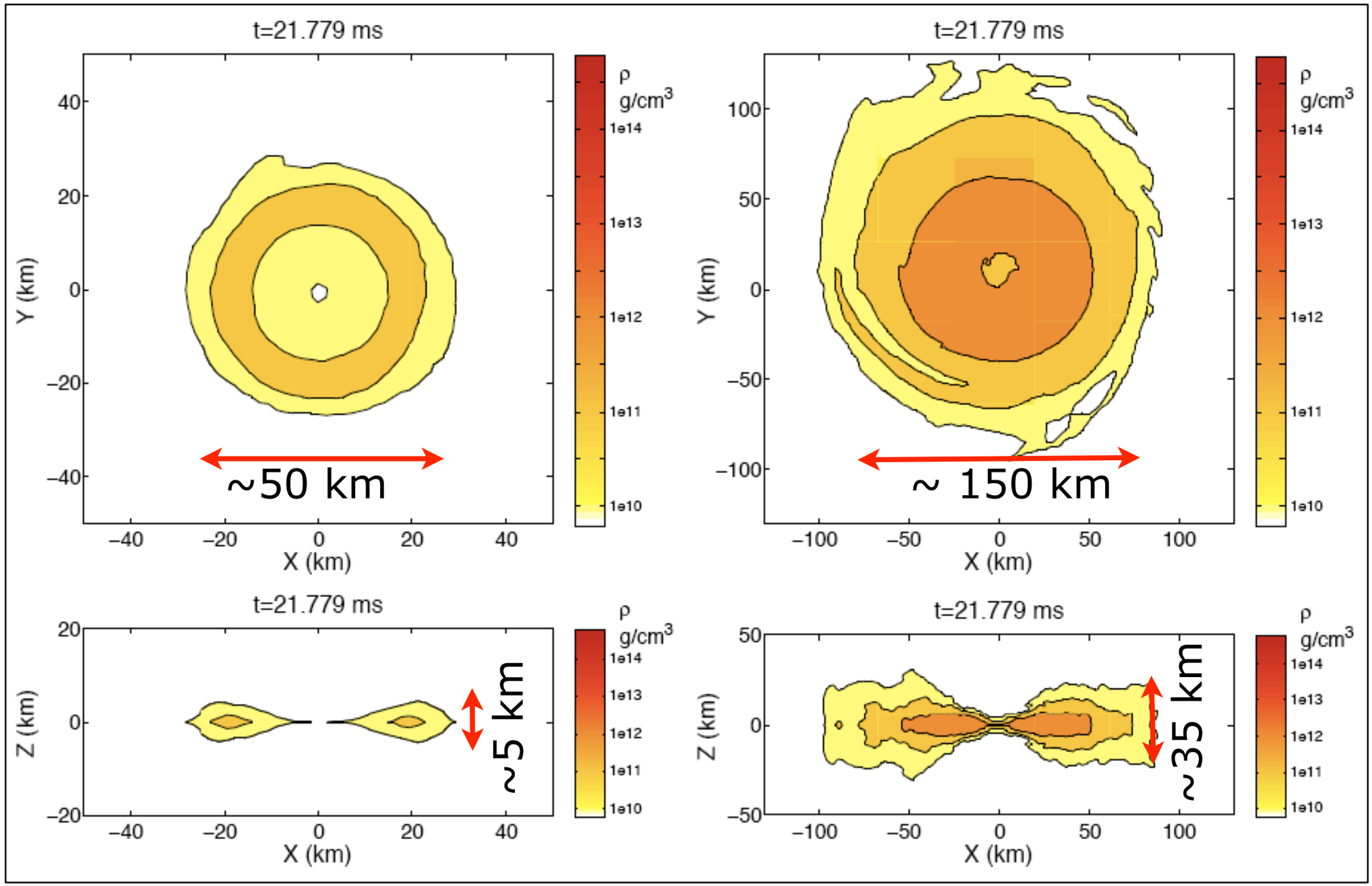

Symmetric. Thin disk. Axisymmetric shape. Thick disk.

Both tori differ in size by a factor ~3 and in mass by a factor ~200.

However, have comparable mean rest-mass densities.

Evolution of total rest mass

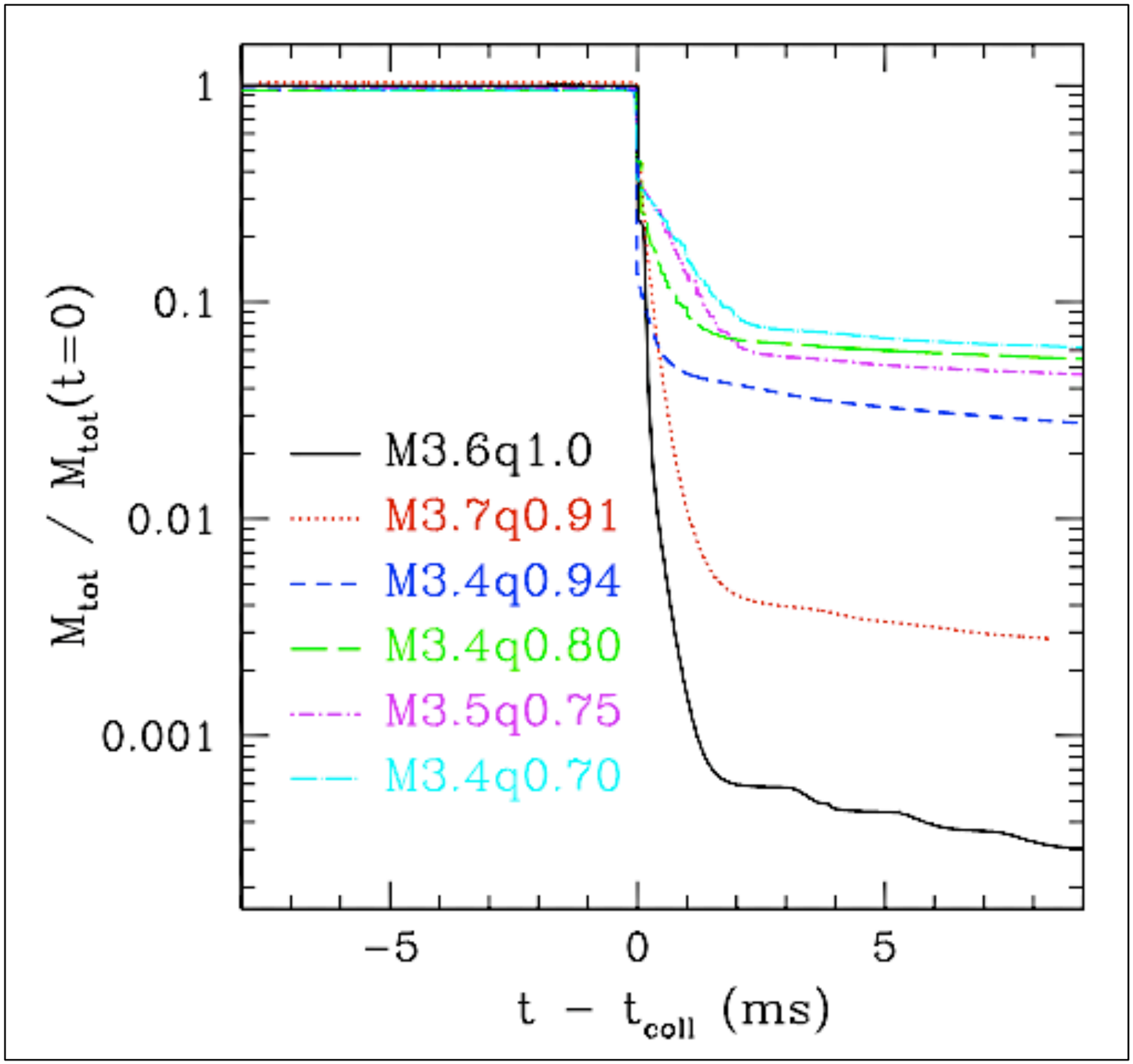

Curves shifted in time to coincide at collapse time.

Mass of resulting disk larger for smaller values of *q*.

Trend not entirely monotone; also influenced by initial total baryonic mass of binary.

Model
M3.6q1.00
M3.7q0.94
M3.4q0.91
M3.4q0.80
M3.5q0.75
M3.4q0.70

Further unequal-mass BNS simulations

- Dietrich et al (2015):

  4 nuclear physics piecewise-polytropic EOS, q=0.66-0.86
  q=0.66 largest mass ratio simulated in NR
  q=0.66 + stiff EOS yields high tidal deformation of secondary which leads to ~0.03M_{sun} of unbound matter. Likely to have a large impact on nucleosynthesis.
  Very large torus mass ~0.3M_{sun}

- Additional work by:

  - Lehner et al (2016) and Sekiguchi et al (2016): nuclear EOS and neutrino effects
  - Rezzolla & Takami (2016): spectrum of post-merger signal
  - Endrizzi et al (2016): magnetic field effects

Conclusion of all these works: **if mass difference is 10% or less, results are fairly similar to those of equal-mass simulations.**

Eccentric BNS mergers (dynamical captures)

Compact-object binaries form through close interaction of compact objects. There might be a significant population of compact-object binaries formed via **dynamical captures** in dense stellar environments like **globular clusters** (O'Leary et al 2009).

Born at small orbital separations and with **large eccentricities**. Hence, close orbital dynamics and GW signal may differ substantially from those of standard quasi-circular BNS systems.

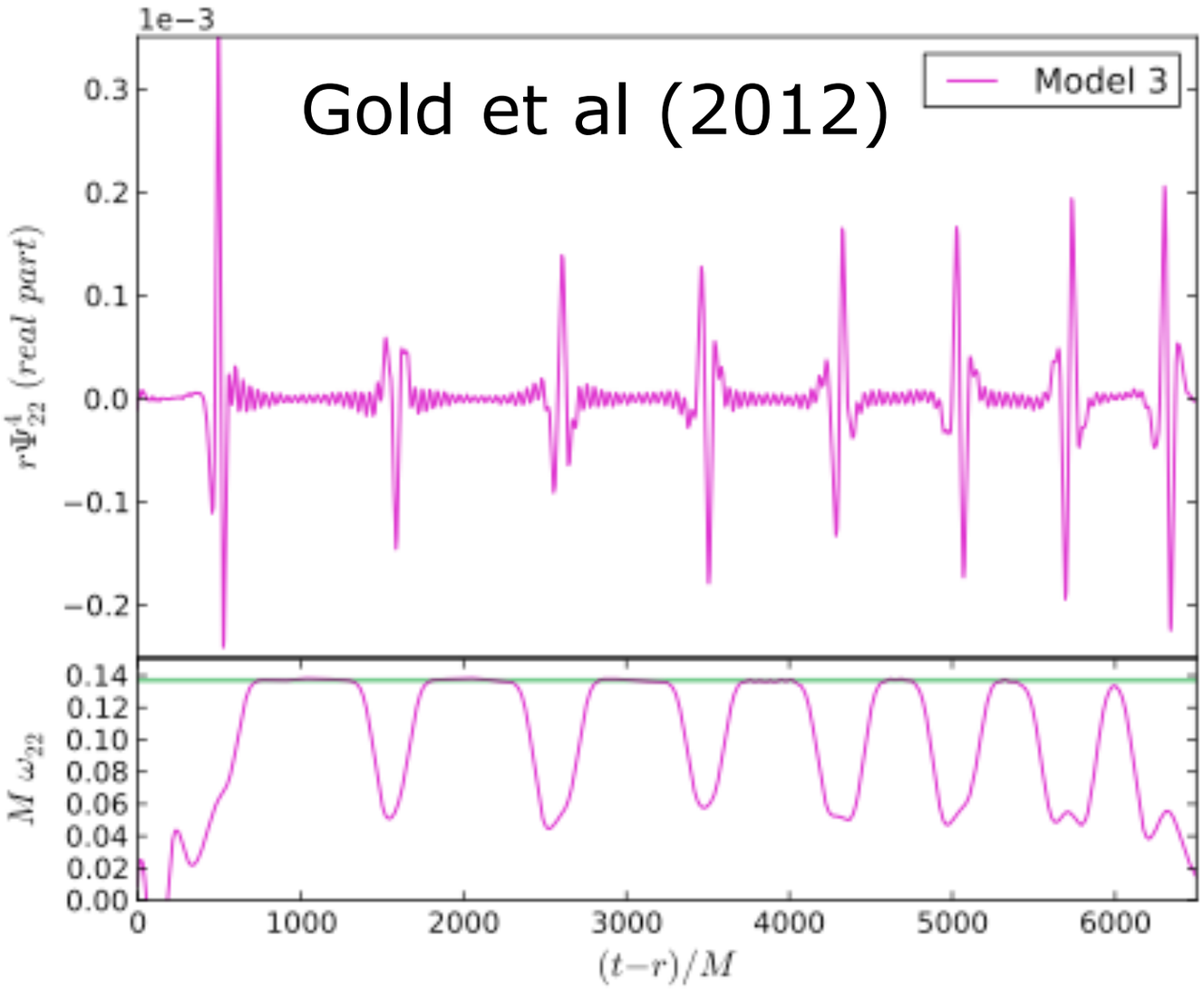

Initially, these systems produce at periastron a series of well-separated, **repeated GW bursts** that lasts from minutes to days. Signal gradually transforms into final inspiral chirp signal of an eccentric binary system.

Largest part of radiation emitted at periastron and at rather **high frequencies**, outside the best sensitivity range of advanced detectors.

Parabolic encounter simulations

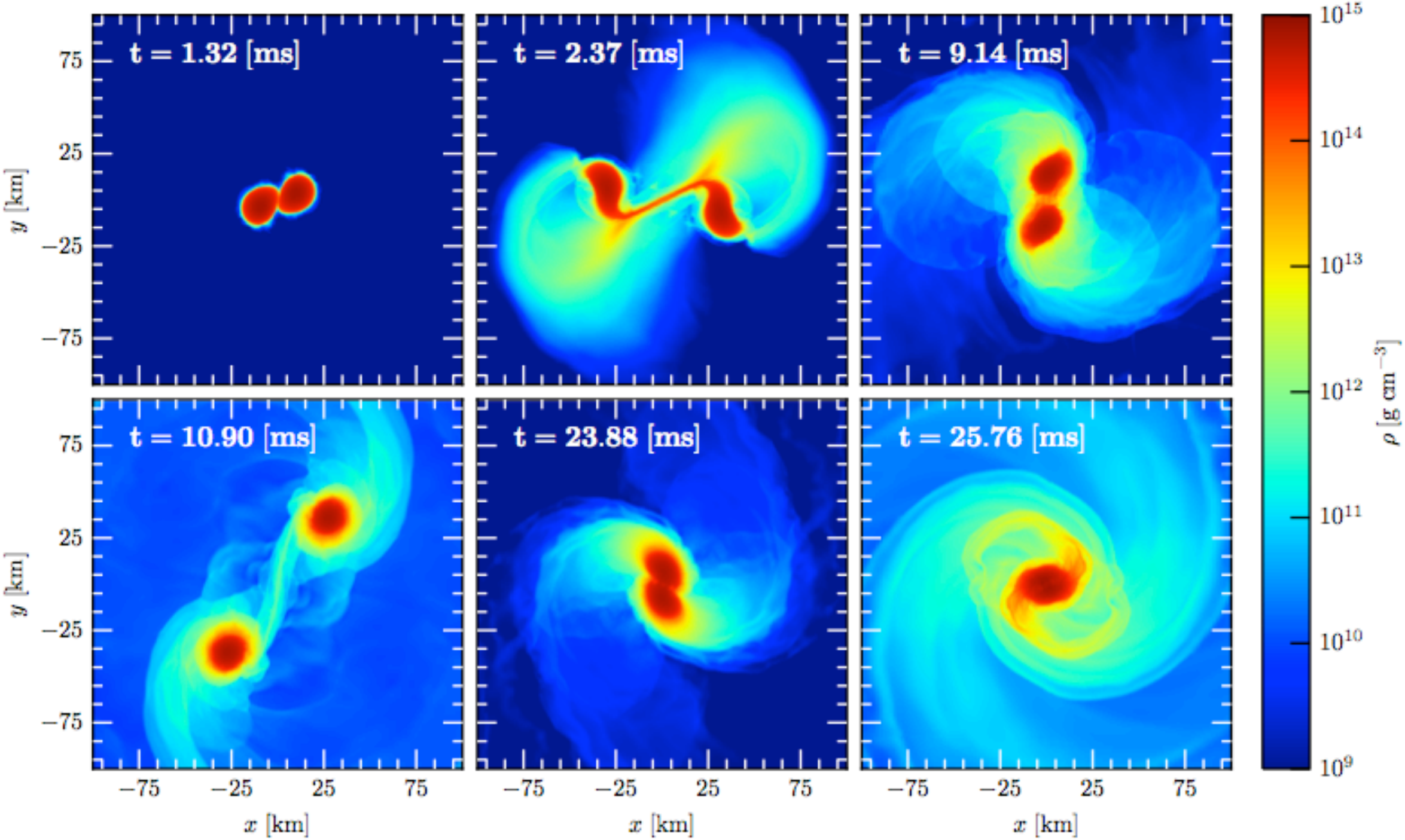

Radice et al (2016)

NS undergo 3 close encounters before merger. Tidal torques at periastron result in large mass ejection and trigger oscillation in NS.

Dynamical captures with NS spin

East et al (2016): Most NS in globular clusters have large **spins**. Even moderate spins can significantly **increase the amount of ejected material**, including the amount unbound with velocities greater than 0.5c leading to brighter electromagnetic signatures associated with kilonovae.

Resulting HMNS develops the **one-arm (m=1) spiral instability**. Imprint on GWs.

$$r_p/M = 8,\ a_{\rm NS,1} = a_{\rm NS,2} = 0.025$$

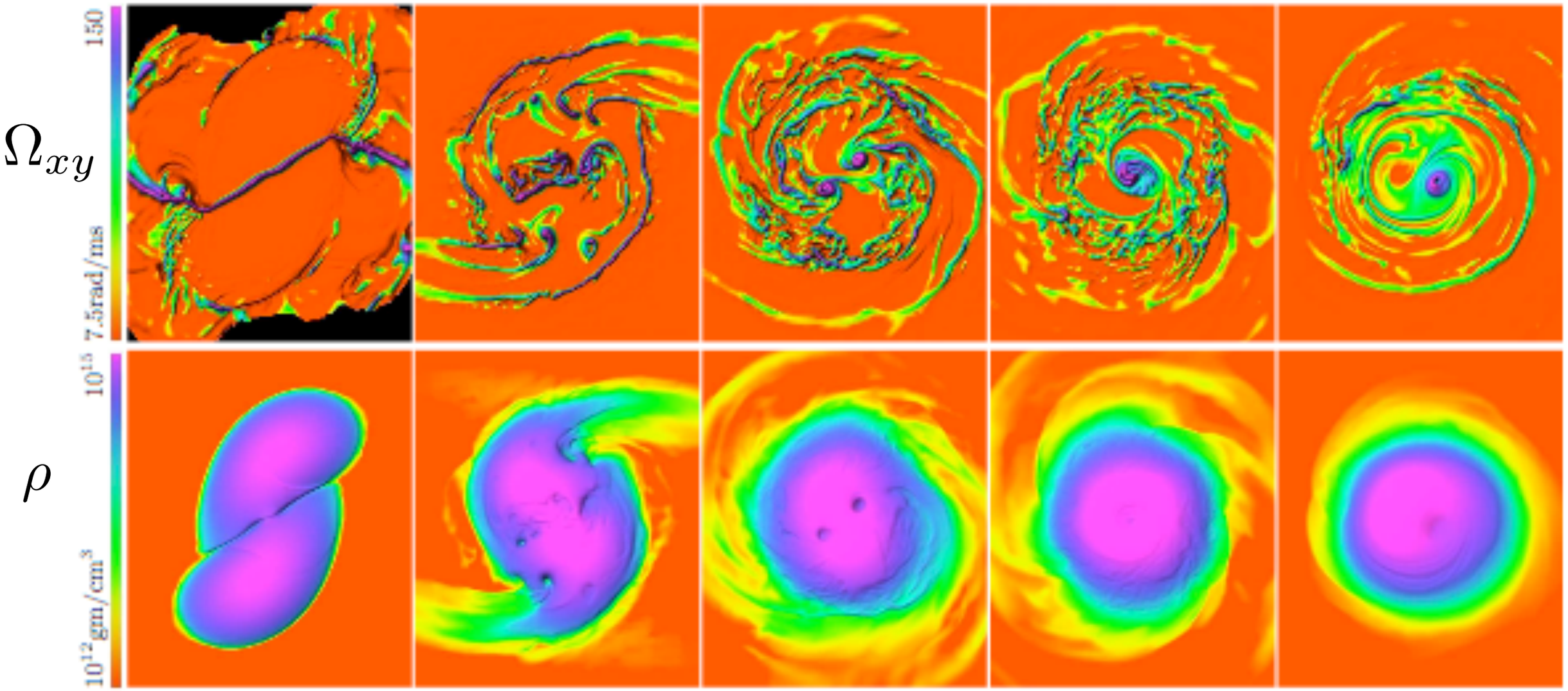

GRMHD BNS simulations

EOS choice in existing GRMHD simulations of BNS mergers:

- **Ideal fluid**

  Anderson et al (2008)

  Liu et al (2008)

  Giacomazzo et al (2009, 2011) (WhiskyMHD)

  Rezzolla et al (2011) (WhiskyMHD)

  Giacomazzo & Perna (2013) (WhiskyMHD)

  Giacomazzo et al (2015) (WhiskyMHD)

  Ruiz et al (2016) (Illinois MHD)

- **Piecewise-polytropic**

  Kiuchi et al (2014, 2015) (SACRA)

  Endrizzi et al (2016) (Einstein Toolkit + Whisky)

  Kawamura et al (2016) (Einstein Toolkit + Whisky)

- **Finite temperature (+ neutrinos)**

  Palenzuela et al (2015)

B-field amplification from KH instabilities

During merger a vortex sheet (shear interface) develops, where tangential component of velocity is discontinuous: unstable to perturbations. It can develop **Kelvin-Helmholtz instability** (KHI), which curls the interface forming a series of vortices at all wavelengths.

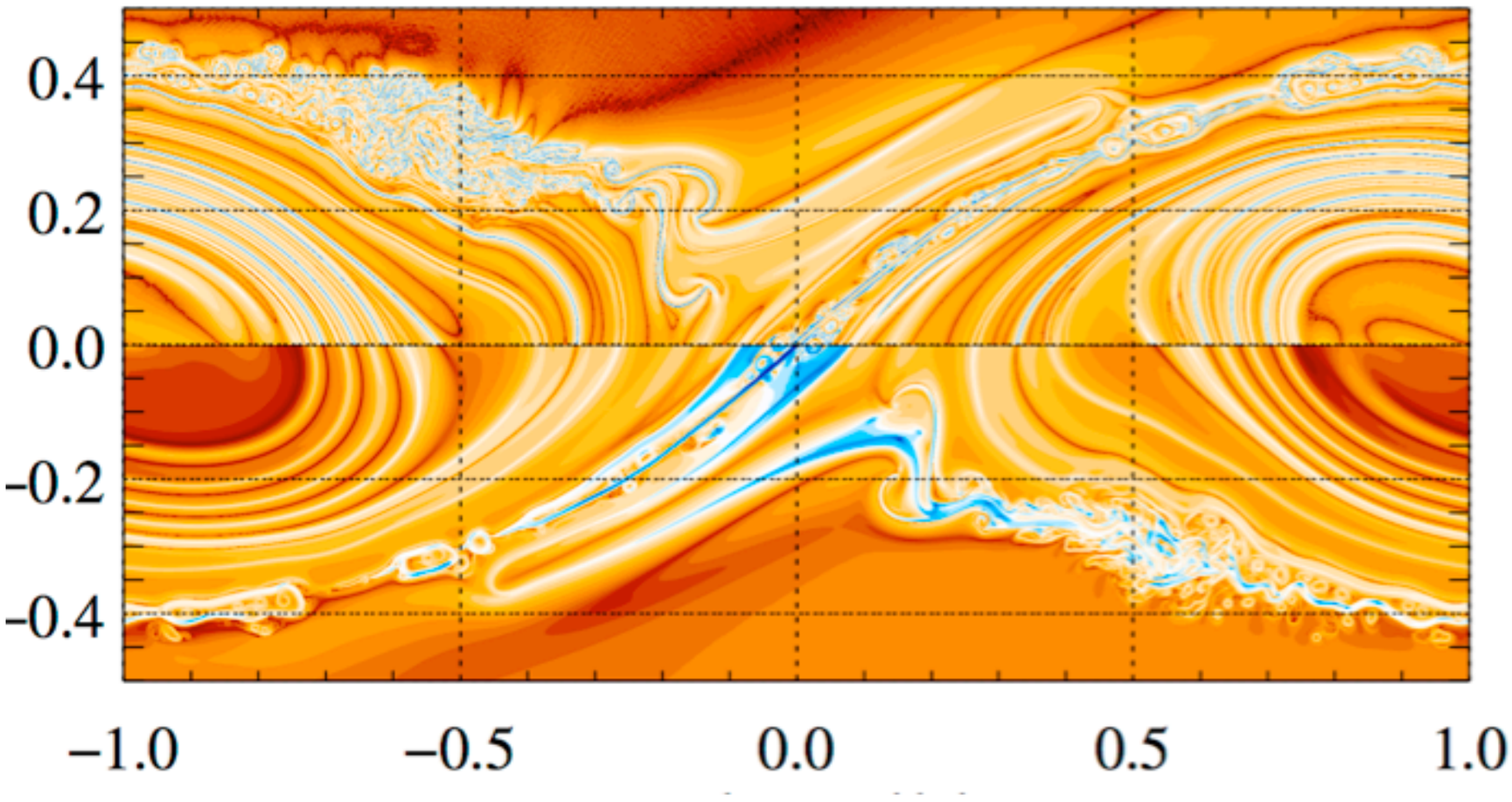

Obergaulinger et al (2010):

local simulations can be performed with sufficient resolution to follow growth and saturation of KHI.

Strong consequences if NS are magnetized (Price & Rosswog 2006). In the presence of an initially poloidal B-field, KHI may lead to an exponential growth of the toroidal component (Rezzolla et al 2011; Kiuchi et al 2014, 2015): rapid formation of vortices that curl poloidal B-field lines. **Overall amplification of ~3 orders of magnitude.**

Development of KHI in a relativistic jet

ambient
$v = 0$

jet $\longrightarrow$
$v \neq 0$

ambient
$v = 0$

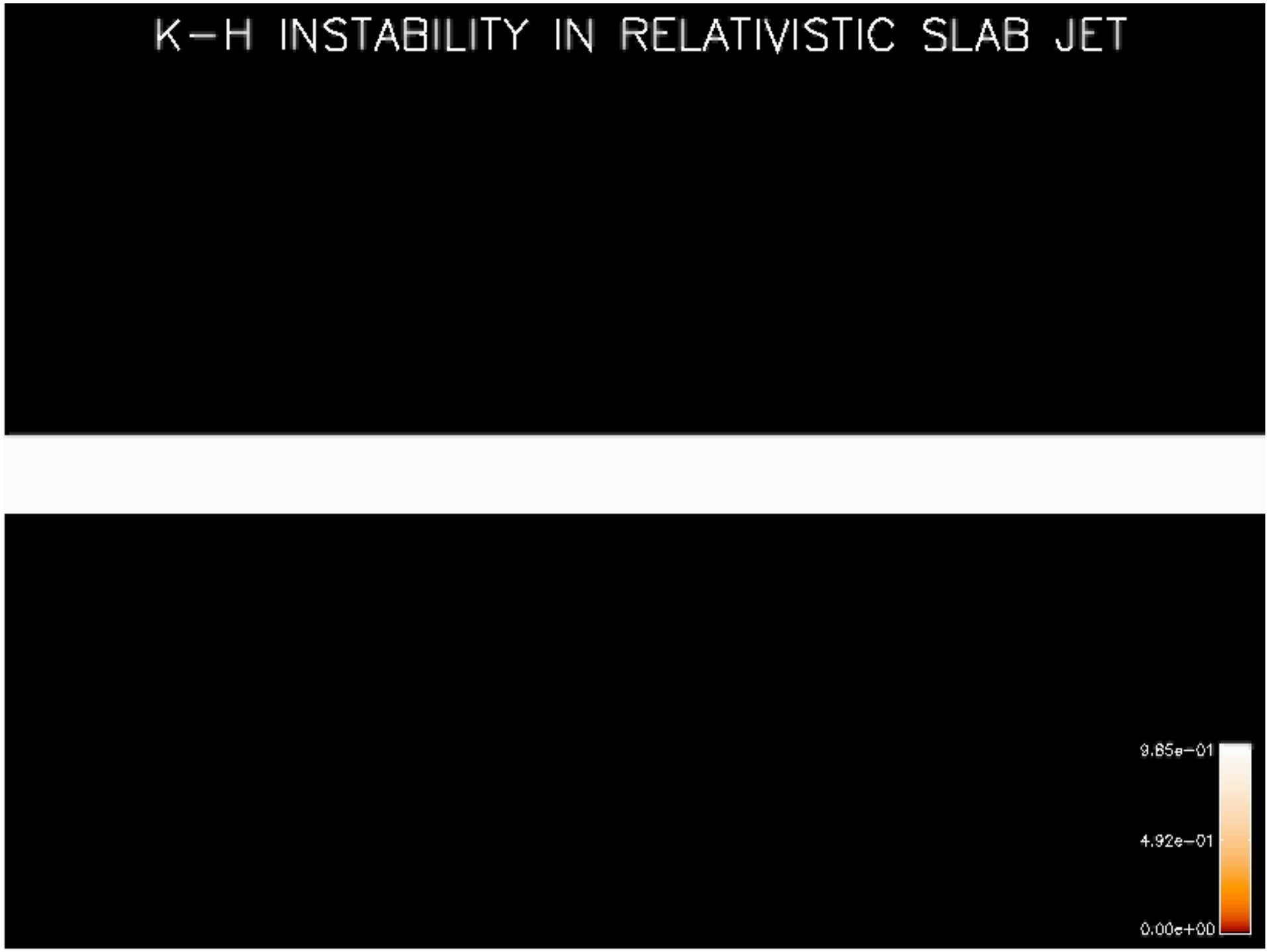

Perucho et al (2005)

Magnetised BNS merger (Rezzolla+ 2012)

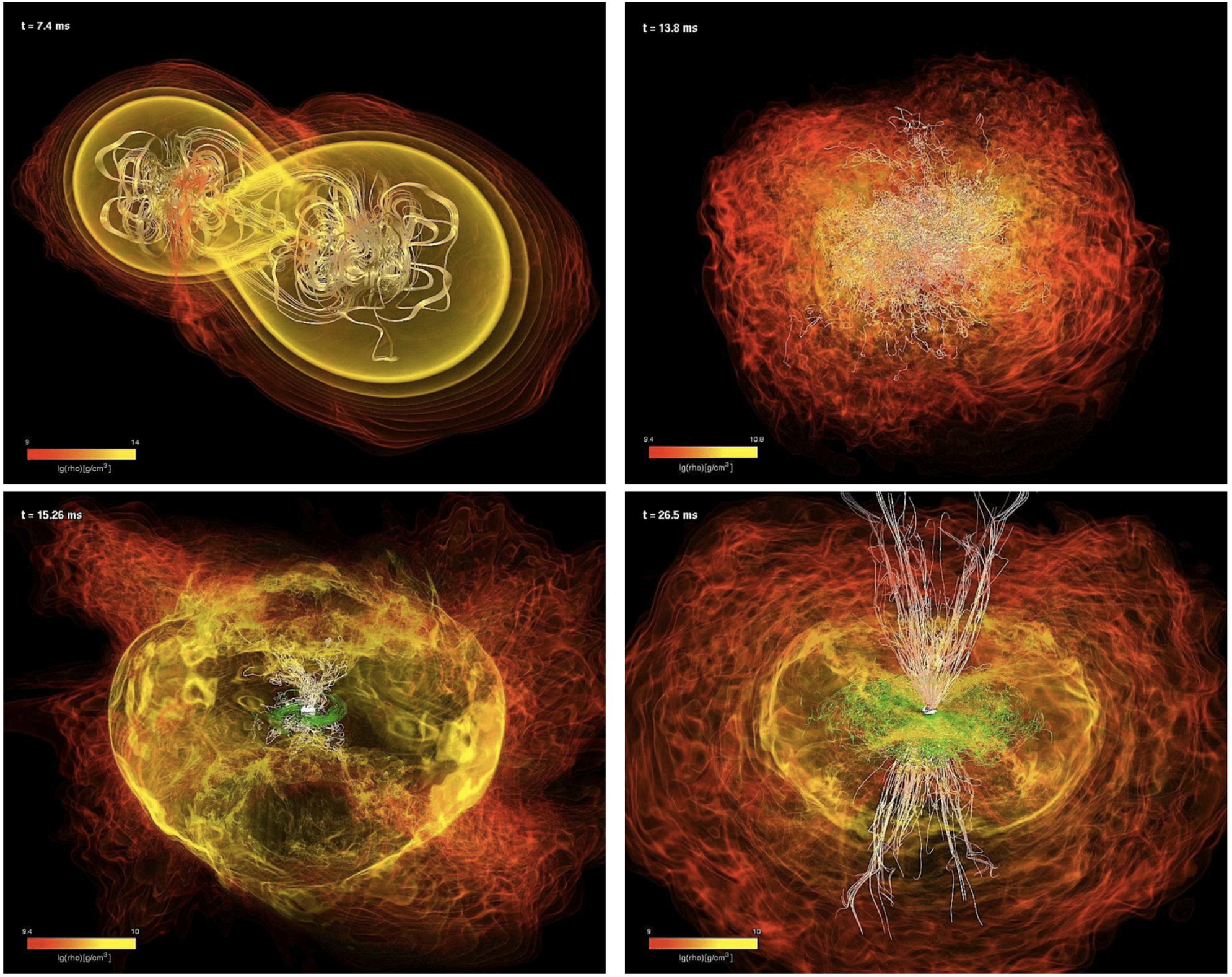

Ab-initio self-consistent formation of polar outflows from MHD effects

Magnetised BNS merger (Kiuchi+ 2014)

Snapshots of density, B-field strength and B-field lines (white curves)

Merger | HMNS | BH+torus

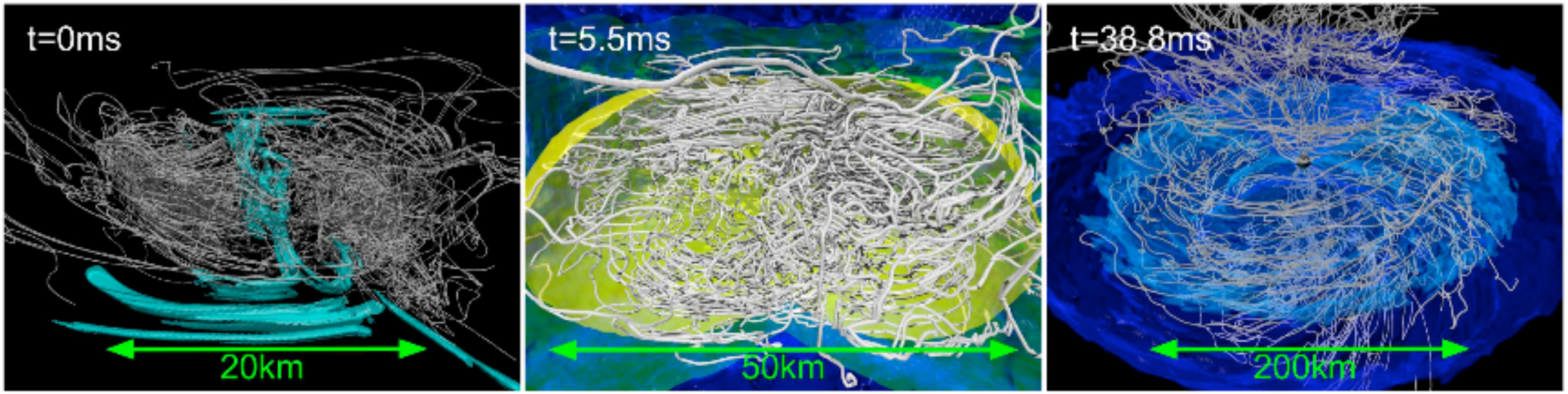

cyan: $B>10^{15}$G

large scale toroidal B-field

no coherent poloidal B-field after BH formation

KH vortices develop and curl the B-field lines, generating strong toroidal fields

Model	Δx_7 [m]	N	$\log_{10}[B_{max}(G)]$
H4B15d70	70	512	15.00

Very high resolution simulations on "K"

MRI and KH instabilities resolved

In the HMNS stage, the B-field strength grows significantly in the **high- and mid-res runs** but not in the low-res run.

$$\lambda^{\varphi}_{\rm MRI}/\Delta x_7 \geq 10$$

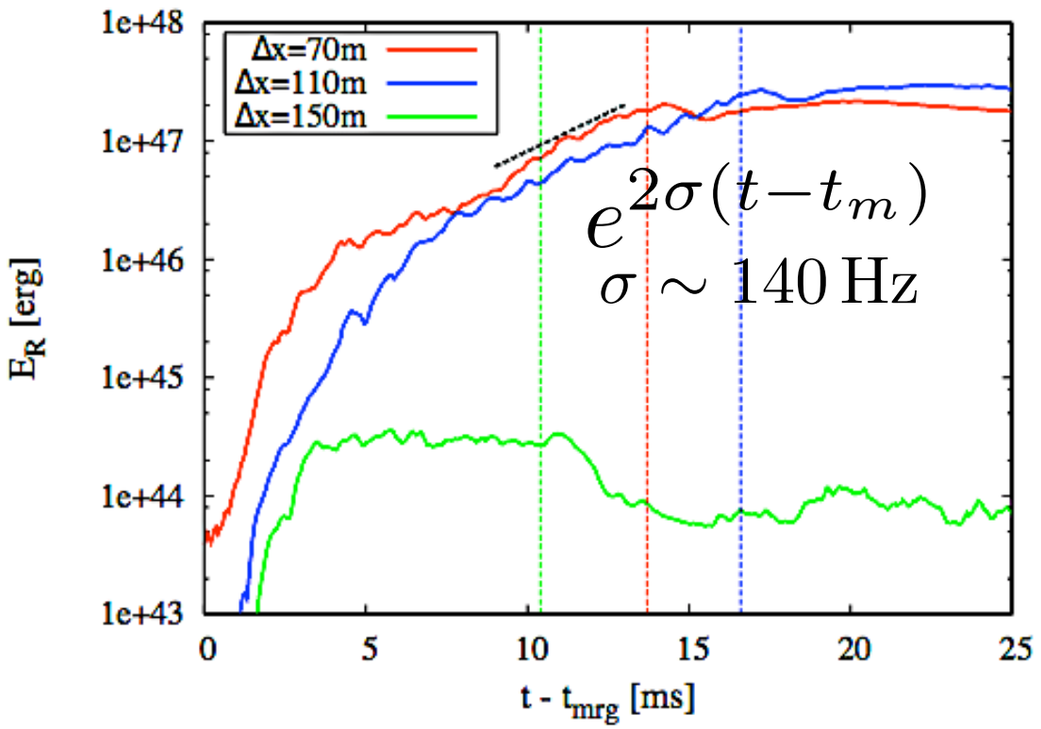

Magnetised BNS merger (Kiuchi+ 2015)

Initial B-field strength of Kiuchi et al (2014) of magnetar class (unrealistic). Kiuchi et al (2015) use more realistic values of 10^{13}G. **Highest resolution simulations ever.**

17 meters !!

density

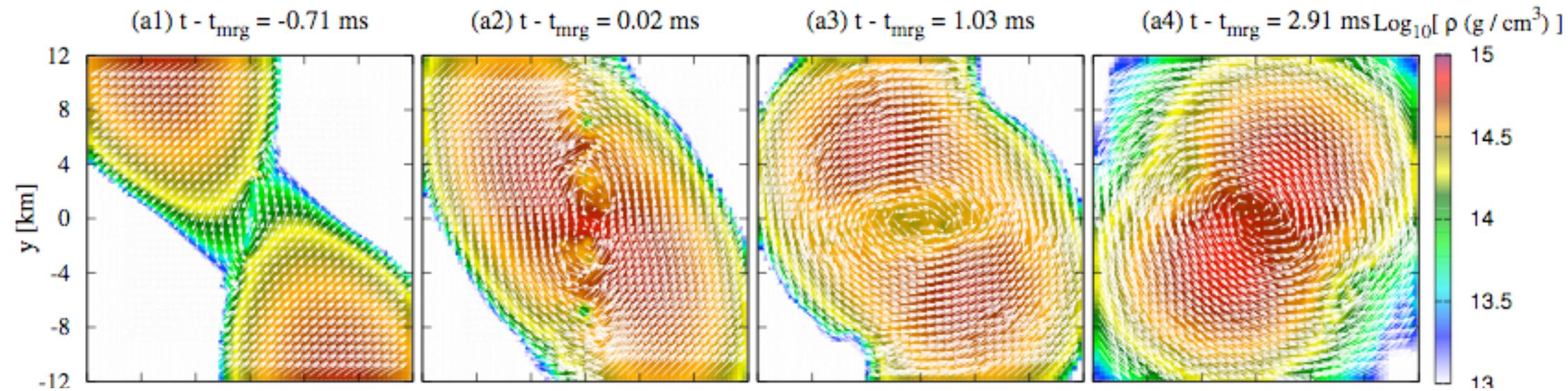

B-field

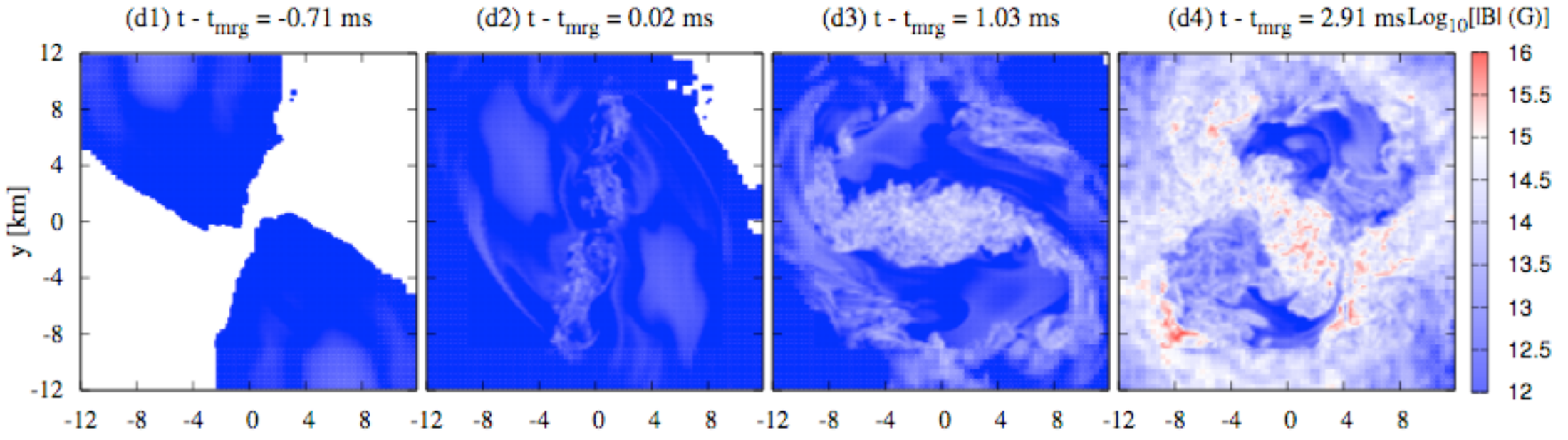

$$B_{\max\,\mathrm{ini}} = 10^{13}\,\mathrm{G} \;\rightarrow\; \text{amplification factor} \sim 10^{6} \text{ at} \sim 4\,\mathrm{ms} \text{ after merger}$$

$$\text{saturation energy} \geq 4 \times 10^{50}\,\mathrm{erg} \;\; \geq 0.1\% \text{ bulk kinetic energy}$$

Conclusion: necessary to consider high B fields for modeling post merger evolution of BNS.

Magnetised BNS merger (Ruiz+ 2016)

In Rezzolla et al (2011) and Kiuchi et al (2014, 2015) initial B-field is confined to NS **interior**. Ruiz et al (2016): initially strong, but dynamically unimportant **dipole** B-field extending into the **exterior** (realistic pulsar model).

$\Gamma = 2$ polytrope

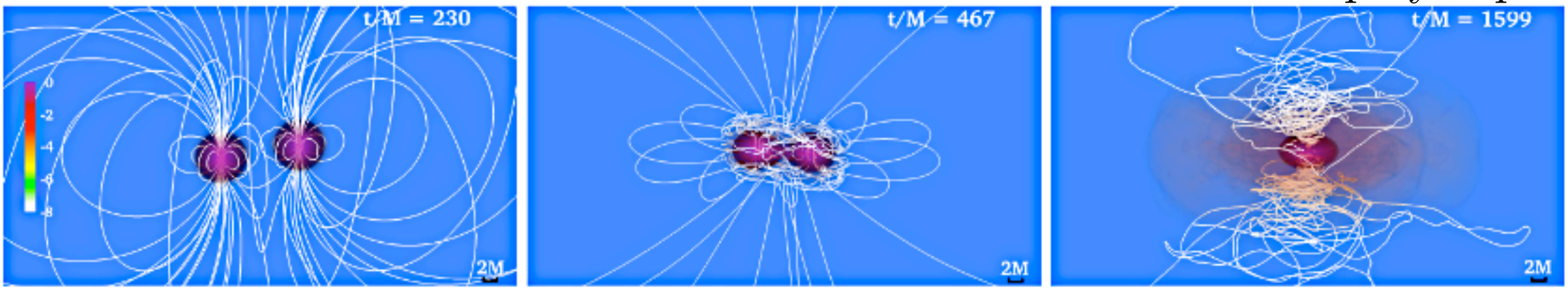

Incipient jets also form if the dipole B-field is confined to the interior of the NS. *This is in contrast to what happens for BH-NS binaries.*

Different EOS affect amount of disk mass and of ejected matter (Hotokezaka et al. (2013); Palenzuela et al. (2015)), and therefore the **ram pressure** of the atmosphere of remnant BH-disk system. Main reason for the non-observance of an incipient jet in the BNS simulations of Kiuchi et al (2014, 2015).

Magnetised BNS merger (Kawamura+ 2016)

Formation of an **organized B-field structure** irrespective of EOS, mass ratio, and initial B-field orientation. **No magnetically dominated funnel and relativistic outflows are (yet) observed.** (Unfeasible) longer simulations required

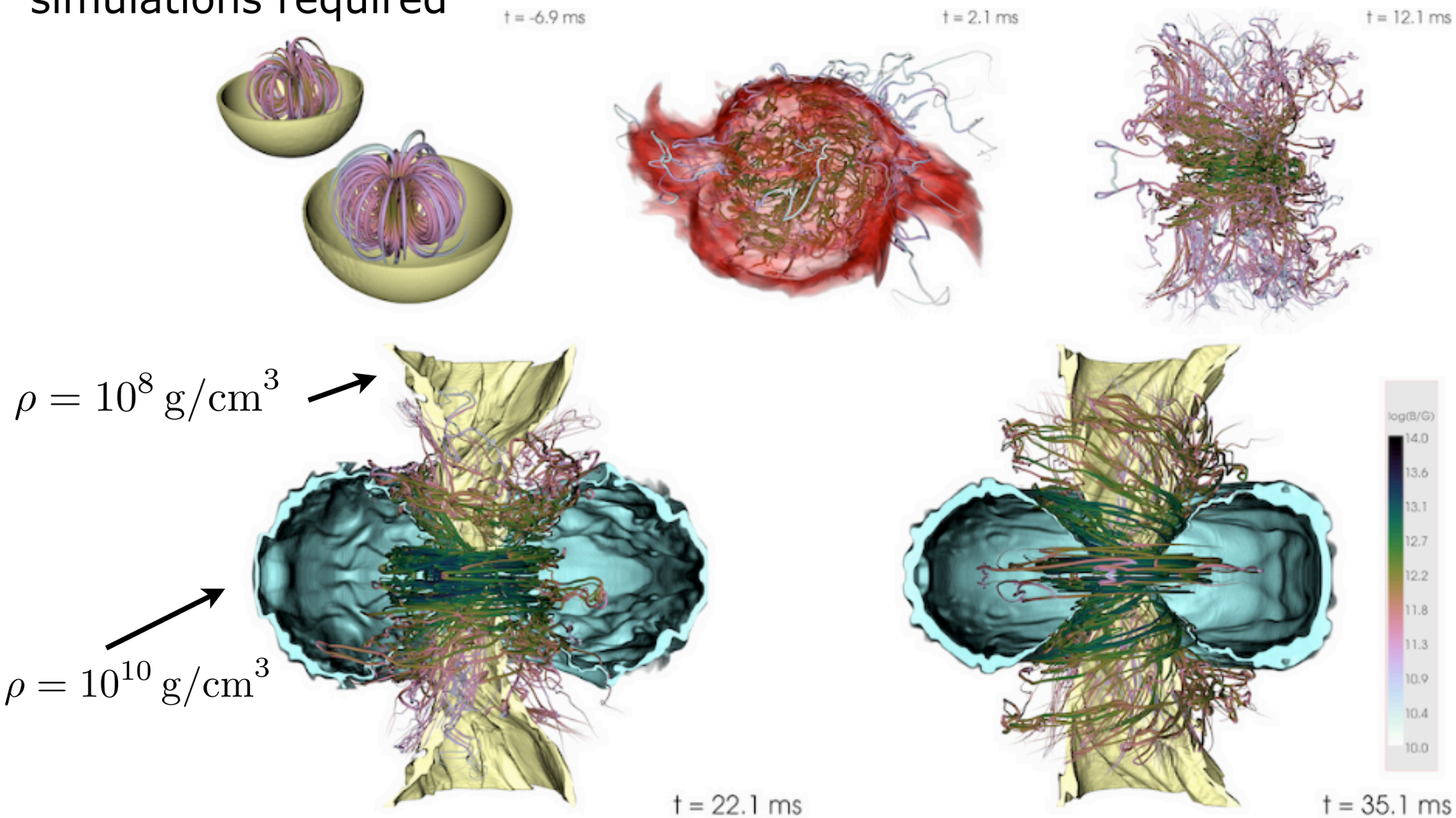

Broad agreement with Kiuchi et al (2014) and Ruiz et al (2016).

Disagreement with Rezzolla et al (2011): Maximum B-field not in funnel but in boundary. Field lines are not straight but helical.

Dynamical ejecta from BNS mergers

NR simulations studying the ejecta are **fairly recent**:

Hotokezaka et al (2013)
Tanaka & Hotokezaka (2013)
Wanajo et al (2014)
Sekiguchi et al (2015, 2016)

Palenzuela et al (2015)
Lehner et al (2016)

Foucart et al (2016)

Radice et al (2016)

There exist **4 different ways to eject neutron rich matter** in BNS (and BH-NS) mergers:

(1) **dynamical** ejection via gravitational torques (tidal ejection) or shocks

(2) through **neutrino-driven** winds

(3) through **magnetically** driven winds

(4) from shock waves in the late-time evolution of **accretion disks**

Most NR simulations have focused on the nucleosynthesis of matter that is dynamically ejected (1) and only a few have considered neutrino-driven ejecta (2). [Cases (3) and (4) not yet studied.]

Dynamical ejecta from BNS mergers

NR simulations show that **<0.1% of total mass of the system becomes unbound**. Ejecta composed of **neutron rich** material.

Rapid neutron capture processes (**nucleosynthesis** of heavy elements) and **radioactive decays** (electromagnetic radiation) take place.

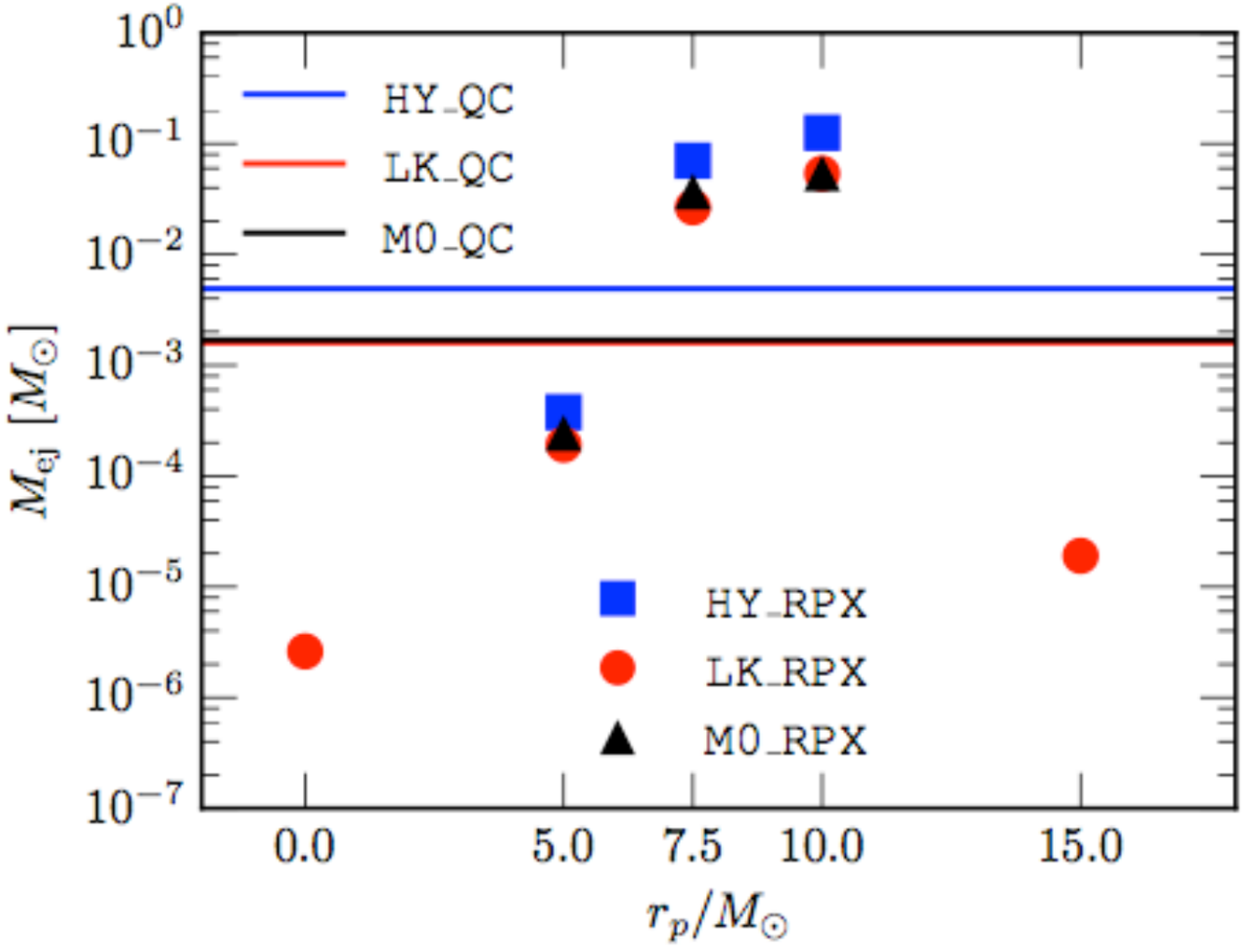

Radice et al (2016)

Eccentric mergers (symbols) eject up to ~0.1M_{sun} and about 2 orders of magnitude more material than quasi-circular mergers.

Neglecting neutrino cooling (blue squares) results in an overestimate of the unbound mass by a factor >2

Nucleosynthesis from the ejecta

Physical conditions to produce elements with atomic number **Z > 90**, i.e. high entropy, low electron fraction, and very rapid expansion, difficult in core-collapse supernovae but **natural in BNS mergers.**

Main result from simulations:

- all studies conclude that **dynamical ejecta** produce strong r-process elements with Z > 130 irrespective of details of merger. In particular, the r-process peaks around Z~130 and Z~195 are independent from details of initial data (quasi-circular or eccentric) or details of radiative losses (pure hydro or neutrinos)

- NR simulations from Wanajo et al (2014), Sekiguchi et al (2015) and Radice et al (2016) using advanced neutrino transport schemes and finite-temperature EOS show that the dynamical and **early-merger neutrino-wind ejecta** of BNS mergers can be the dominant origin of all the Galactic r-process nuclei.

Wanajo et al (2016)

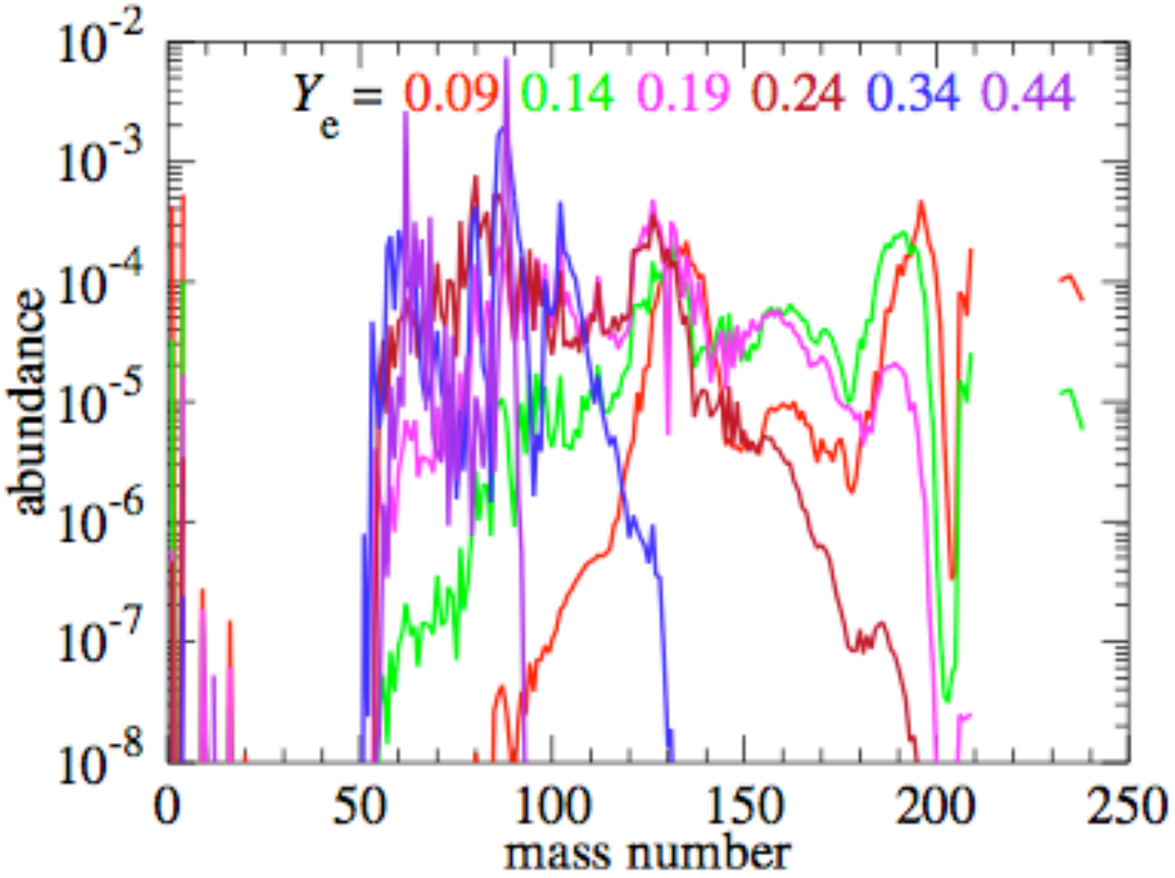

Final nuclear abundances for selected trajectories with given electron fraction.

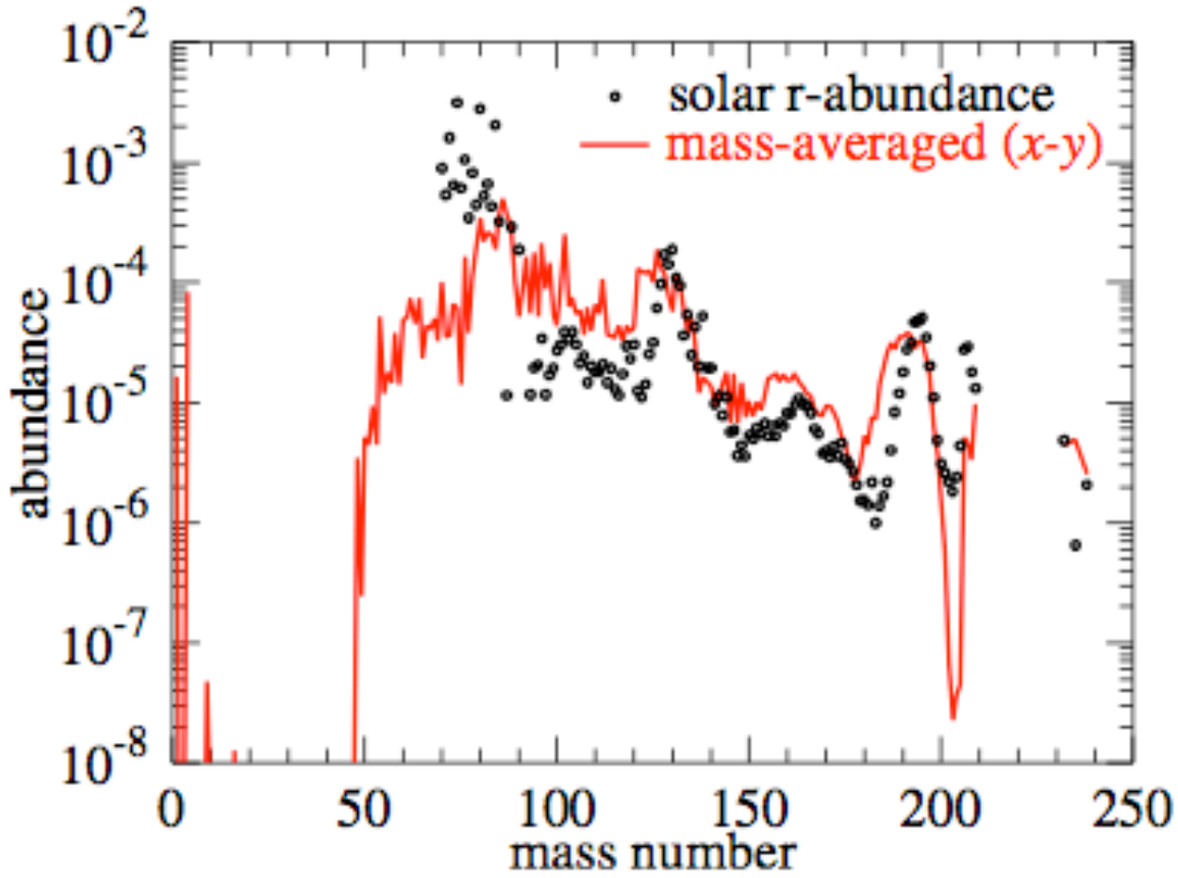

Comparison between solar r-process abundances and mass-averaged nuclear abundances

Remarkable agreement with solar r-process abundance distribution over full mass number range of Z ≈ 90 – 240.

Note: to fully study the nucleosynthesis from **neutrino-driven ejecta** one needs to explore **timescales** which are of the order of **seconds**. Only feasible through **approximations** as e.g. CFC employed in the work of Just et al (2015).

Results from BH-NS merger simulations

Main results from BH-NS simulations

Merger: NS either tidally disrupted or swallowed by companion BH.

$$
\begin{aligned}
a &= 0, Q = 2 \\
M_{\rm BH} &= 2.7 M_\odot,\ M_{\rm NS} = 1.35 M_\odot,\ R_{\rm NS} = 15.2\,{\rm km}
\end{aligned}
$$

$$Q = \frac{M_{\rm BH}}{M_{\rm NS}}$$

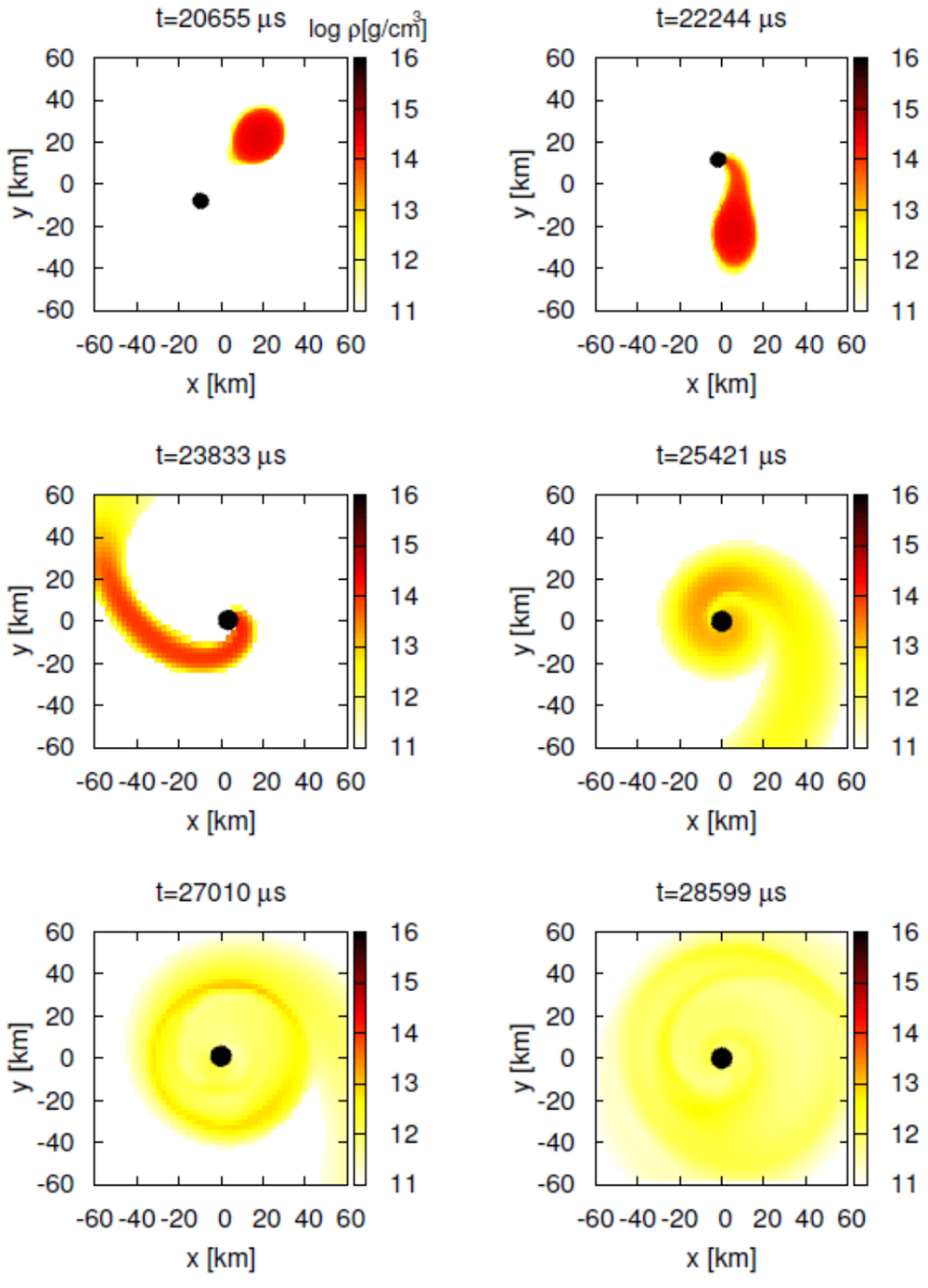

$$
\begin{aligned}
a &= 0, Q = 3 \\
M_{\rm BH} &= 4.05 M_\odot,\ M_{\rm NS} = 1.35 M_\odot,\ R_{\rm NS} = 11.0\,{\rm km}
\end{aligned}
$$

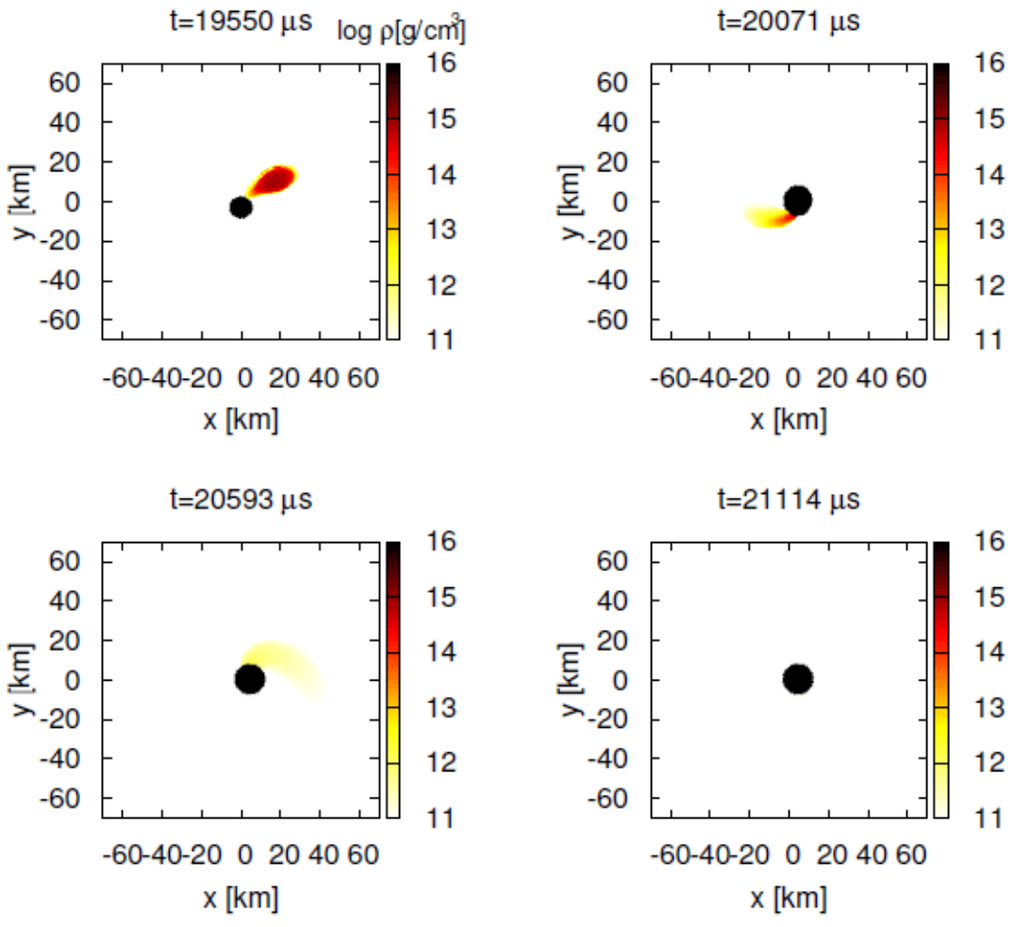

Kyutoku et al (2010)

BH spin effect

$Q = 3,\ a = 0$

$Q = 3,\ a = 0.75$

4 orbits to merger

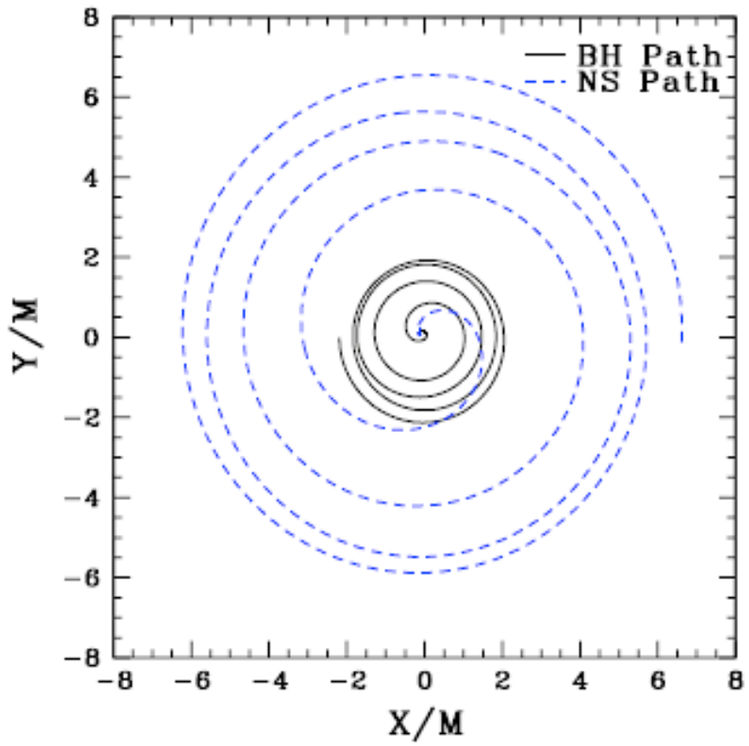

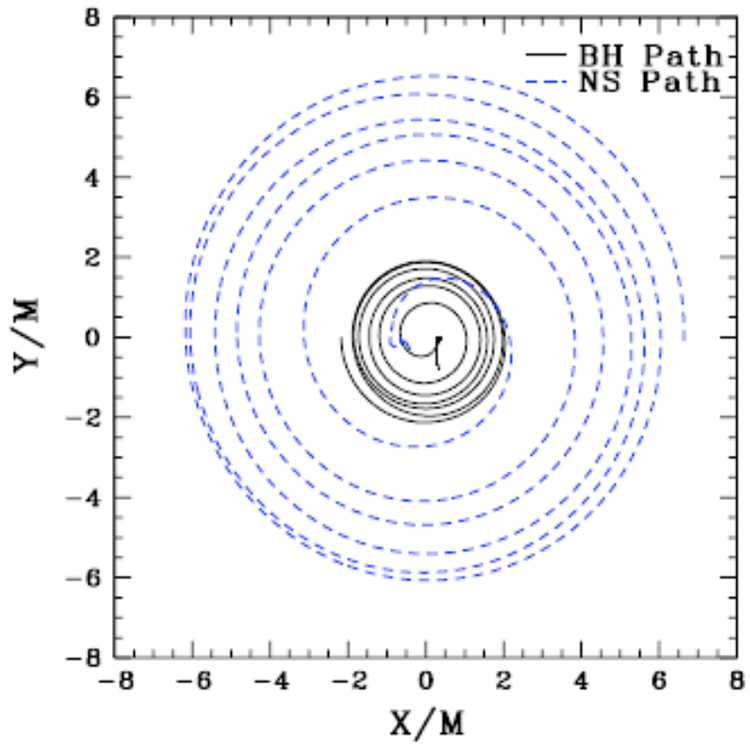

6 orbits to merger

disk mass ~4% of total rest mass

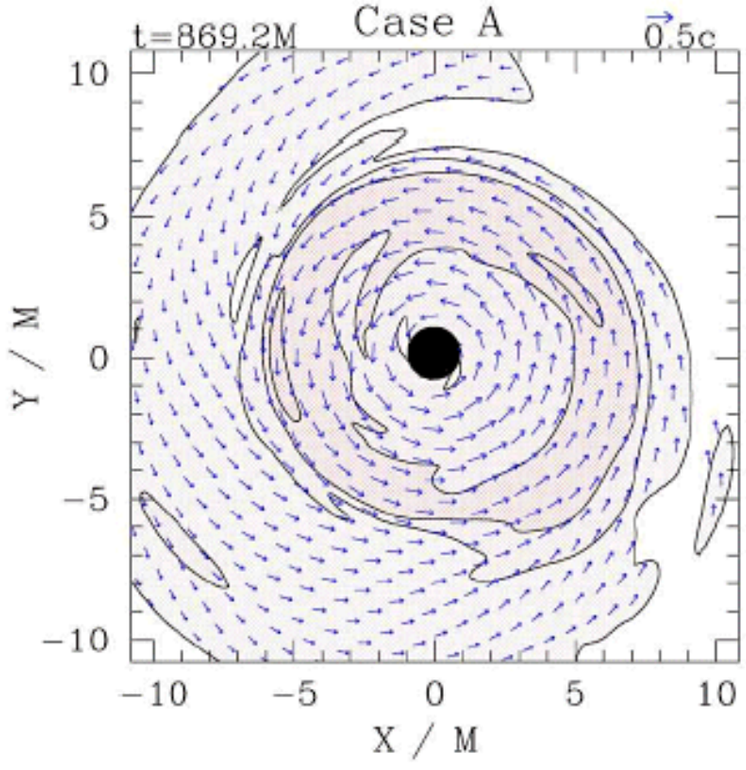

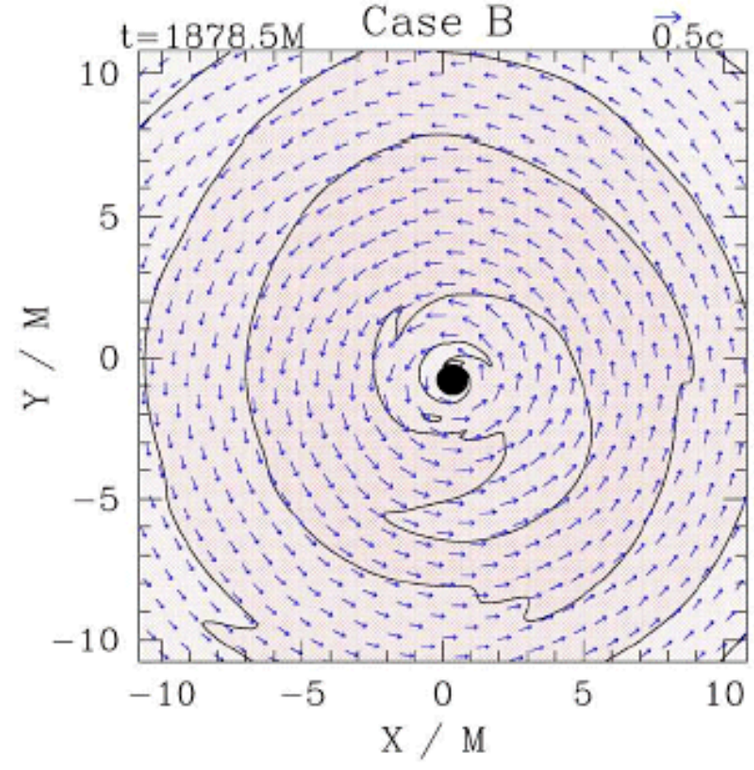

disk mass ~13% of total rest mass

spin-orbit coupling effect: additional repulsive force for *a>0.*
Binary lifetime longer.

Etienne et al (2009)

Main results from BH-NS simulations

- **<u>Tidal disruption and mass of the disk:</u>**

For $\mathcal{C} = 0.14 - 0.2,\ a = 0$ tidal disruption occurs outside the ISCO for $Q \leq 3$

Final remnant is a BH surrounded by a disk of $M_{\rm d} \leq 0.1 M_{\odot}$

BH spin enhance the possibilities for tidal disruption and for disk formation.

$$\mathcal{C} = 0.17,\ a = 0.5 \ \Rightarrow\ Q \leq 5$$

$$\mathcal{C} = 0.145,\ a = 0.9 \ \Rightarrow\ M_{\rm d} \geq 0.5 M_{\odot}$$

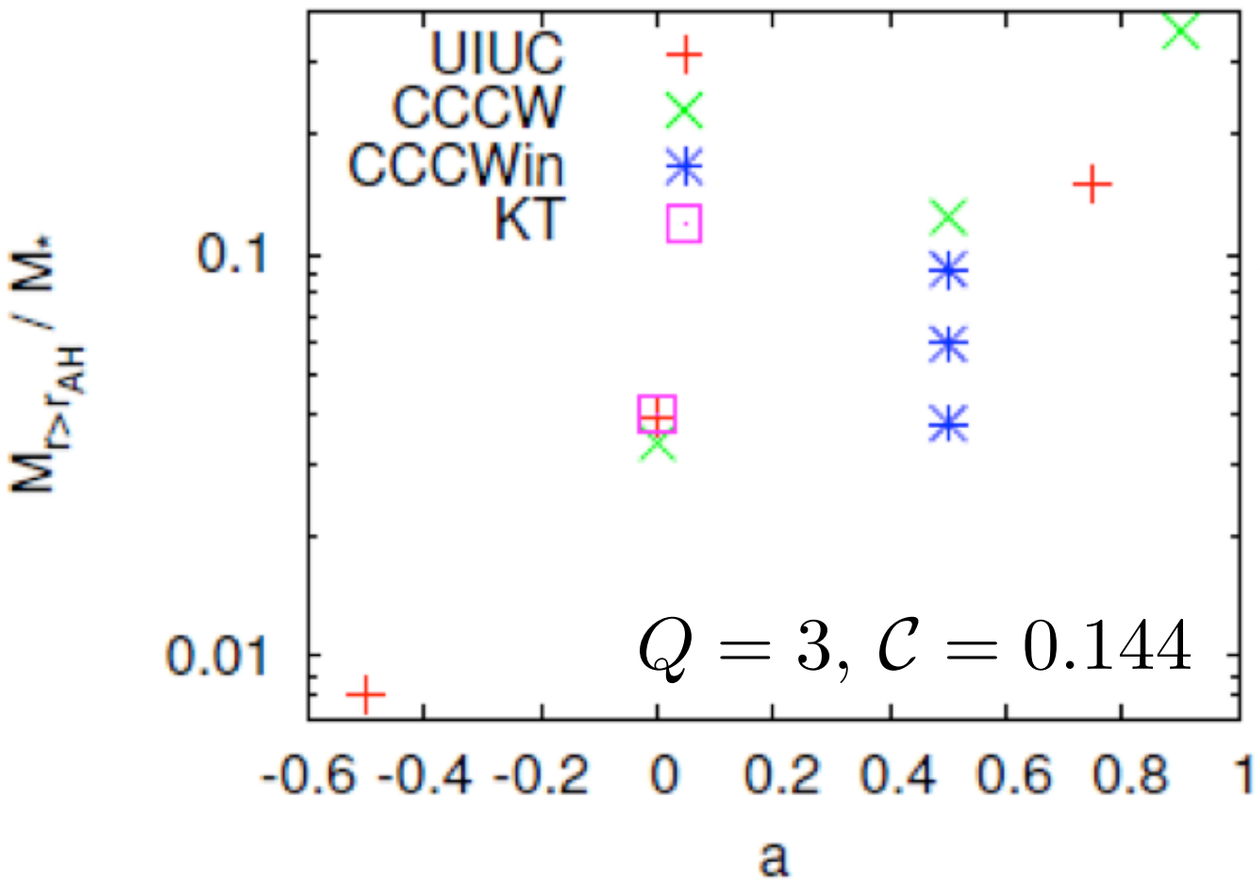

disk mass increases steeply with BH spin

40°
60°
80°

disk mass decreases with the increase of the inclination angle of the BH spin

Foucart et al (2011)

Kyutoku et al (2011)

For $a \sim 1$ the NS may be tidally disrupted even for a high mass ratio $Q \sim 20$

(Wiggins & Lai 2000)

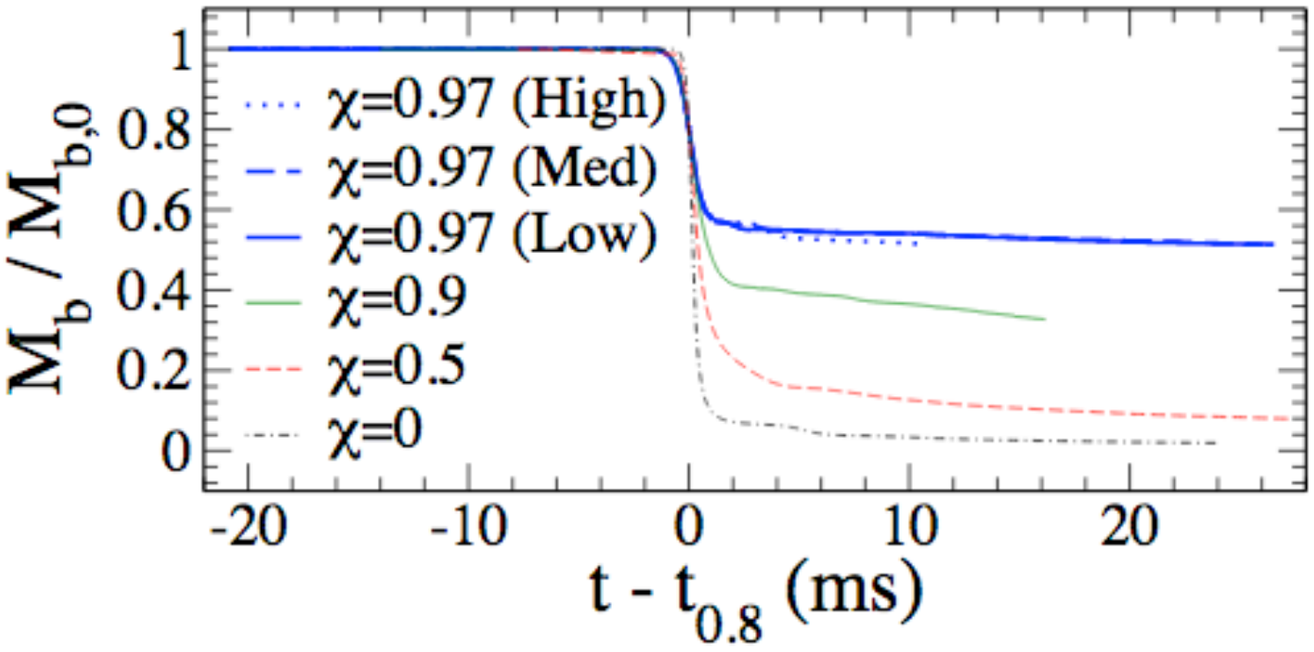

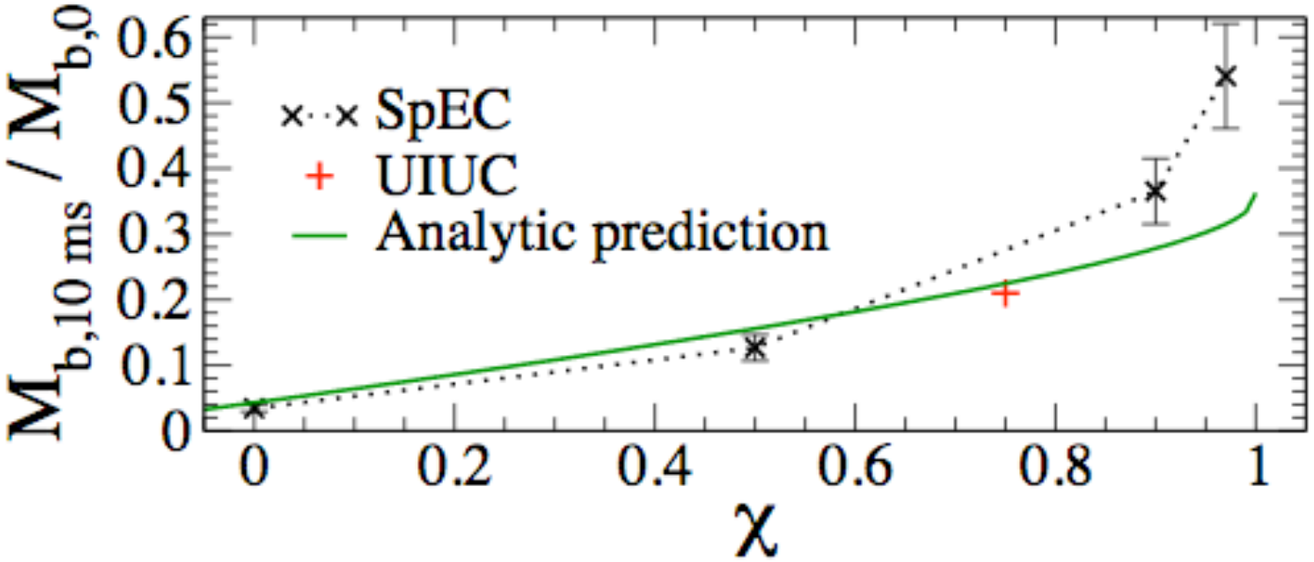

From Lovelace et al (2013)

$$Q = 3,\ \mathcal{C} = 0.144$$

a=0.97 results:

60% of the NS matter avoids falling into the BH during the initial plunge and merger. Most of this matter settles into a massive accretion disk. Early disk mass is 50% larger than for an a=0.9 system.

$$\frac{M_{\rm d}}{M_{\rm NS}} = 0.288 \left(\frac{3M_{\rm BH}}{M_{\rm NS}}\right)^{1/3} \left(1 - 2\frac{M_{\rm NS}}{R_{\rm NS}}\right) - 0.148\frac{R_{\rm ISCO}}{R_{\rm NS}}$$ (Foucart 2012)

Analytic predictions perform well for low-spin black holes with $a < 0.9$

Strong deviations visible for higher spin configurations. Not surprising as analytic results are only supposed to be valid for relatively low mass disks $M_{\rm d} < 0.2 M_\odot$

● Mass ejection

Mass of the ejecta: $$M_{\rm ej} \equiv \int_{r>r_{\rm AH},u_t<-1} \rho\, d^3x$$

Unbound material is generated primarily by tidal torque exerted on the elongated NS during tidal disruption.

Ejecta mass as large as	$\sim 0.1 M_\odot$
Average velocity of ejecta	$\sim 0.2 - 0.3c$

Matter can be ejected through different processes during and after the merger:

1. Tidal disruption: M_{ej} ~ 0.01-0.1 M_sun (depending on binary parameters) (Kyutoku et al 2013, Foucart et al 2013, 2014).

Amount can even be larger for rapidly spinning, low mass BH (Deaton et al 2013, Lovelace et al 2013). Tidally ejected material very neutron rich (Ye<0.1), cold (T<1 MeV), confined close to the equatorial plane, and strongly asymmetric.

2. Formation of the accretion disk and at the interface between the disk and the tidal tail (Foucart et al 2015).

3. Disk winds may be triggered by magnetic effects (Kiuchi et al 2015) and/or neutrino absorption (Foucart et al 2015).

4. Over longer timescales (seconds) 2D Newtonian simulations have shown that viscous heating can drive strong outflows in the disk.

From Foucart et al (2015), disk evolution using LS220 and M1:

1. $\sim 0.06 M_\odot$ cold, neutron rich material. Strong r-process nucleosynthesis and (infrared) EM emission.

2. $\sim 3 \times 10^{-4} M_\odot$ higher latitudes, timescale ~10ms after merger

3. $\sim 10^{-3} M_\odot$ estimate due to neutrino-driven winds on timescale of 100 ms

4. $\sim 0.01 M_\odot$ estimate due to viscous heating on timescales of 1s

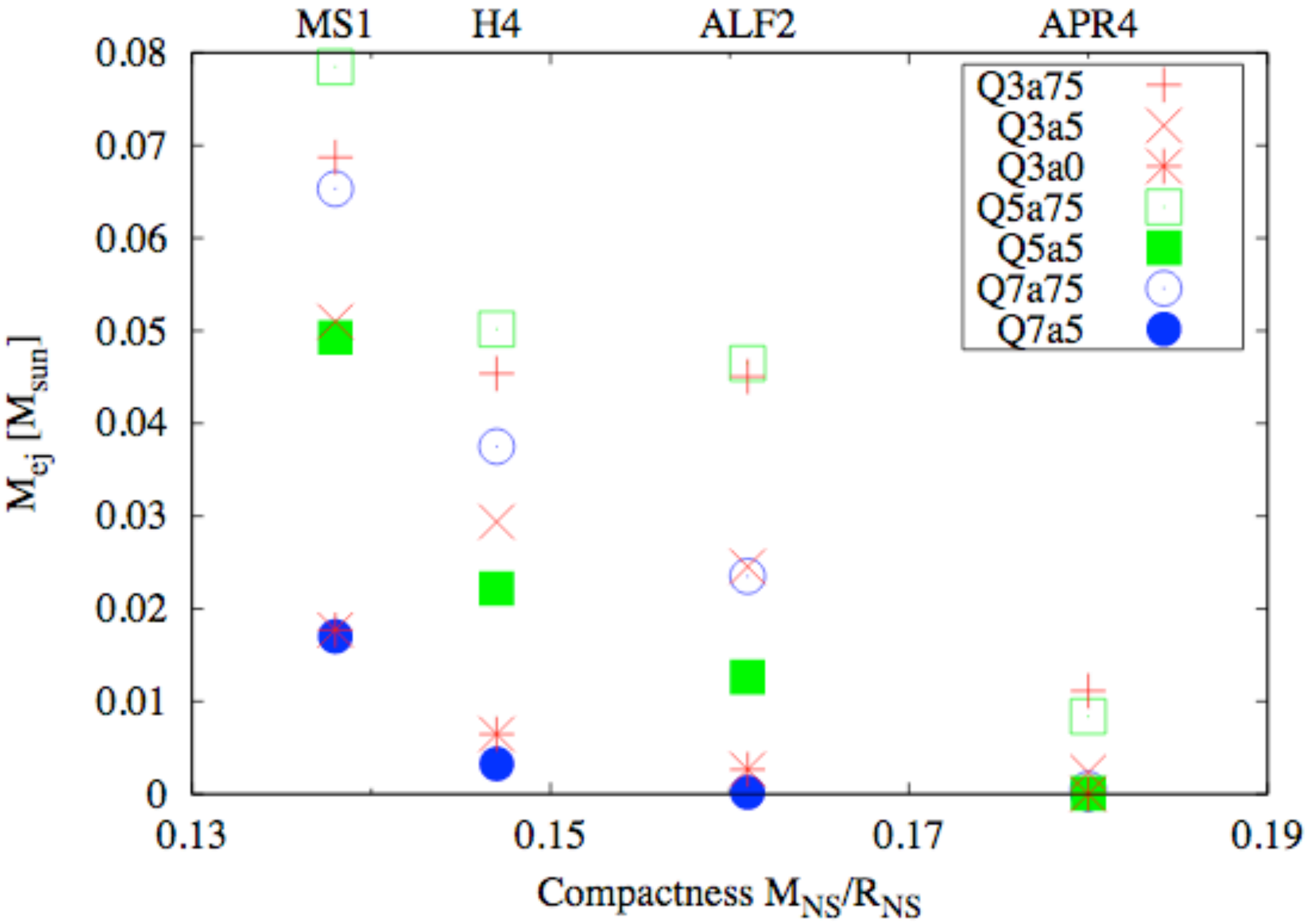

Dynamical mass ejection more efficient when NS compactness is small, mass ratio is small, and/or the BH spin is large.

Kyutoku et al (2015)

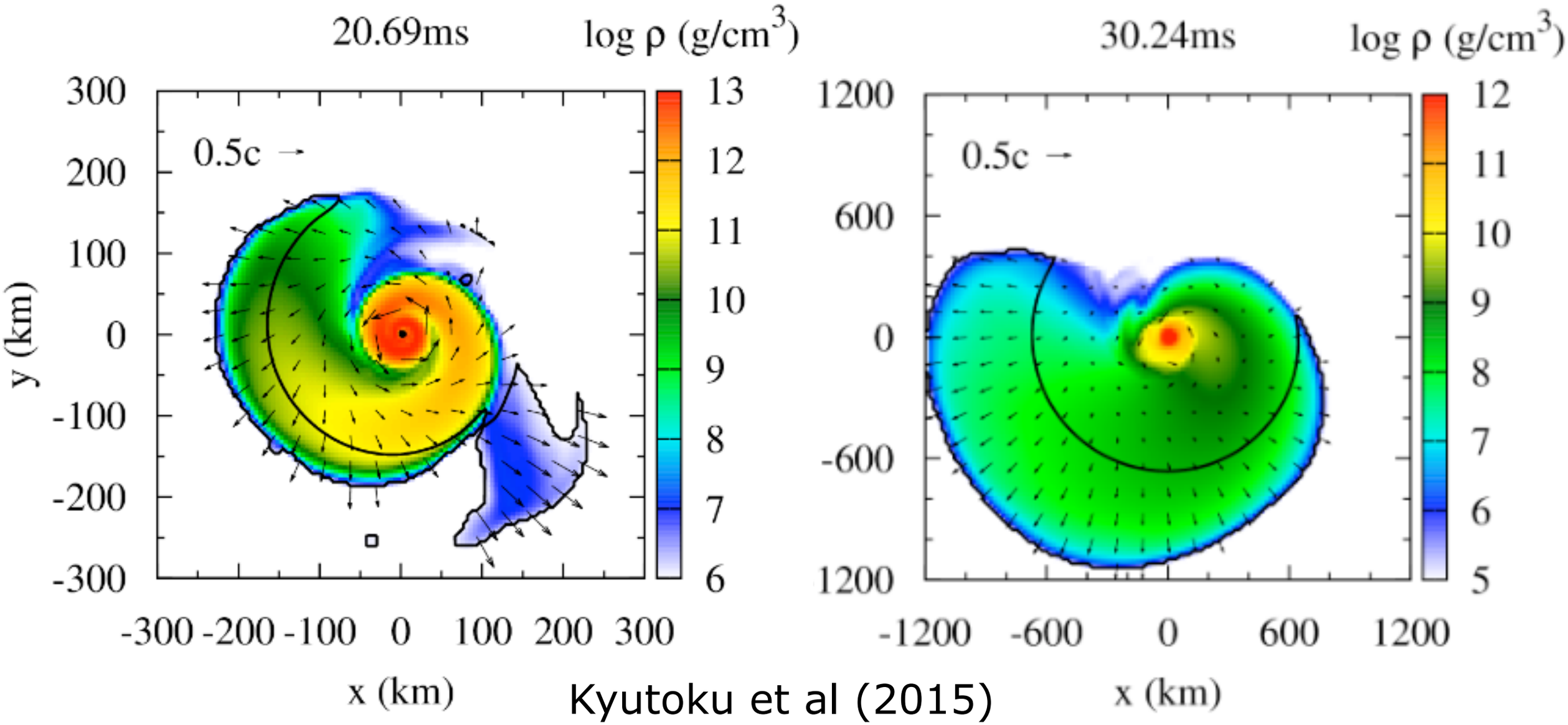

Kyutoku et al (2015)

Tidal tail exhibits a trailing **one-armed spiral** structure, and the BH exerts tidal torque on the tail, increasing its orbital angular momentum.

Anisotropic (crescent-like) ejection: BH-disk system receives a kick.

Ejecta mostly on equatorial plane. Different to dynamical ejection from BNS, in which quas-iradial oscillations of HMNS eject appreciable amount of material toward polar regions via shock interaction.

Kilonova/Macronova (KM)

Quasithermal radiation from the ejecta heated by decay of unstable r-process elements. Best target for EM counterpart of BH-NS and BNS mergers (Li & Paczynski 1998).

Dynamical ejecta composed primarily of neutrons which trigger synthesis of r-process elements (Lattimer & Schramm 1974). After neutrons are exhausted, within a few seconds, beta-decay and fission of radiactive nuclei heat the ejecta, which emits radiation primarily in **red-optical and infrared bands** on a day-to-month time scale (Tanaka et al 2014).

Simultaneous detection of KM and GWs will be:

- useful to determine the **host galaxy** of the source.
- as **lightcurve** reflects the binary parameters, useful for extracting the physical information of the binary.

Kawaguchi et al (2016): semi-analytic model for KM emission using fitting formulas for mass and velocity of dynamical ejecta. Model calibrated with results of a multi-frequency radiation transfer simulation of Tanaka et al (2014).

Model predictions: at 400 Mpc, KM as bright as 22-24 mag for cases with a small chirp mass and a high BH spin, and >28 mag for a large chirp mass and a low BH spin. KM could be observed in the optical wavelength by 8 meter class telescopes within 3 days.

BH-NS coalescence: GW spectrum

$Q = 1$

$f_{\rm cut} \sim 1 - 2\,{\rm kHz}$

$Q = 3$

$Q = 5$

$f_{\rm cut} \sim 2 - 3\,{\rm kHz}$

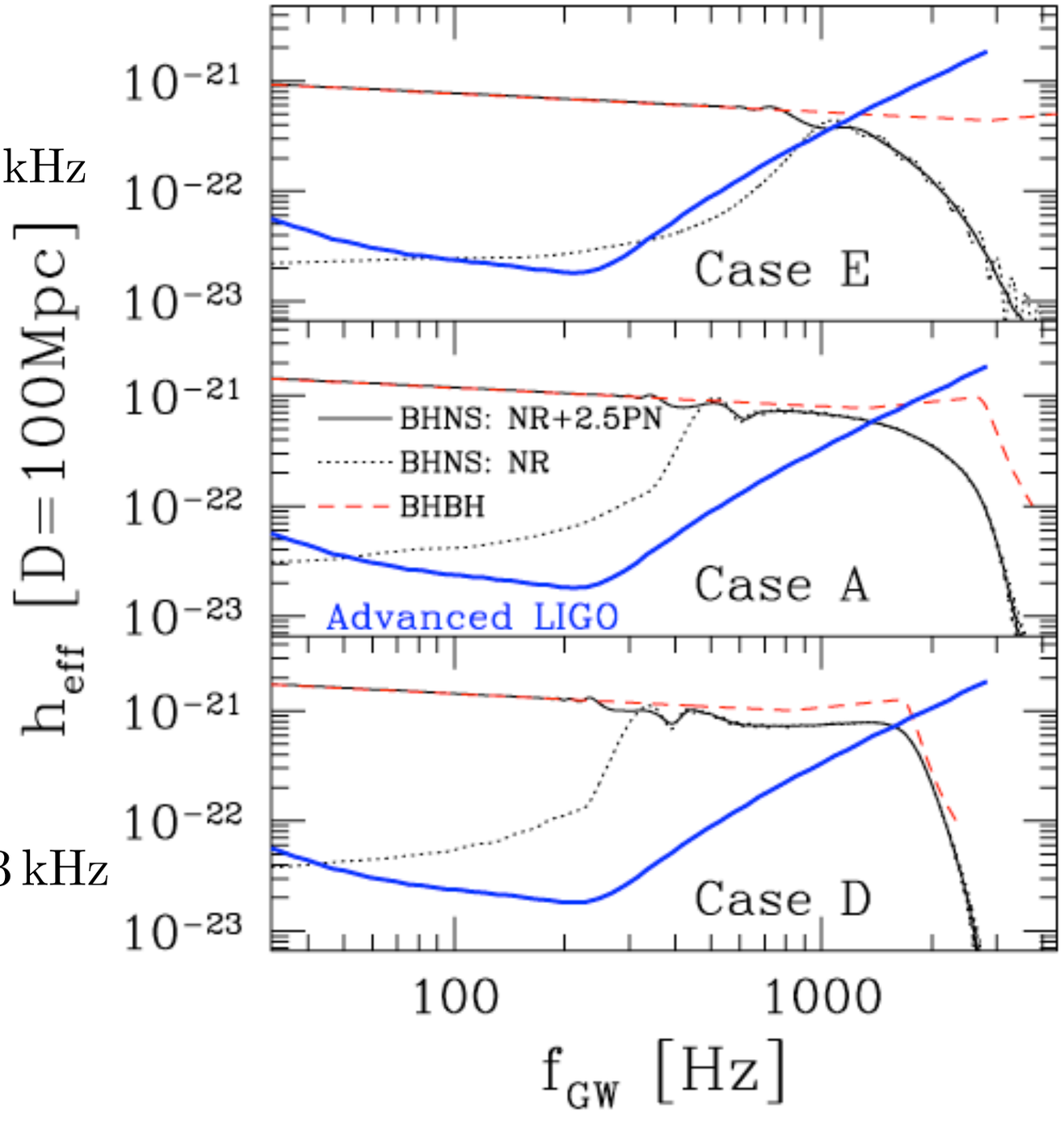

Amplitude of GW spectra damps steeply above a **"cutoff" frequency**, equal to a frequency in the middle of inspiral phase.

Cutoff frequency determined by:

a) frequency of GW emitted when the NS is tidally disrupted for the stiff EOS or

b) frequency of a QNM of the remnant BH for the soft EOS.

Etienne et al (2009)

Simulations show that cutoff frequency decreases with decreasing NS compactness and with increasing BH spin.

Cutoff frequency provides potential information on EOS (tidal deformation).

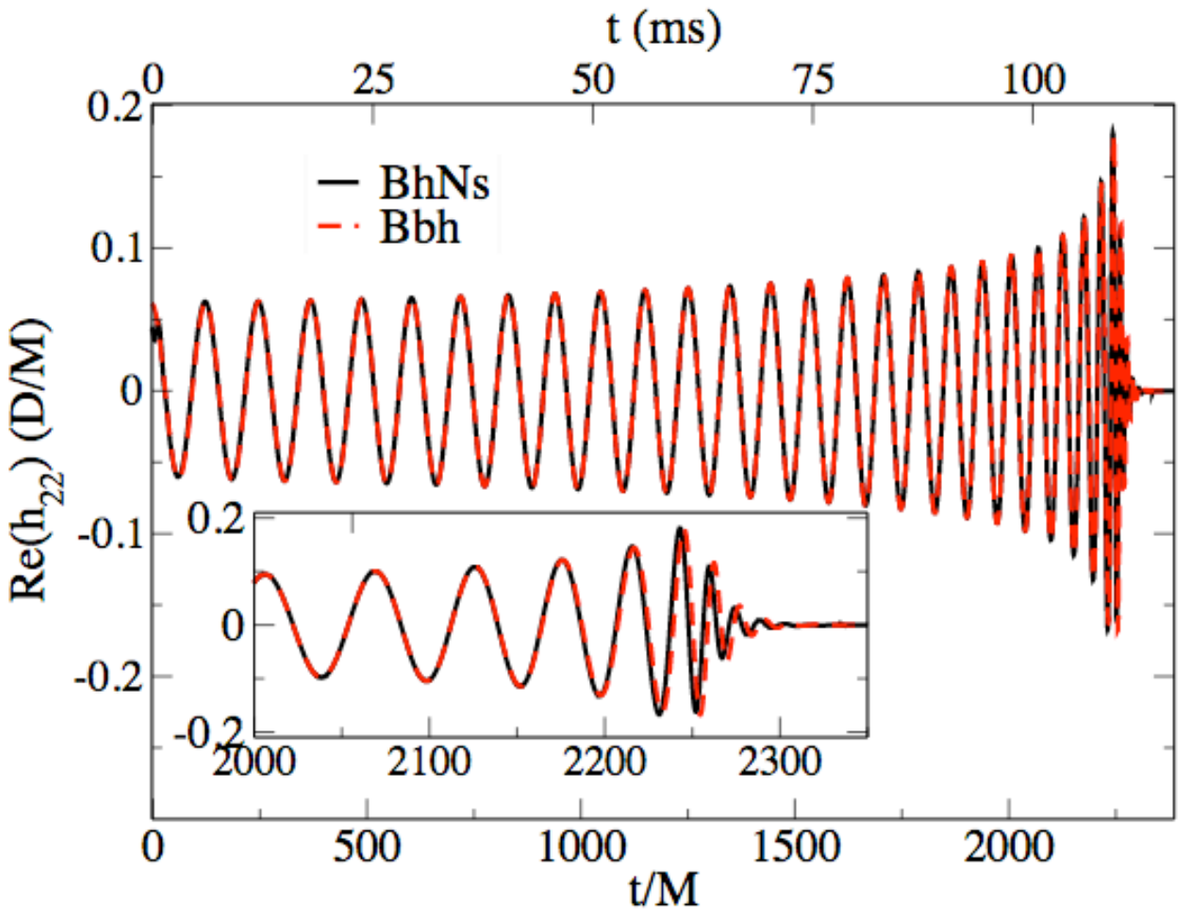

If NS not tidally disrupted, steep damping of spectrum determined by the swallowing of the NS by the BH.

Cutoff frequency is thus characterized by ringdown GWs associated with the QNM of the remnant BH.

Because finite-sized effect of the NS not very important in this case, the GW spectrum is remarkably similar to that of the BH-BH binary merger with the same mass ratio.

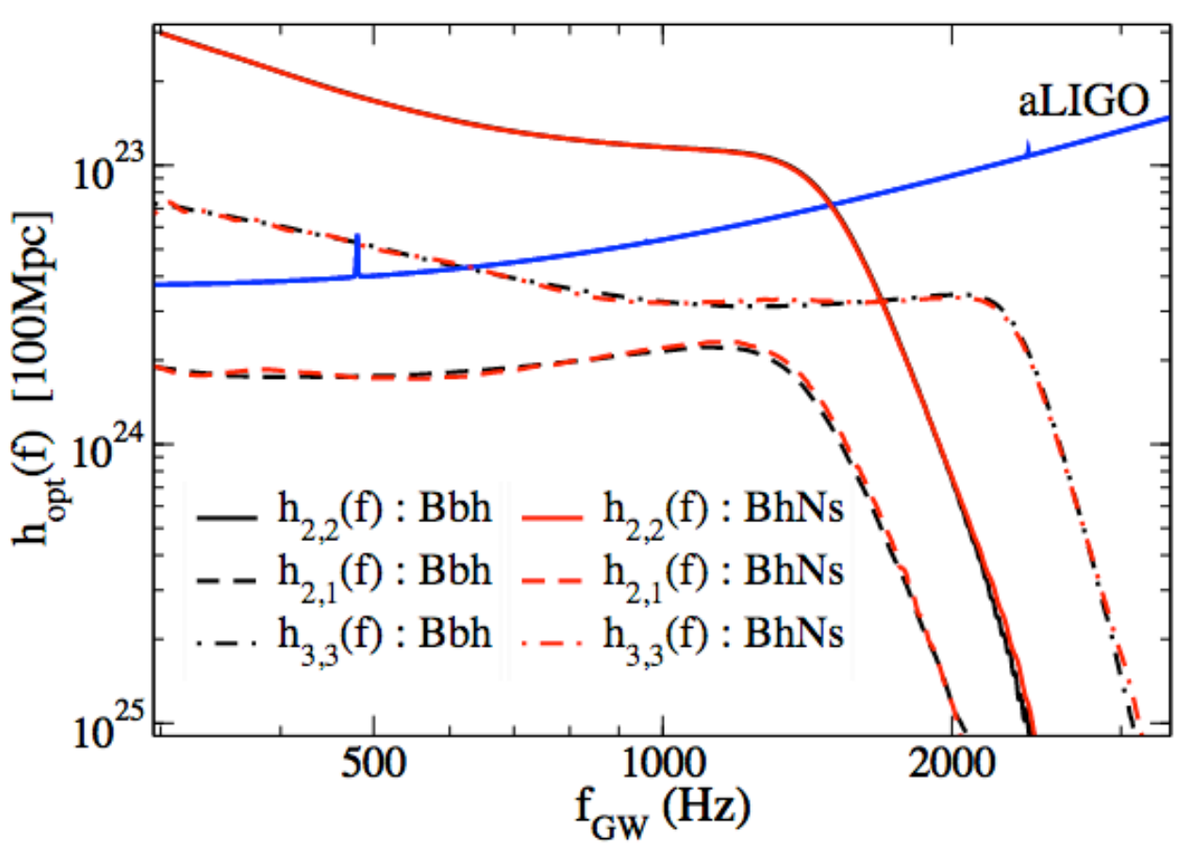

$$Q = 6$$

Final BH mass and spin agreement within:

$$\delta M_{\rm BH} < 5 \times 10^{-4} M_{\rm BH}$$

$$\delta \chi_{\rm BH} < 5 \times 10^{-3}$$

Foucart et al (2013)

Cutoff frequency depends strongly on the EOS

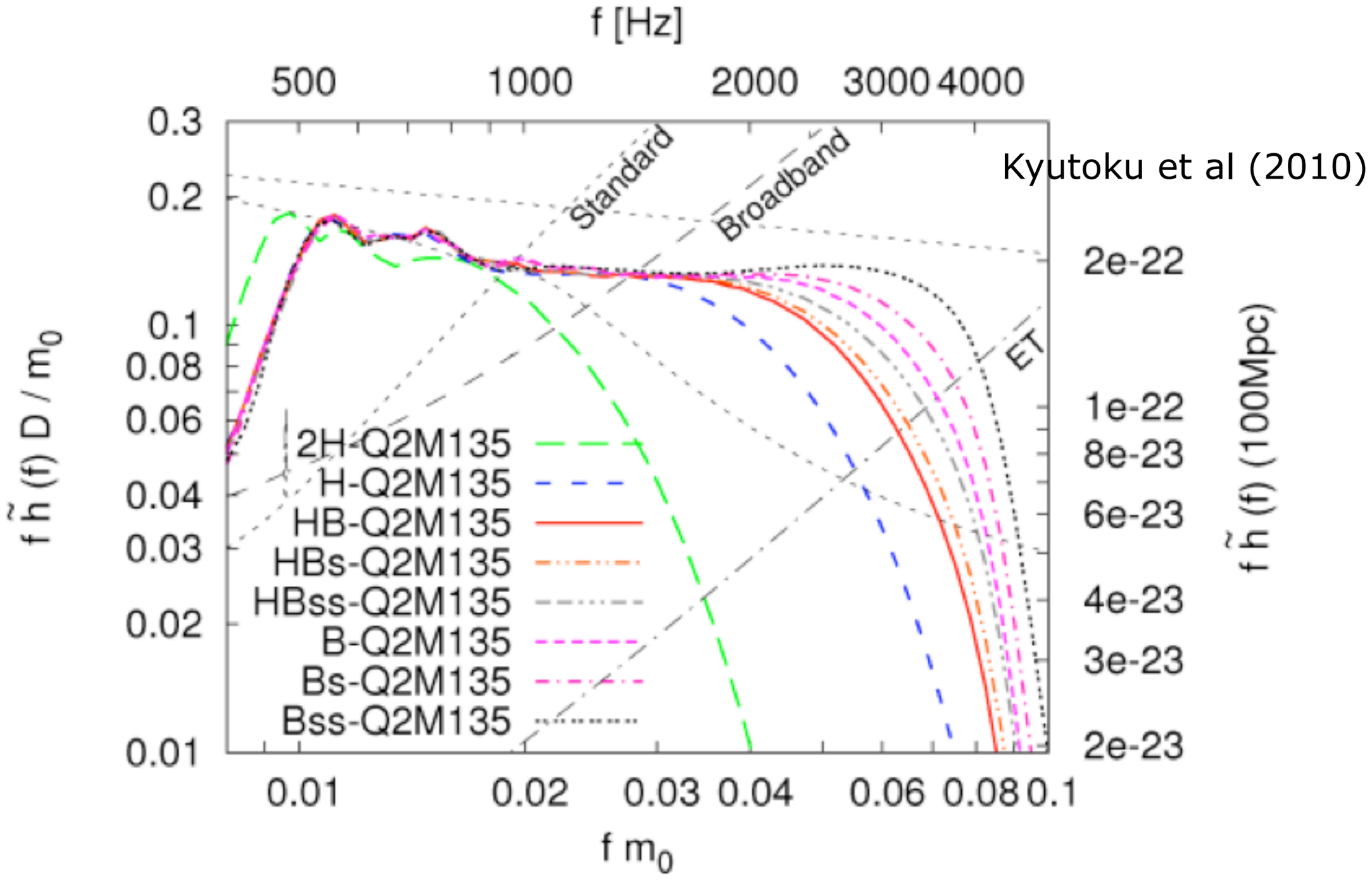

Kyutoku et al (2010)

If cutoff frequency is determined for a detected GW signal, the EOS of the NS will be constrained. (see Lackey et al (2013), 134 BH-NS simulations)

BH-NS: MHD simulations

Presence of strong B-fields is one of the most characteristic properties of NS. However, role of B fields in their merger process still poorly known. Ongoing work by Etienne et al (2012), Paschalidis et al (2015), Kiuchi et al (2015).

An **accretion torus**, expected to be formed around the remnant BH, is subject to the magnetorotational instability (**MRI**) (Balbus & Hawley 1991), and the B-field will be amplified.

High-resolution essential to resolve MRI. Kiuchi et al (2015) performed the highest resolution simulations to date.

While the simulation starts with an ad hoc localized seed magnetic field for the NS, the resulting torus becomes in a turbulence-like state and a global B-field is naturally formed.

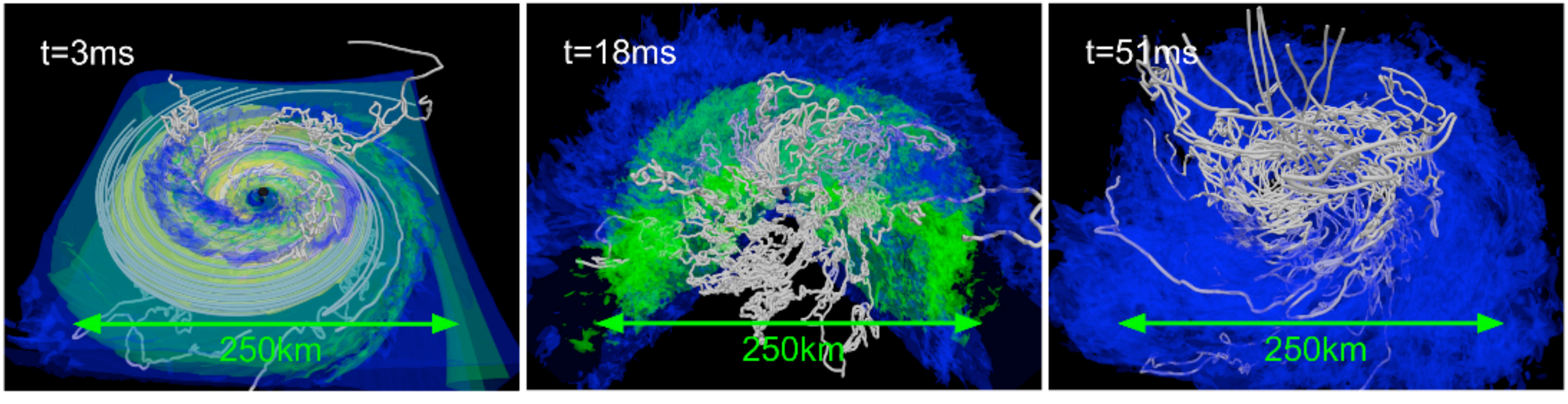

Kiuchi et al (2015)

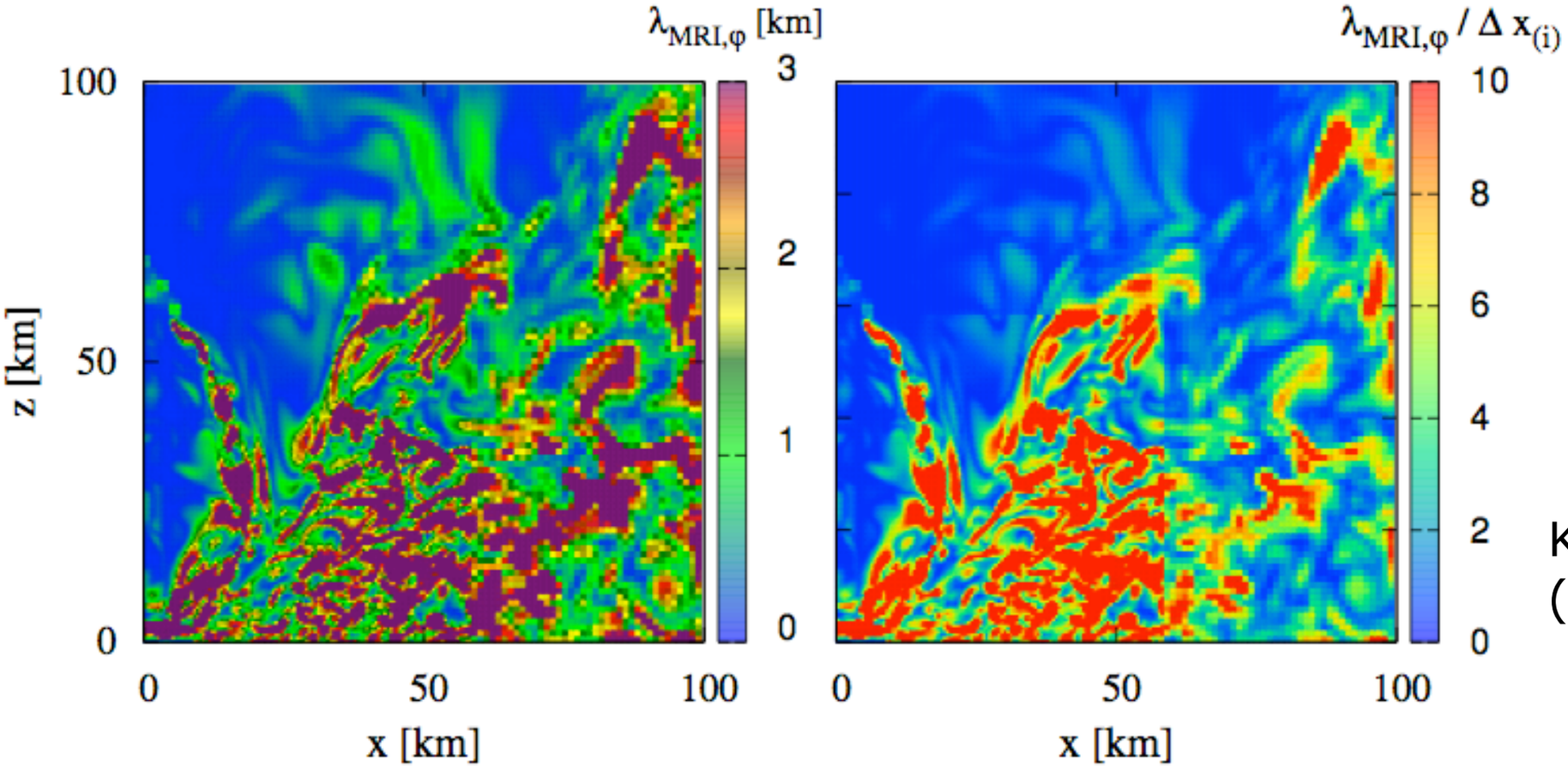

Kiuchi et al (2015)

FIG. 3. Profiles of wavelength of the fastest growing mode for non-axisymmetric MRI (left) and the wavelength divided by the grid resolution (right) on a meridional plane (x-z) at $t - t_{\rm mrg} \approx 15.0$ ms for the lowest-resolution run.

$$\lambda_{\rm MRI,\varphi} = \frac{2\pi}{\Omega} \frac{b_\varphi}{\sqrt{4\pi\rho h + b^\mu b_\mu}}$$

Wavelength longer than ~3 km in large portion of the region. Fastest growing MRI mode covered by more than 10 grid points even in the lowest-resolution run.

MRI properly resolved: turbulence-like motion produced by MRI plays an important role in mass ejection from the accretion torus.

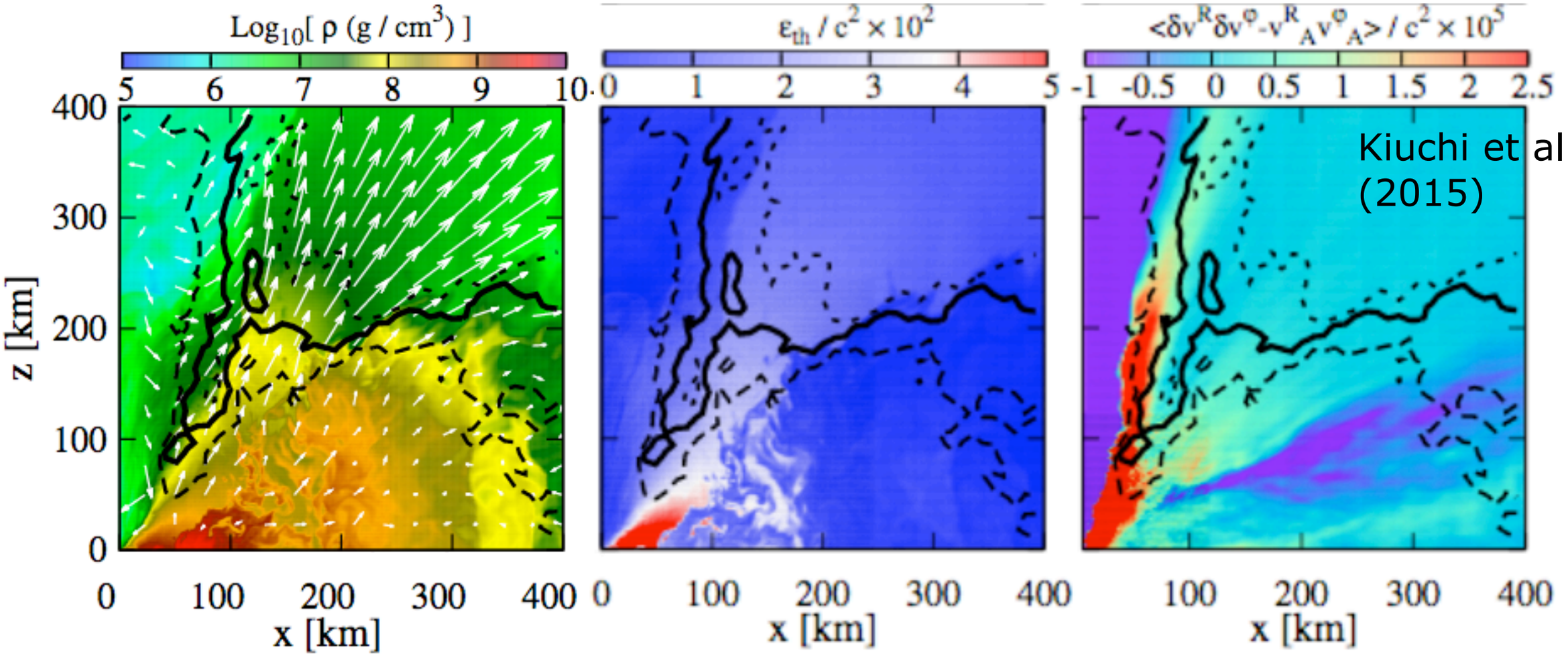

MRI-triggered turbulence drives mass accretion and converts kinetic energy into thermal energy resulting in the generation of a **strong wind.**

Funnel wall and magnetosphere with collimated poloidal magnetic fields.

Formed magnetosphere could help **launching a jet** by the Blandford-Znajek mechanism. The high outgoing Poynting flux found in the simulations of Kiuchi et al (2015) could be the main engine for sGRBs.

$\sim 0.06 M_\odot$ in the torus wind component, 6 times larger than that of the dynamical ejecta component.

Torus wind may contribute significantly to r-process nucleosynthesis of heavy elements, and to KM, in BH-NS mergers.

(Incipient) jet emergence

Under "right conditions" (i.e. initial seed poloidal B field) jets can be magnetically launched from BHNSs (Etienne et al 2012). Paschalidis et al (2015): GRMHD simulations of BHNS systems. Incipient jets launched if NS is initially endowed with a dipolar B field extending into the exterior. "Existence proof": large interior B field strength (~10^{17}G) but dynamically weak $\beta^{-1} \ll 1$

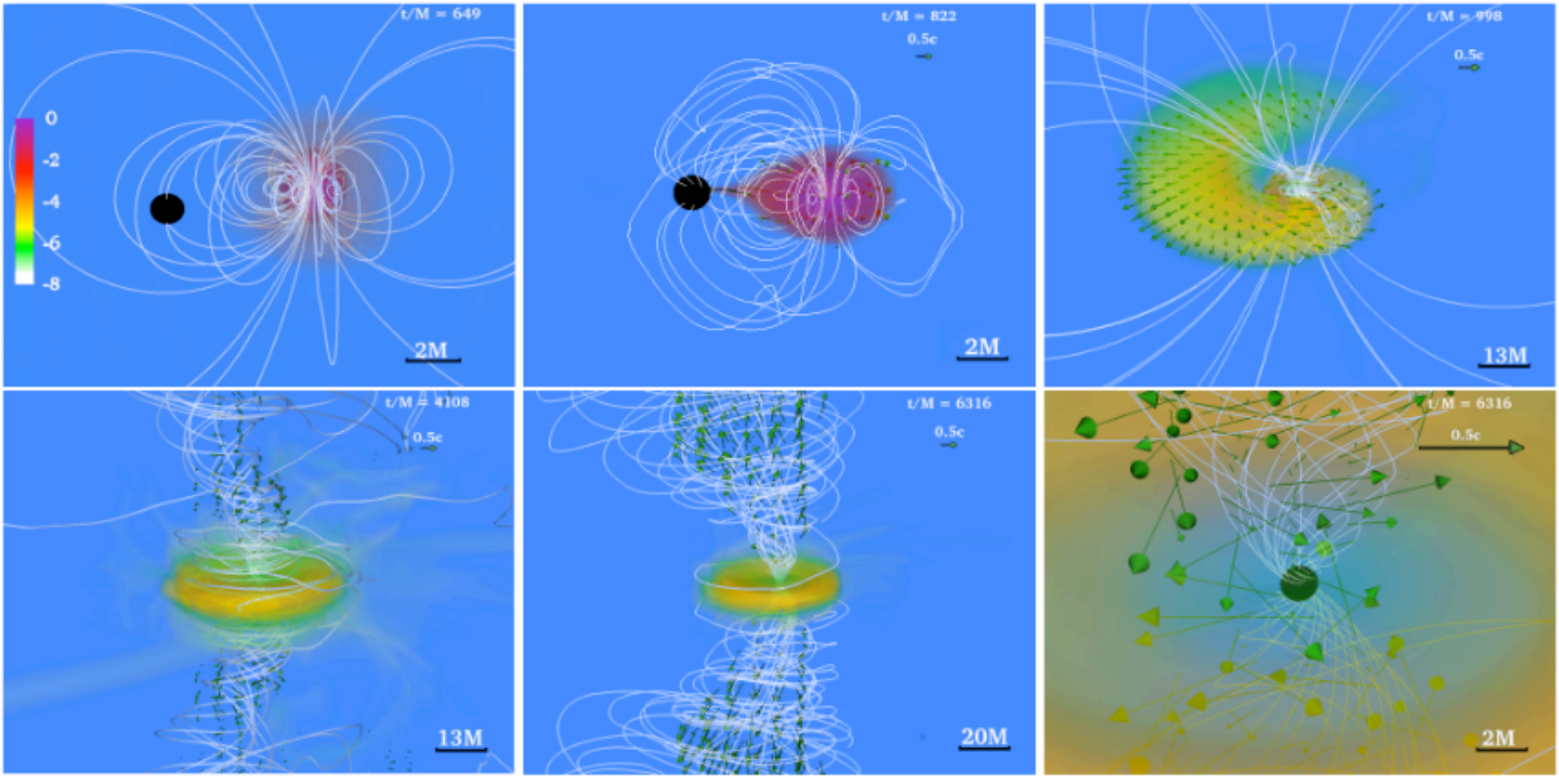

FIG. 1.— Snapshots of the rest-mass density, normalized to its initial maximum value $\rho_{0,\max} = 8.92 \times 10^{14}(1.4M_\odot/M_{\rm NS})^2$g cm^{-3} (log scale), at selected times. Arrows indicate plasma velocities and white lines show the magnetic field lines. Bottom panels highlight the system after an incipient jet is launched. Here, M $= 2.5 \times 10^{-2}(M_{\rm NS}/1.4M_\odot)ms= 7.58(M_{\rm NS}/1.4M_\odot)$km.

Paschalidis et al (2015)

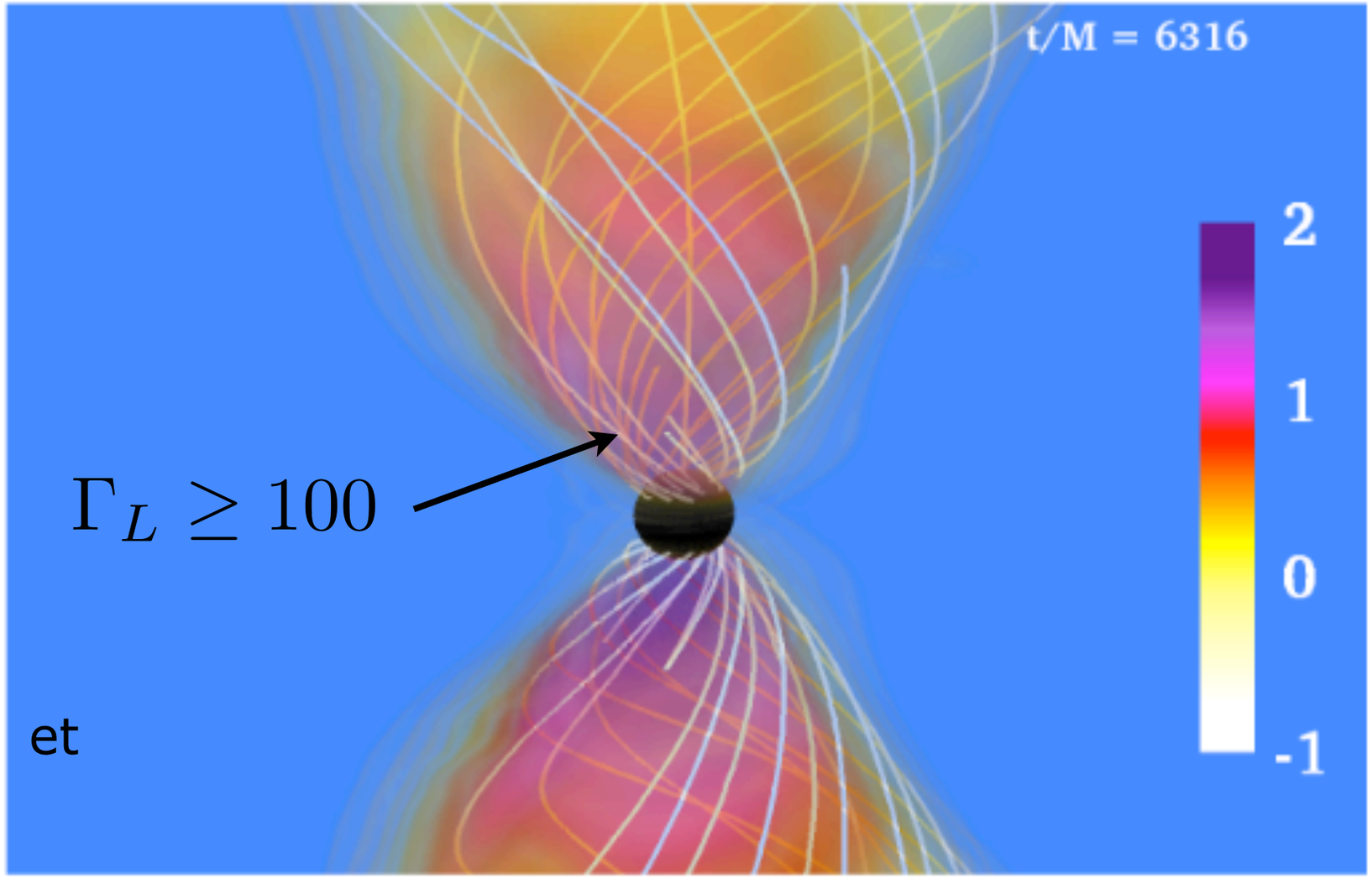

FIG. 3.— The ratio $b^2/2\rho_0$ (log scale) at $t - t_{\rm acc} = 5316$M.

For steady-state, axisymmetric Poynting-dominated jets, the maximum attainable Lorentz factor in the (asymptotic) jet is equal to the energy-to-mass flux ratio (Vlahakis & Königl 2003)

$$\Gamma_L \sim b^2/2\rho_0$$

As required by short GRB models, incipient jets can be accelerated to Lorentz factors of about 100 or larger (at the nearly force-free regions in the funnel)

Eccentric mergers of BH with NS

In dense stellar regions, such as galactic nuclei and globular clusters, BH-NS binaries can form through dynamical capture and merge with **non-negligible eccentricities** (e.g. Samsing et al 2014).

Repeated-burst nature of eccentric GW mergers. Compared to quasi-circular inspirals, eccentric mergers emit more GW energy. Small changes in the energy of the binary at each pericenter passage can lead to relatively large changes in the time between GW bursts.

GRHD simulations performed by Stephens et al (2011), East et al (2012, 2015) explored the effects of impact parameter, BH spin, NS EOS, and NS spin.

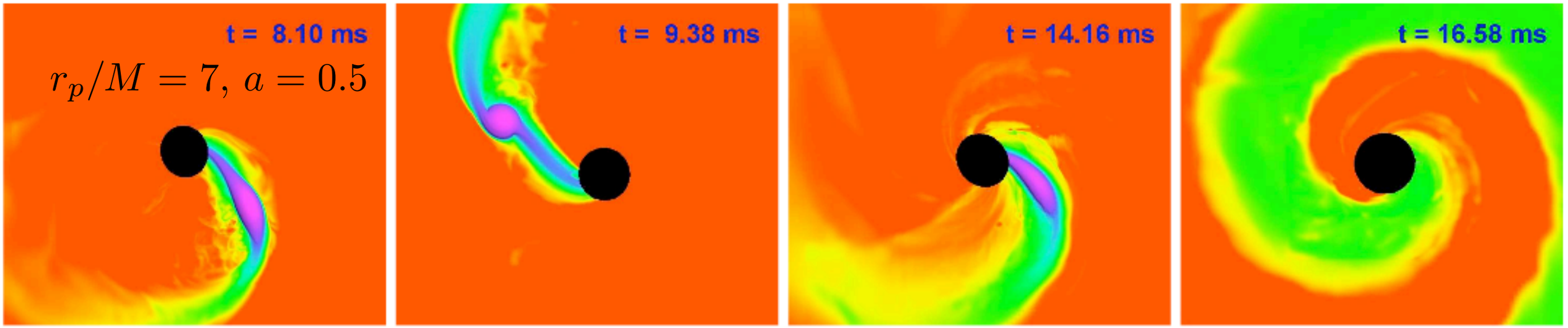

NS survives first encounter and is tidally disrupted during second encounter.

NS spin can significantly increase the amount of mass in unbound material.

East et al (2015)

East et al (2012)

Trajectories of NS center-of-mass

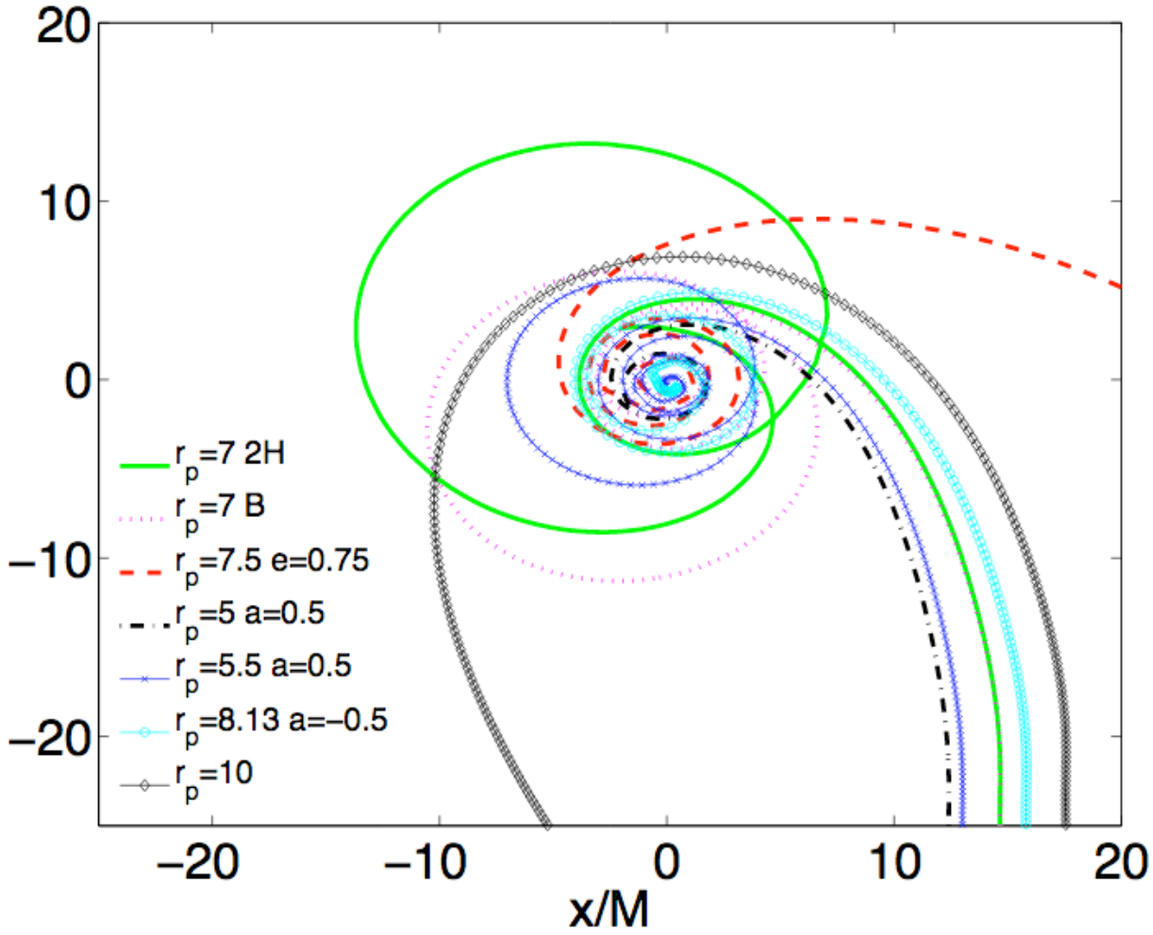

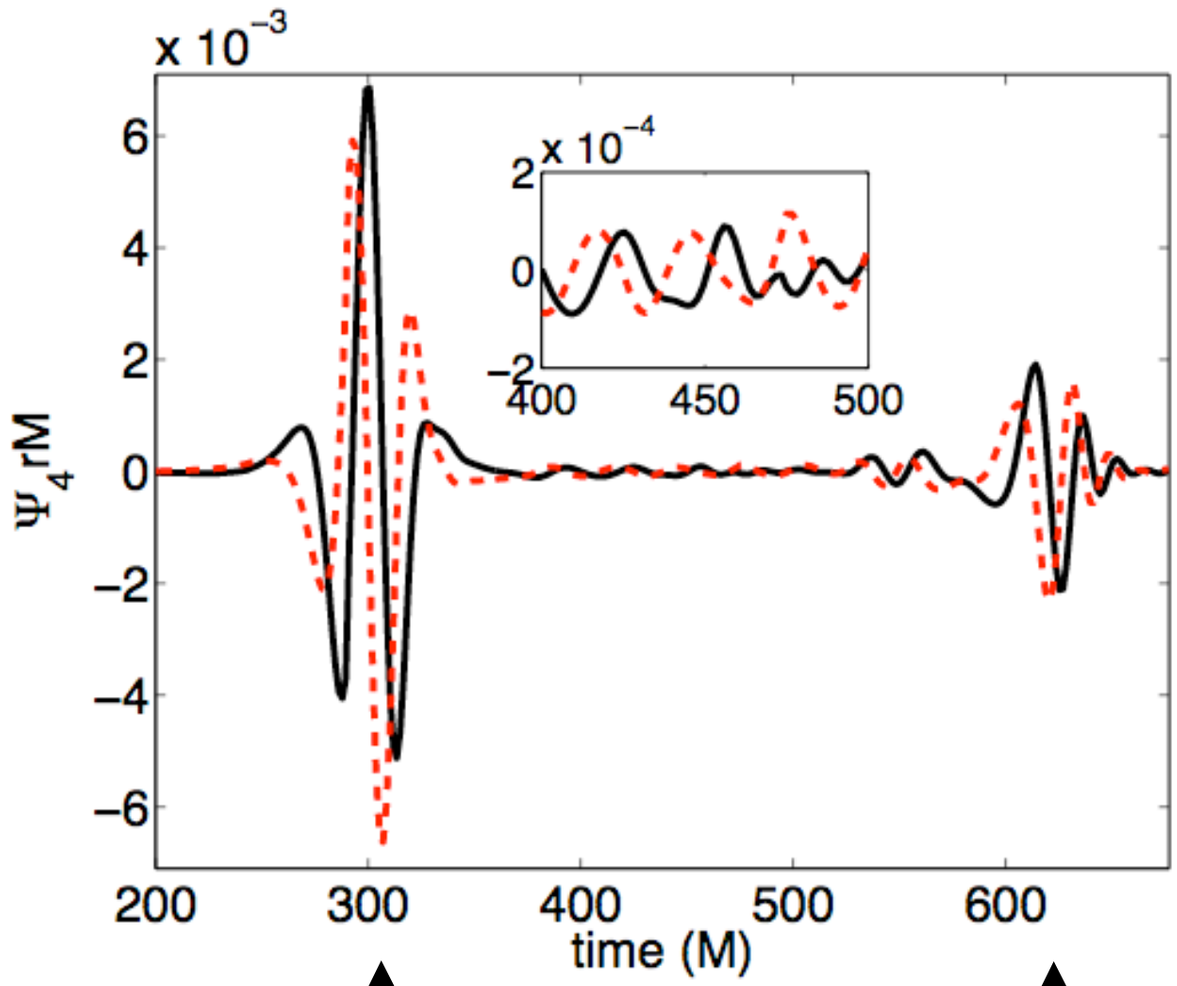

r_p=7, EOS 2H and B: close encounter (fly-by) followed by short elliptic orbit and merger.

r_p=10 long period elliptical orbit.

All other cases show merger on first encounter (while displaying various degrees of whirling behaviour).

initial fly-by

merger

tidally induced oscillations of NS (f-modes)

Black hole + accretion torus system: GRB

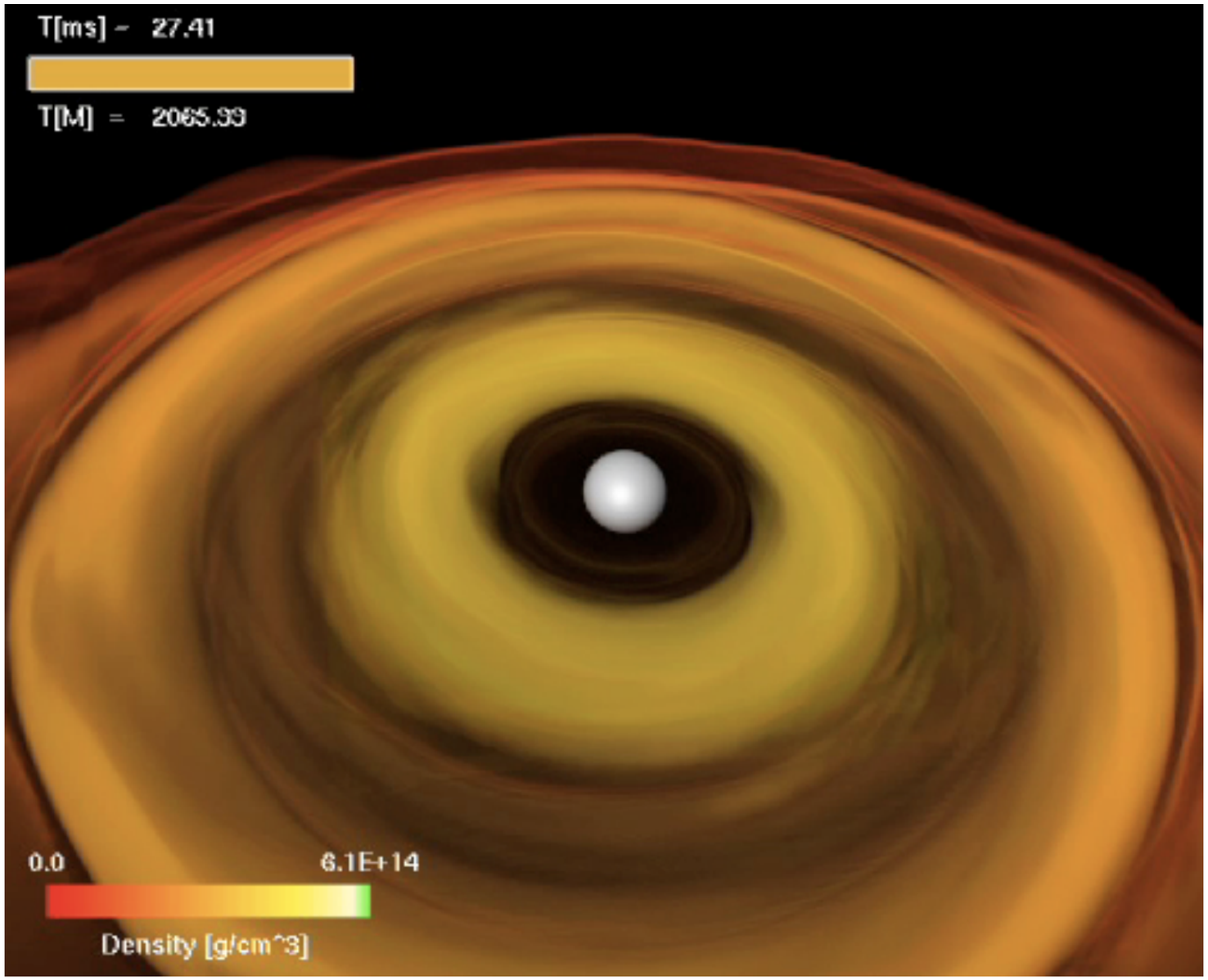

GRB hypothesis requires a **stable enough system to survive for a few seconds** (Rees & Meszaros 1994). Any instability which might disrupt the system on shorter timescales, such as the runaway instability and the Papaloizou-Pringle instability, could pose a severe problem for the accepted GRB models.

The runaway instability (e.g. Font & Daigne 2002)

Recent numerical relativity simulations have shown that **the runaway instability does not have a significant impact on the dynamics.**

- 2D axisymmetric: equilibrium ID. Stable tori irrespective of angular momentum distribution (Montero, Font & Shibata 2010)
- 3D: ID resulting from BNS simulation (Rezzolla et al 2011)

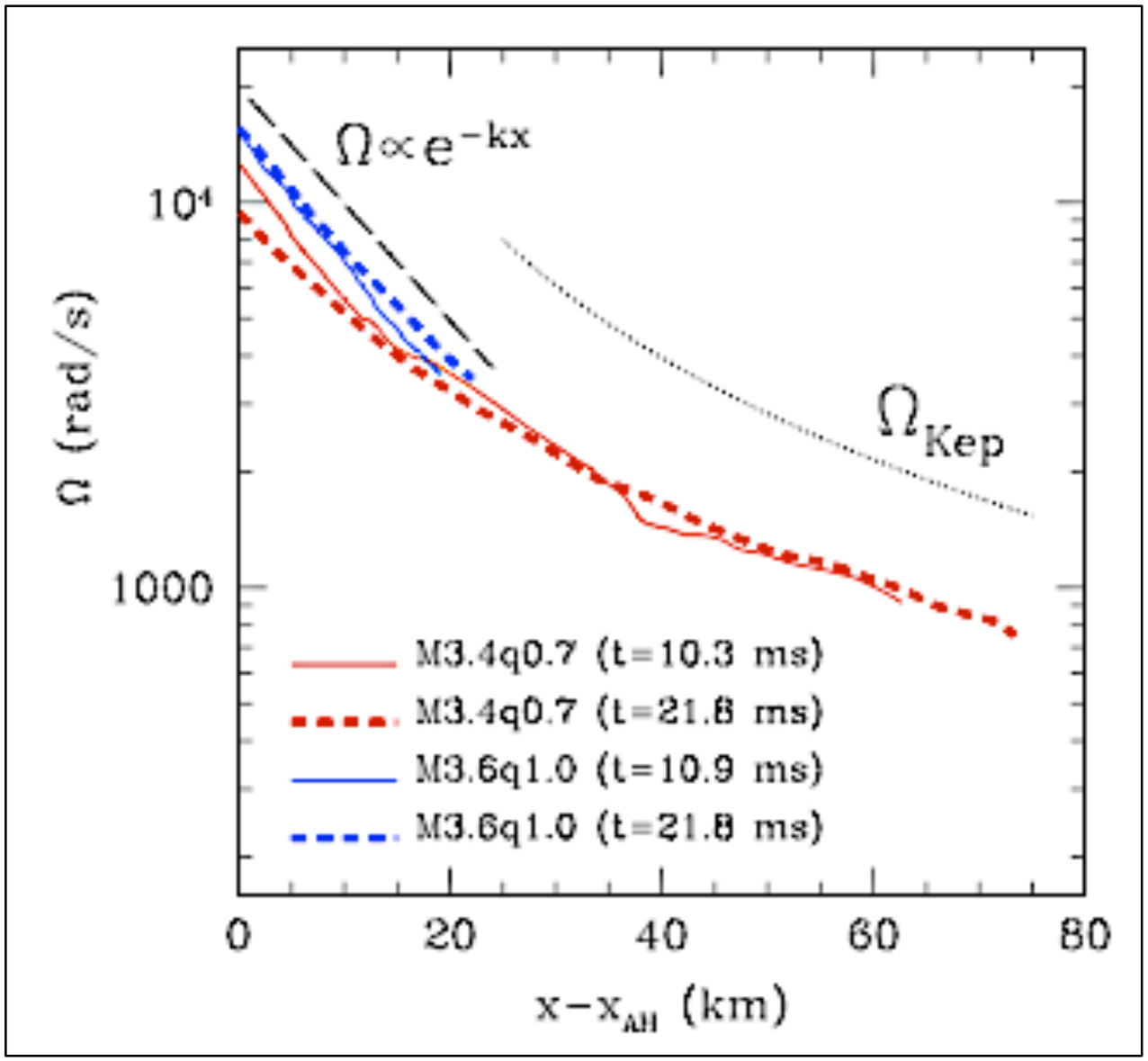

Rezzolla+ 2011

Unequal-mass binary reaches a **Keplerian** profile, $x^{-3/2}$. Explains scaling of specific angular momentum as $x^{1/2}$ and provides **firm evidence that tori produced self-consistently are dynamically stable.**

Note: Assuming *constant* specific angular momentum leads to runaway unstable disks (Korobkin+ 2013). Validity of assumption uncertain.

On longer timescales m=1 PP-instability sets in.

Korobkin+ 2011, Kiuchi+ 2011, Mewes+ 2015, 2016

Papaloizou-Pringle instability in tori

Papaloizou and Pringle (1984): tori with constant specific angular momentum unstable to non-axisymmetric global modes. Perturbation theory.

Basic idea: Global unstable modes have a co-rotation radius within the torus, located in a narrow region where waves cannot propagate. This region separates inner and outer regions where wave propagation is possible. Waves can tunnel through corotation zone and interact with waves in the other region. Transmitted modes amplified only if there is a feedback mechanism, in the form of a reflecting boundary at the inner and/or outer edge of the torus.

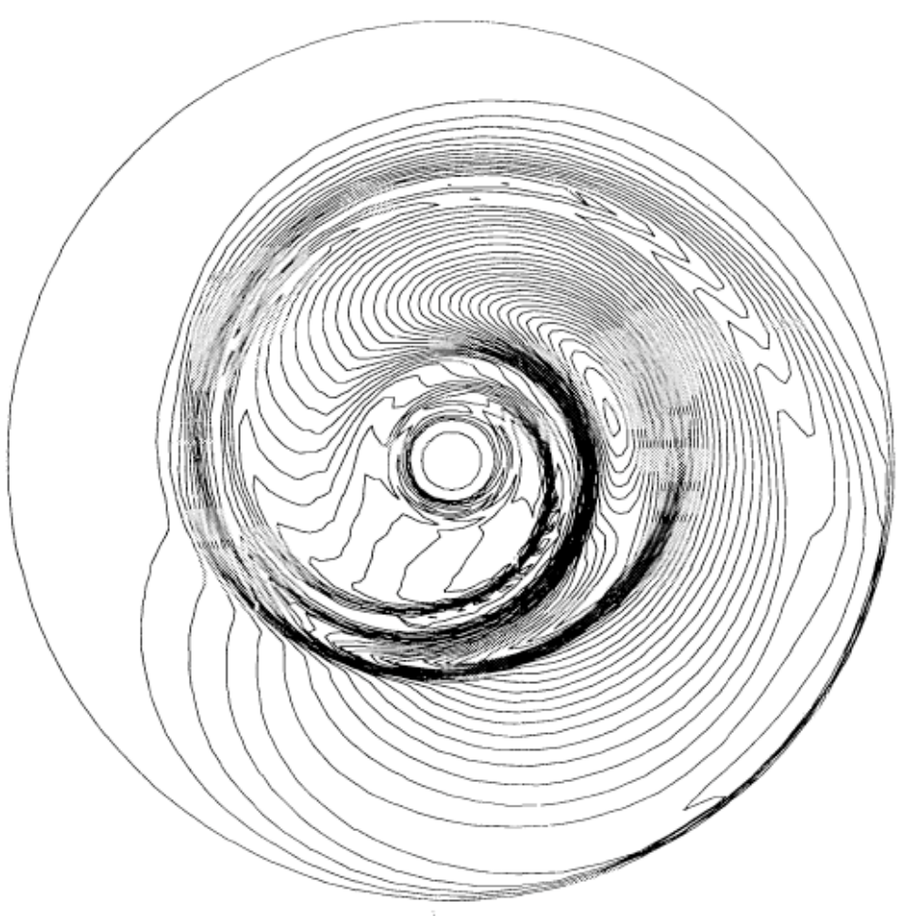

Manifestation of the PPI: counter-rotating epicyclic vortices, or **"planets"**, with m planets emerging from the growth of a mode of order m.

Early non-linear work by Hawley, Blaes, et al. Fixed metric computations.

Hawley (1991)

Animation model NC1: x-y plane

Development of the m=1 PPI

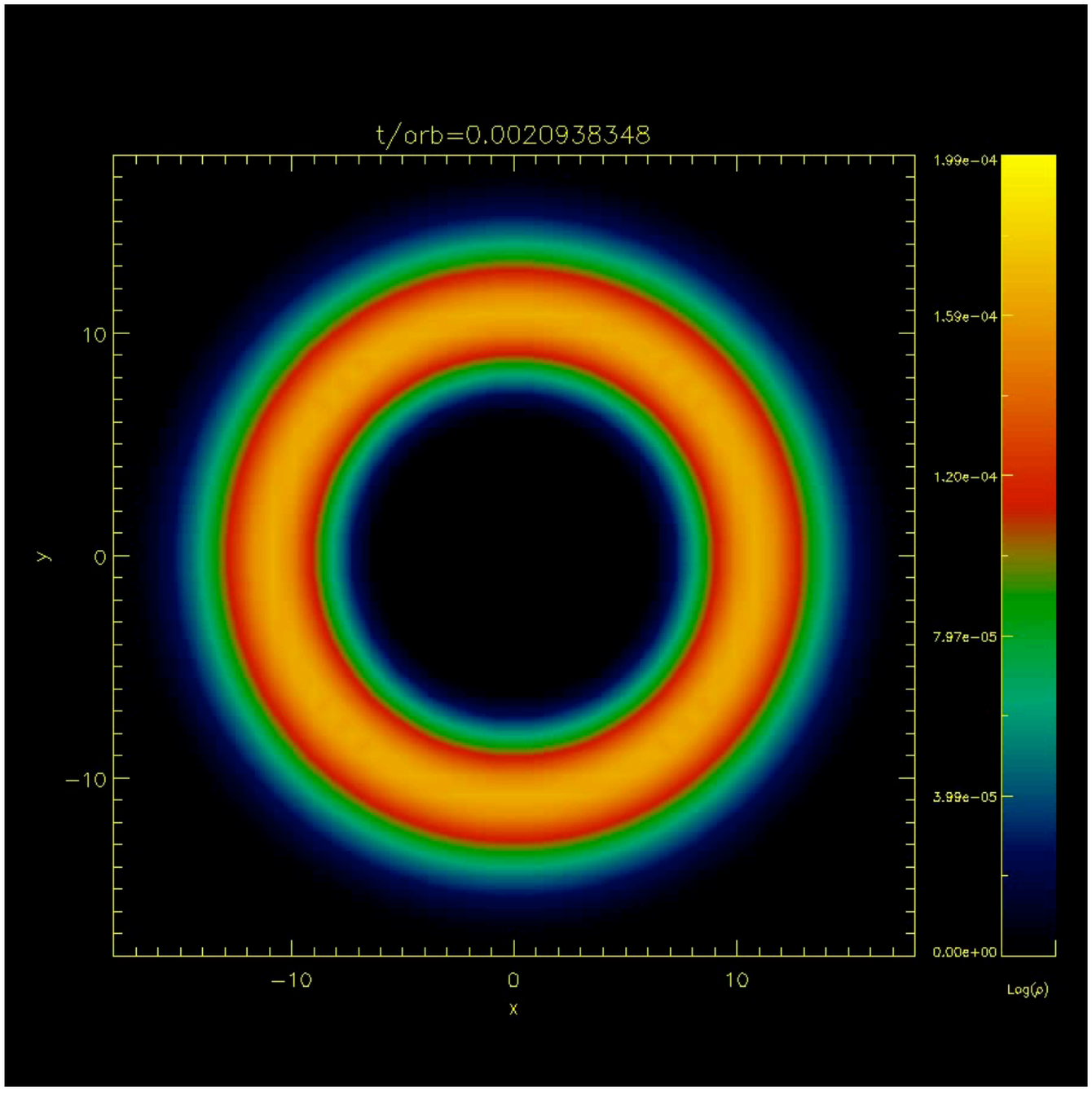

Full NR simulations.

Initial data built following the approach by Shibata (2006). Both constant and non-constant angular momentum tori.

Evolved using fixed mesh refinement NR code **SACRA** (Yamamoto, Shibata & Taniguchi 2008)

Kiuchi, Shibata, Montero & Font (2011)

m=1 mode grows for all j profiles

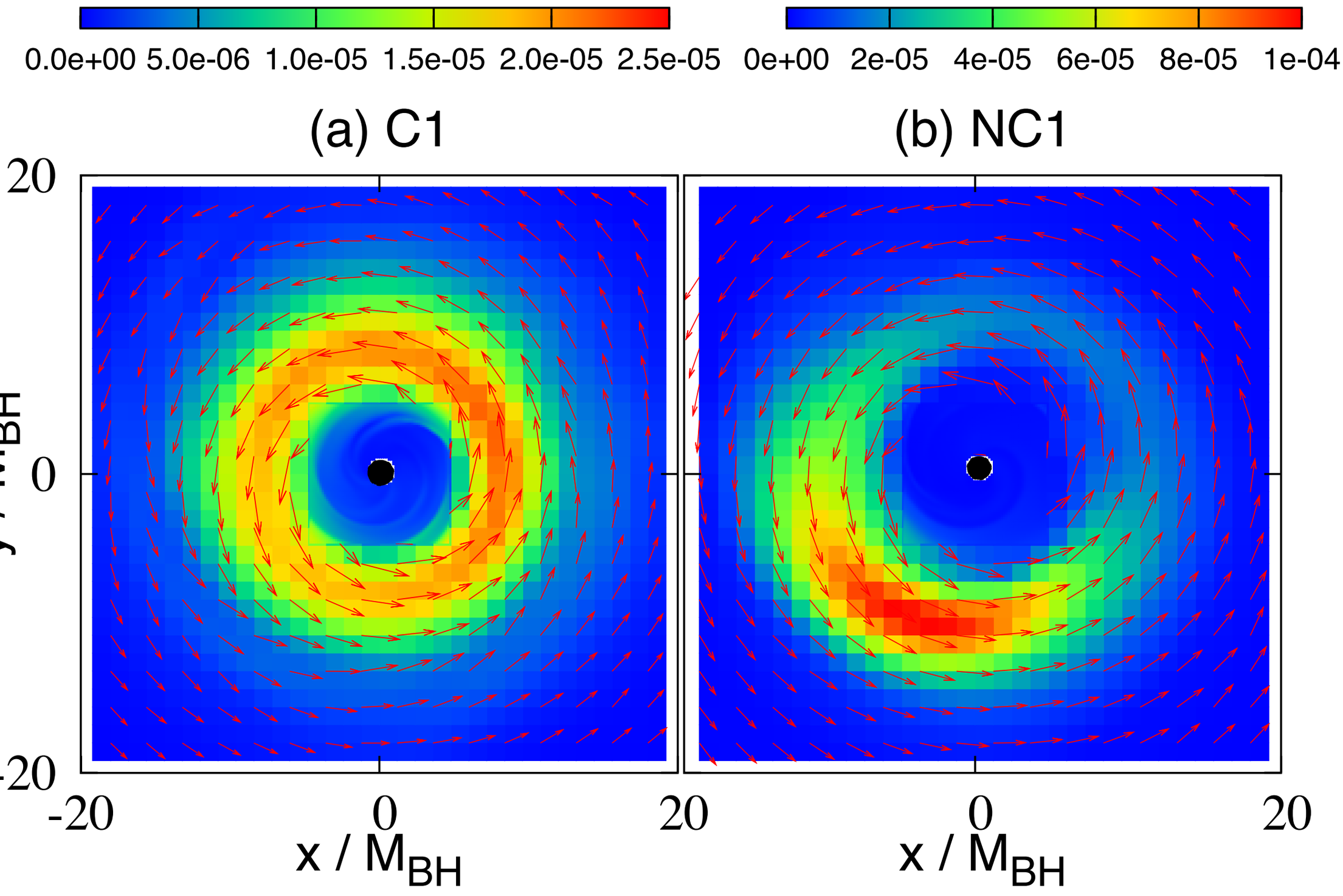

m=1-3 Fourier mode-amplitude and GW

$$D_m = \int \rho\, e^{im\varphi}\, d^3x$$

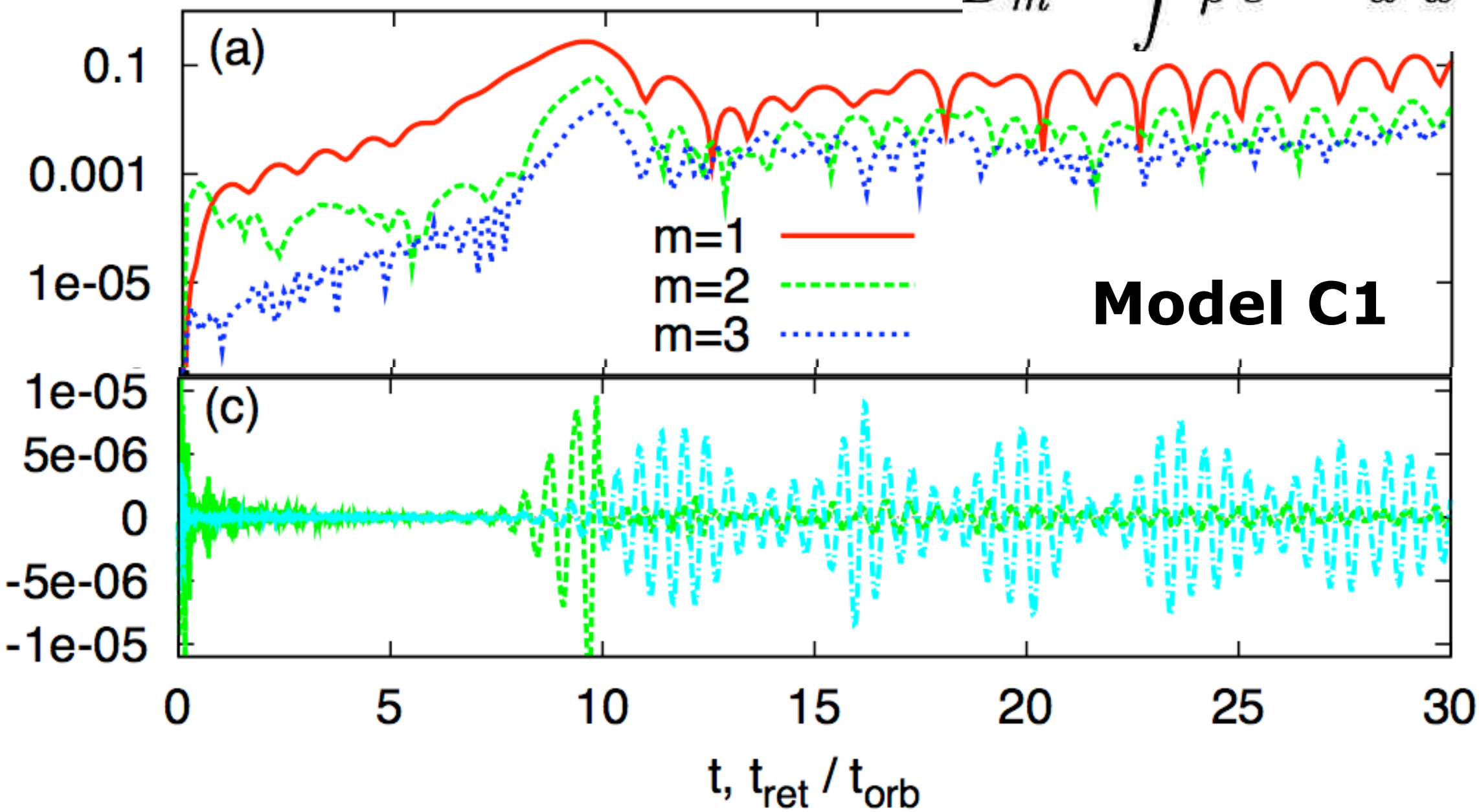

The m=1 mode is the fastest growing mode.

After saturation, m=1 structure survives for many rotation periods and tori become good GW emitters.

Summary

- NR BNS and BH-NS simulations are coming of age.

- Brief review on main results from NR simulations of BNS and BH-NS mergers.

- NR simulations (may) provide a plethora of information on pressing issues in relativistic astrophysics:
  - Gravitational wave astronomy
  - High-density nuclear physics
  - Short GRB central engines (gamma-ray emission)
  - r-process nucleosynthesis and KM (infrared EM emission)

- Continuously pushing forward the state-of-the art:
  - GRHD/GRMHD
  - Einstein equations (evolution & ID; spin, eccentric orbits)
  - High-order numerical methods & AMR
  - Nuclear physics EOS
  - Radiation transport